New Perfluoropolyether Surfactants for Water-in-Oil Emulsions

DISSERTATION

to obtain the academic degree
Doctor rerum naturalium (Dr. rer. nat.)
submitted to the Department of Biology, Chemistry, Pharmacy
of the Freie Universität Berlin

by
Mohammad Suman Chowdhury
from Manikganj, Bangladesh

November 2020

Declaration of honesty

I hereby declare and confirm the authenticity of my PhD thesis. It is the result of my own research work. Collaborations with other research groups are specified in the respective projects. All annotations, which have been used from published or unpublished sources, are identified as such. Any other sources than those cited have not been used.

_____

Mohammad Suman Chowdhury

November 2020

To Mazlum Jananeta Mawlana Bhashani

1. Reviewer: Prof. Dr. Rainer Haag, Freie Universität Berlin

2. Reviewer: PD Dr. Kai Licha

Date of Defense: 09.12.2020

Acknowledgments

I would like to acknowledge my advisor **Prof. Dr. Rainer Haag** for giving me the wonderful opportunity to work on much exciting and challenging research of fluorosurfactant synthesis for high-throughput droplet-based applications. I would also like to appreciate the freedom he gave me to explore novel ideas to try and push the limit of droplet-based research. Most importantly, I would like to thank him for introducing me to the research community and giving me the incredible opportunity to work at Harvard University in the group of Prof. Dr. David A. Weitz.

I would like to sincerely thank **PD Dr. Kai Licha** for being the second advisor of this thesis. I highly acknowledge the mentorship of **Dr. Pradip Dey** who I started with as an intern student and who guided me during my master thesis. I sincerely appreciate all his support, suggestions, and advice for challenging research work.

I sincerely thank **Prof. Dr. David A. Weitz** (Harvard University) for inviting me to work in his lab couple of times as a visiting scholar, introducing me to highly talented scientists in his working group, and being a highly productive collaboration partner. I also greatly acknowledge all knowledge, scientific teachings, and advice he gave me during my research stays in his working group.

I thank **Dr. Wenshan Zheng** (Harvard University), **John A. Heyman** (Harvard University) and **Dr. Xingcai Zhang** (Harvard University) for their scientific inputs on my research work. I would also like to thank **Prof. Esther Amstad** (École Polytechnique Fédérale de Lausanne) for her highly efficient collaboration. Additionally, I would like to greatly thank all other cooperation partners for their scientific suggestions and inputs.

Hereby, I would like to thank to all the former and present members for the incredible atmosphere. I sincerely thank, **Dr. Christoph Schlaich**, **Dr. Sabine Reimann**, **Dr. Shalini Kumari**, **Dr. Sumati Bhatia**, **Dr. Pallavi Kiran**, **Dr. Jose Luis Cuellar Camacho**, **Dr. Manoj Kumar Muthyala**, **Dr. Daniel Stöbner**, **Dr. Olaf Wagner**, **Dr. Abhishek Kumar Singh,** and **Dr. Abbas Faghani** for all their scientific discussions during our daily lab work. I am also thankful to **Dr. Pamela Winchester** for language polishing of my publications and

List of abbreviations

PDMS	Poly(dimethylsiloxane)
PEG	Poly(ethylene glycol)
PCR	Polymerase chain reaction
W/O	Water-in-oil
O/W	Oil-in-water
W/O/W	Water-ion-oil-in-water
O/W/O	Oil-in-water-in-oil
W/O/W/O	Water-in-oil-in-water-in-oil
UV	Ultraviolet
CAD	Computer aided design
CAC	Critical aggregation concentration
HLB	Hydrophilic-lipophilic balance
PFPE	Perfluoropolyether
PPO	Poly(propylene oxide)
mRNA	Messenger RNA
ePCR	Emulsion polymerase chain reaction
kHz	Kilo hertz
dPCR	Droplet polymerase chain reaction
3D	Three-dimensional
Dox	Doxorubicin
APC	Antigen-presenting cell
SPAAC	Strain promoted azide-alkyne cycloaddition
mCPBA	Meta-chloroperoxybenzoic acid
DBCO	Dibenzylcyclooctyne

Table of contents

1 Introduction

1.1 Emulsions and droplet microfluidics

1.1.1 Basic concept of emulsion

Emulsions are, typically, opaque dispersions comprised of two immiscible liquids, in which one being the inner phase is dispersed as droplets in the outer continuous phase.[1-2] Milk is a classical example of such emulsion systems, in which fat molecules are dispersed in the continuous water phase, generating an oil-in-water (o/w) emulsion. By contrast, tuning the ratio of the two immiscible phases, a water-in-oil (w/o) emulsion can also be created.[3] However, irrespective of the emulsion types, man-made emulsion droplets are primarily polydisperse in nature, when no templating approach is employed, and unlike naturally occuring milk, mixing of the two unlike phases needs extra energy, typically, in the form of a mechanical agitation (Figure 1 a).[2] These dispersion systems are metastable,[4], reflecting their tendency for sedimentation, creaming, flocculation, and coalescence, and, ultimately, they phase separate (Figure 1 b).[5]
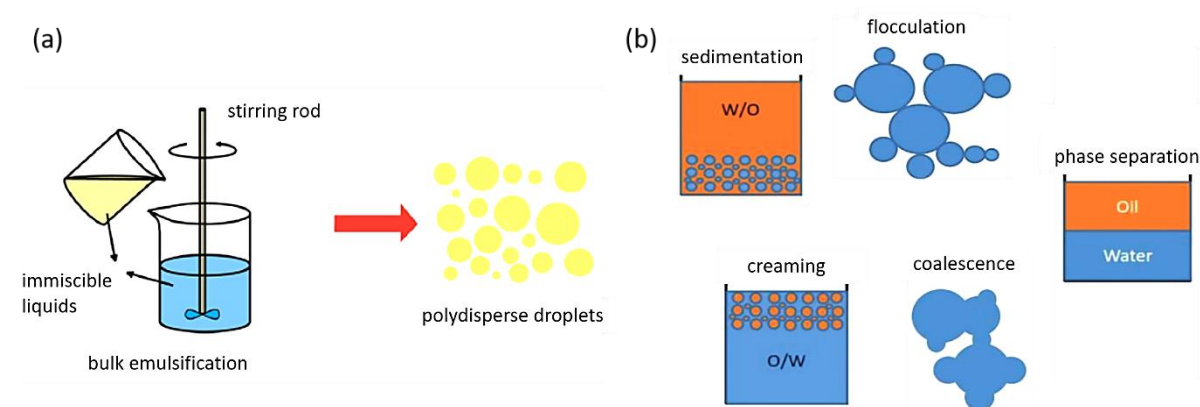
Figure 1. (a) Schematic illustration of the polydisperse droplet generation by agitating two immiscible liquids. Reused from ref.[2] (b) Pathways showing the de-emulsification of two unlike phases. Reused with the permission from ref.[5] Copyright 2018 Canadian Society for Chemical Engineering.

To circumvent the de-emulsification tendency and/or to increase the metastability of the dispersed phase, a third component, as a stabilizer, is often introduced into the emulsion system. Typically, amphiphilic moieties comprised of polar and non-polar segments, are used to stabilize the dispersed phase.[6] However, colloidal particles, polymers, block copolymers, stimuli-responsive polymers, and ionic polymers are also used to generate different kinds of emulsions for many applications, including release of active cargos, oil harvesting, skin-care

product, Janus particles, and fiber formation (Figure 2).[7-11] Besides, Hasemnejad *et al.* described a nano-emulsion system that used Pluronics, a biocompatible tri-block copolymer, to stabilize the o/w nano-emulsions.[12] Irrespective of the polymer types used to stabilize the dispersed phase, the dispersions are often polydisperse, limiting their use in many research and product developments.[13]
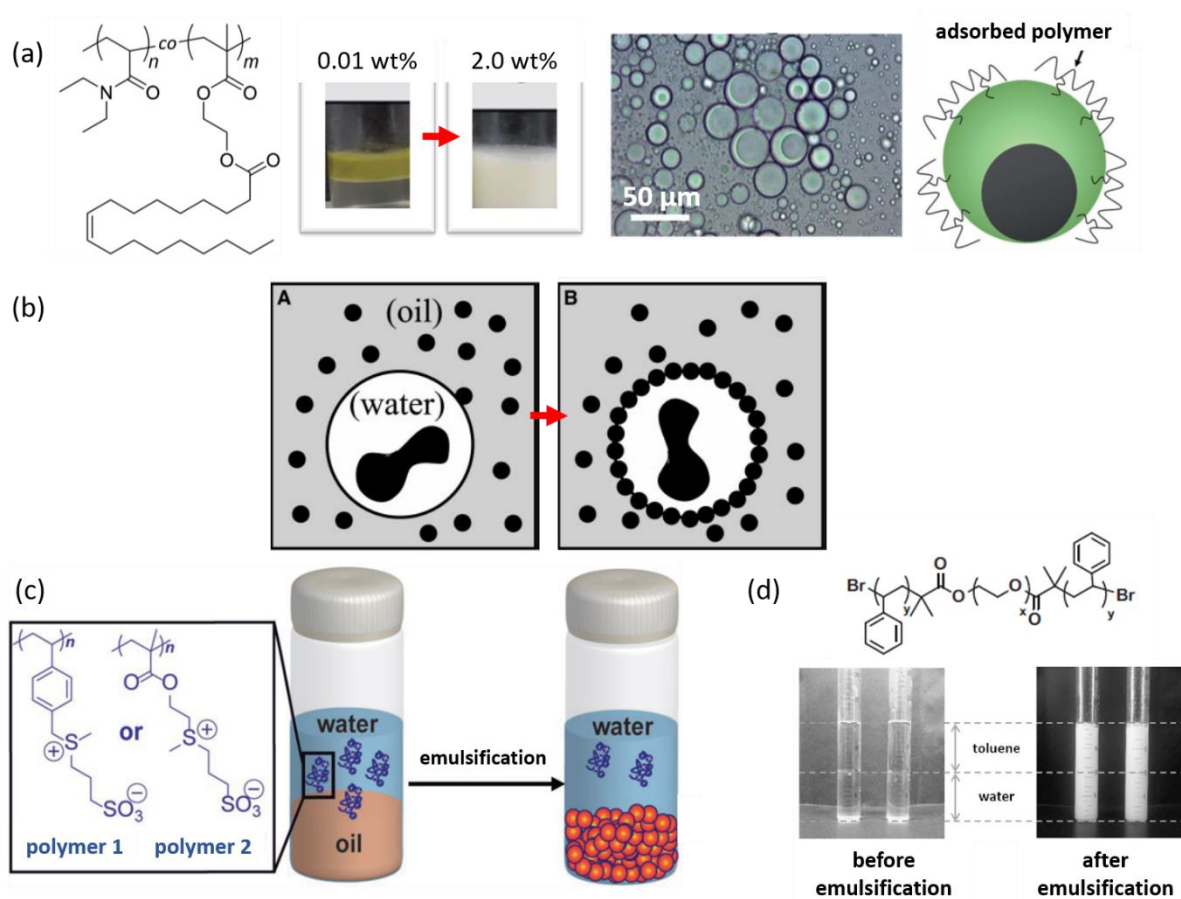
Figure 2. (a) Schematic showing thermo-responsive polymer-based Janus emulsion generation. Adapted from ref.[7] Copyright 2019 The Royal Society of Chemistry. (b) W/O emulsion stabilization with colloidal particles. Reprinted with the permission from ref.[11] Copyright 2002 American Association for the Advancement of Science. (c) Zwitterionic polymer-based emulsification. Reprinted with the permission from ref.[9] Copyright 2018 Wiley-VCH, Weinheim. (d) Non-ionic block-copolymer-based emulsification of toluene in water. Reprinted with the permission from ref.[10] Copyright 2015 The Society of Polymer Science, Japan (SPSJ).

1.1.2 Glass-capillary- and PDMS-based droplet microfluidics

Microfluidics is a platform technology that offers exquisitely precise control over fluid manipulation using tens to hundreds of micron-sized channels.[4, 14] These channels can be made with different materials, including silicon, glass, and plastics.[14] Silicon- and glass-based channels, although useful for some applications, are not widely explored because of their high

cost, low scale-up, biological incompatiblity, and rigid characteristics.[14] Additionally, silicone-based microchannels are not suitable to synchronise with the conventional optical detection setup.[14] By contrast, elastomeric-polymer materials addresses all of these problems, because they can be impermeable to water but permeable to gases, which are essential for cells. These polymers should be cost effective, optically transparent to be coupled with the regularly used optical detection setup, and, most importantly, non-toxic to cells.[15]

Consequently, poly(dimethylsiloxane) (PDMS), being an elastomeric polymer material, has been widely used over the past decades in microfludics-based biochemical assays.[4, 15] Droplet microfluidics is one of the crucial innovations that allows flexibility in biological applications by permitting micron-sized droplet generation with unprecedented control over the droplet size distribution, reflecting a key aspect of quantitative analyses.[16]

Glass-capillary-based droplet microfluidics is far from industrial use, but it is widely used in basic academic research for the generation of complex double emulsions such as water-in-oil-in-water (w/o/w) and oil-in-water-in-oil (o/w/o), and triple emulsions such as water-in-oil-in-water-in-oil (w/o/w/o), in which multiple droplets can be captured in one large droplet.[17-19] A typical glass-capillary-based microfluidic device for droplet emulsions consists of glass capillaries with blunt and/or sharp orifice, needles, and glass slides (Figure 3 a-b).[20-21] Using such a device, emulsions with multiple compartments can be created, analyzed, and controlled for cargo release (Figure 3 c-d).[18, 22-23]
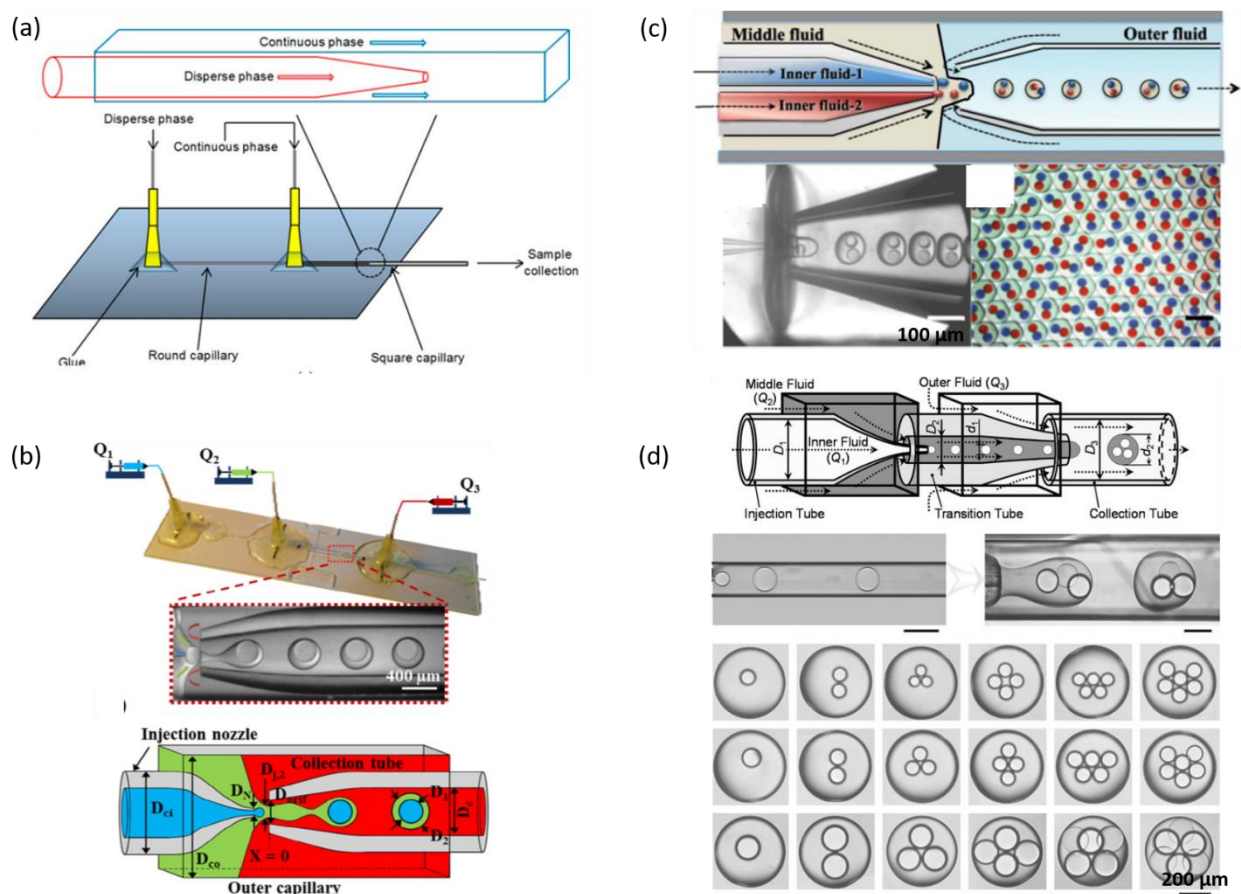
Figure 3. (a) Schematic showing key elements: capillary, needle, and glass slide which are required to fabricate a glass-capillary-based microfluidics device. Reused from ref.[20] Copyright 2016 MDPI, Basel, Switzerland. (b) Glass-capillary-based device using three inlets to produce double emulsions (top). Diagram showing the device geometry and liquid types (bottom). Adapted from ref.[21] Schemes showing generation of complex emulsions with multiple compartments in one. Reprinted with the permission from ref.[18, 22] Copyright 2012 The Royal Society of Chemistry (c). Copyright 2007 Wiley-VCH, Weinheim (d).

However, the extremely low scale-up of device facbrication is one of the major drawbacks of the glass-capillary-based droplet microfluidics platform.[24] Also, glass capillaries are not permeable to respiratory gases, on chip droplet incubation with the glass-capillary devices is not possible, limiting their use in many biological applications.[15] On the other hand, the PDMS-based device fabrication does not suffer from the scale-up problems. In addition, it offers many distinct advantages over the glass capillary devices, including fabrication of multiple channels at once in one single chip.[14] A typical PDMS chip fabrication needs multiple steps: (i) spin coating of photoresist on silicon wafer; (ii) UV exposure of the unmasked area; (iii) washing of the non-crosslinked photoresist; (iv) pouring PDMS solution on the developed silicon master and polymerize it; (v) removal of the cross-linked patterned PDMS slab; (vi) making holes for the inlets and outlets; (vii) gluing the punched slab on glass slide by means

of plasma surface activation of both the design side of the PDMS and glass slide; and (viii) the device needs to be treated with a suitable chemical to make it either hydrophilic or hydrophobic (Figure 4a).[25] Due to computer aided design (CAD) of the microfluidic channel, each PDMS chip glued onto the glass slide can have multiple channels, reducing the time and cost of manufacturing.[15, 25] A channel is composed of several parts: multiple inlets for oil and aqueous streams and an outlet for the emulsion droplets (Figure 4b).[25] Although PDMS chips have many advantages, they have some limitations too; for example, unlike glass capillary-based devices, organic solvents cannot be used with the PDMS device for a long-time emulsion generation because this causes swelling of the PDMS slab and, consequently, it changes the microchannel's geometry.[26-27]
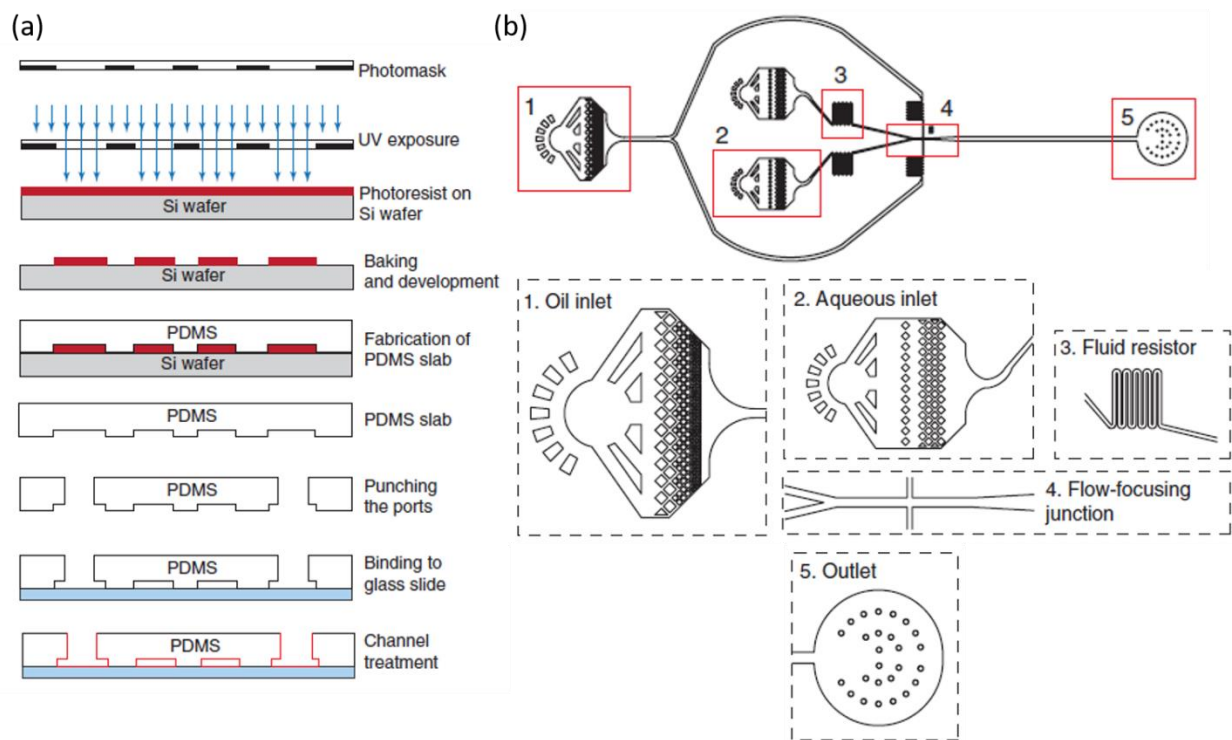
Figure 4. (a) Schematic drawing of PDMS device fabrication steps. (b) Microfluidics device (top) and its associated parts in offset images. Reprinted with the permission from ref.[25] Copyright 2013 Nature America, Inc.

1.2 Surfactants

1.2.1 Surfactants in emulsion and compartmentalization

Surfactants, by definition, are surface active agents that are soluble in both aqueous and organic medium and that reduce the interfacial energy between the two immiscible liquids.[5] They, classically, contain a hydrophilic segment, showing affinity towards water, and a hydrophobic segment, having tendency to interact with organic liquid such as oil. Thus, they assemble at the interface of water and oil, and play a crucial role to minimize the high interfacial energy

between the two liquids. The mixing of the two liquids under mild stirring, generates emulsion droplets of different sizes.[4-5, 28] Depending on the volume fractions of the two different liquids, w/o or o/w emulsions can be created. However, a more complicated emulsion systems can also be prepared where drops in drops are formed.[27] Droplet size distribution and type of surfactants used are two key features that, primarily, dictate the stability of the emulsion droplets.[29-30] Accordingly, different types of emulsion systems have been used to compartmentalize active ingredients for many different applications in food and pharmaceutical industries, inlcuding petroleum industry, skin care industry, and perfume industry.[29, 31-33]
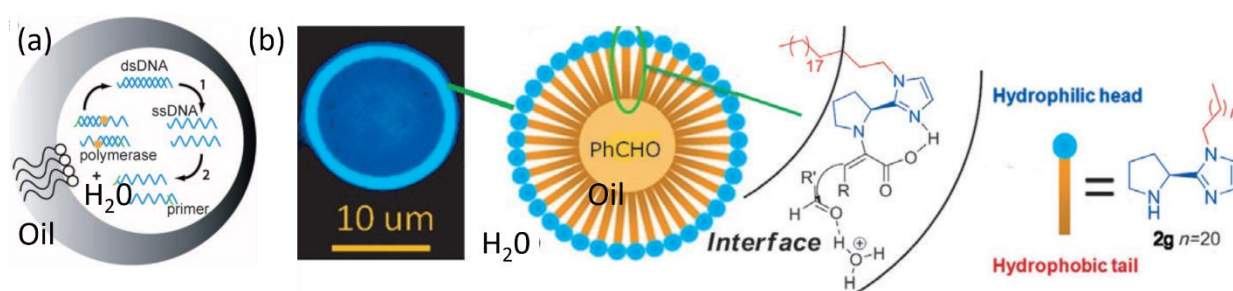
Figure 5. (a) Image showing surfactant-stabilized w/o emulsion droplet for nucleic acid synthesis in water. Reprinted with the permission from ref.[4] Copyright 2010 Wiley-VCH, Weinheim. PDMS device fabrication steps. (b) Photo image showing o/w emulsion droplet stabilized with functional surfactants for a chemical reaction at the interface. Reused with the permission from ref.[34] Copyright 2012 Wiley-VCH, Weinheim.

1.2.2 *Physicochemical Characteristics*

Above a certain critical aggregation concentration (CAC) of the surfactant molecules, the aggregation morphology is dictated by the energetically favorable conformation of the molecules.[35] Using the shape of a surfactant molecule, a critical packing parameter, which is a dimensionless number, can be calculated to predict: (i) the solubility of the surfactant, (ii) the structure of the aggregates it will form above the CAC, and (iii) the type of emulsions it will support (Figure 6a).[35-36] Hydrophilic-lipophilic balance (HLB) value is another dimensionless number for the surfactant molecules that can be calculated by Griffins' method and/or Davies' method. Using the HLB value, the solubility and emulsification type of a surfactant can also be predicted (Figure 6b).[37]
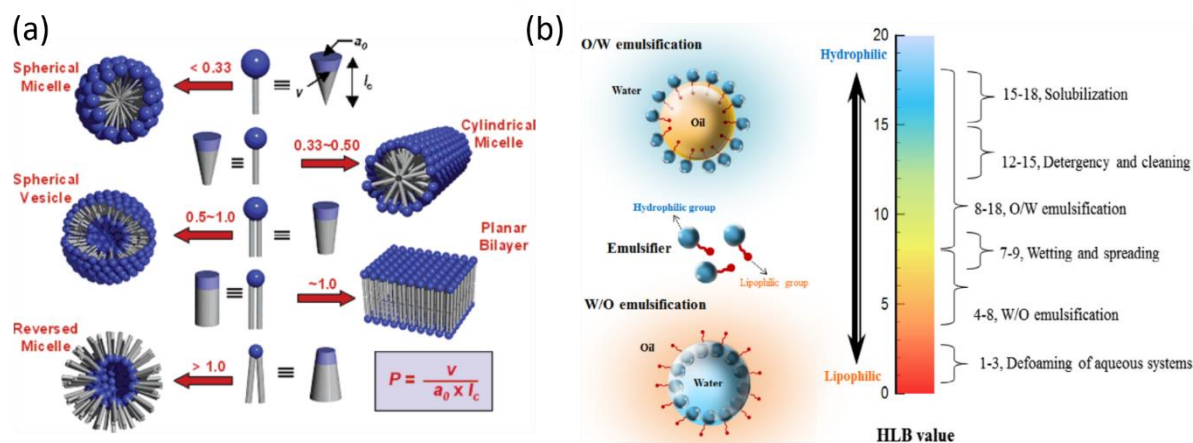
Figure 6. (a) Mophological structures predicted by the packing parameter. Reprinted with the permission from ref.[35] Copyright 2005 American Chemical Society. (b) Scheme showing o/w emulsification (top left), w/o emulsification (bottom left), and a HLB scale of 0-20. Reprinted with the permission from ref.[37] Copyright 2016 Elsevier Ltd.

1.2.3 *Low molecular mass surfactants and polymeric surfactants*

Surfactants, irrespective of their molecular masses, can be broadly classified into four categories: anionic, cationic, zwitterionic, and non-ionic. Low molecular mass surfactants have been widely used in drug delivery, oil harvesting, coacervation, gene therapy, skin care products, and capsule preparation.[33, 38-40] But, they suffer from several issues, including high surface tension, weak surface adsoption, low mechanical strength of the interfacial film, low multivalency, poor stability, high CAC, and low safety profile.[5, 41-44] While the polymeric surfactants address these issues and offer many possibilities to tailor them by means of controlled polymerizations, and by integrating many functionalites into the pendant groups or, alternatively, into the main-chain backbones.[41-42, 45-46] Among different types of surfactants, the non-ionic surfactants are particularly important for many biological applications bacause they provide anti-fouling features.[47] Accordingly, they have been exploited in anti-fouling coatings, molecular biology or as nanocarriers.[46, 48-49]

1.3 Fluorosurfactants for biology and chemistry in droplets

For quantitative assays it is of crucial importance to generate monodisperse droplets and for doing so the best choice is to use PDMS-based microfluidic devices. However, as mentioned earlier that when conventional silicon oil and hydrocarbon oils are used to generate water-in-oil emulsion droplets, they cause shrinking or swelling of the PDMS devices, resulting in clogging of the channels. Morever, the use of these oils may also delaminate the device.[50] To

address these issues, fluorocarbon oils are used as the continuous phase.[30] However, the two most important aspects that make the fluorocarbon oils very attractive and useful for microfluidics emulsions are (i) their extremely high hydrophobicity and lipophobicity, inhibiting biological reagents from the aqueous phase to be soluble in them, and (ii) their higher permeability of respiratory gases in comparison to water, providing an appealing three-dimensional environment for cell cultures.[4, 25, 30, 50] Additionally, these oils have high boiling point, making them suitable for assays requiring high temperature. To capitalize on these benefits of fluorocarbon oils, fluorinated surfactants are used that are readily soluble in fluorous oils, and can stabilize the microdroplets against uncontrolled coalescence by populating the oil-water interface.[25] Due to the robustness of carbon-fluorine compared to carbon-hydrogen bonds, the perfluorinated surfactants are highly stable at elevated temperature, and are thus appealing in the emulsion systems.[50]

1.3.1   PEG-based di- and tri-block surfactants

Droplet stability against coalescence is affected by the diffusion time of the surfactant molecules while the diffusion time is affected by the properties of the surfactants.[25] For a droplet to be stable it takes about several miliseconds.[51] Therefore, it is of crucial importance that surfactant molecules must populate the entire droplet interface within miliseconds. For biochemical assays in droplets, surfactants must be bio-inert to avoid any interference with the biomolecules or cellular functions.[30, 52] Moreover, for a long-term droplet stability, surfactant molecules must also provide a robust droplet interface. Hence, commercially available long chain perfluoropolyethers (PFPEs) are more useful than the short chain fluorotelomers with chain length below ~ C_{10}.[30] Also, the high molecular weight PFPEs are available with carboxylic acid groups, making them readily interact with the oppositely charged molecules.[53] Due to the ionic interactions, the organic molecules from the aqueous phase can migrate easily into the continuous fluorous oil phase, reducing the compartmentalization efficiency and making the miniaturization process questionable.[1] Moreover, biomolecules such as proteins may lose their native structures or functions through the ionic interactions between surfactant and protein molecules.[54] Therefore, to ensure fast enough surfactant diffusion to the droplet interface, to achieve a long-term emulsion stability, and to provdie a non-ionic droplet interface, the poly(ethylene glycol) (PEG) coupled PFPEs have been reported (Figure 7).[30] A wide variety of molecular weights of PEG, including the oligomeric PEG, is commercially available. PEG-based surfactants have been exploited to design fluorosurfactants with different morphologies. However, only a tri-block copolymer fluorosurfactant comprised of PEG600

and a high molecular weight PFPE of 6000 g mol^{-1} was found to be the most effective one, which is the only commercially available fluorosurfactant for droplet microfluidics until now.[30, 55] In addition to PEG600, poly(propylene oxide) (PPO)- and PEG-based di- and tri-block copolymers, Jeffamine®M and Jeffamine®ED derivatives, respectively, were also used as polar parts to design a multi-block copolymer fluorosurfactants for droplet microfluidics, but these fluorosurfactants are not commercially available, and lack robustness and efficiency for challenging applications.[1, 56]
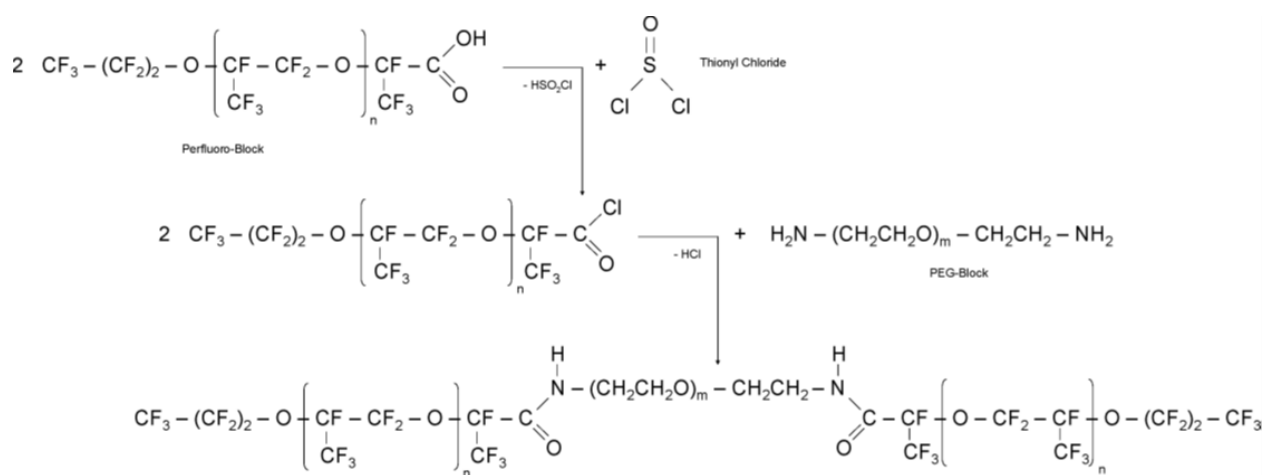
Figure 7. Scheme showing the synthesis of a tri-block copolymer fluorosurfactant comprising PEG and PFPE. Adopted with the permission from ref.[30] Copyright 2008 The Royal Society of Chemistry.

1.3.2   *Miscellaneous polar head-based di- and tri-block surfactants*

Although PEG is widely considered to be biologically inert, some studies show that it is actually not a fully bio-inert macromolecule, because PEG has hydrophobic characterisitcs that affect the bioactivity of certain proteins.[57] Therefore, for a droplet-based biological affinity assays that rely on hydrophobic interactions between proteins, PEG-based surfactants may not be the best choice to compartmentalize the biomolecules. Consequently, alternative polar head groups have been explored to create di- and tri-block fluorosurfactants in combination with short and/or long chain fluorinated tails (Figure 8).[50, 58-59]
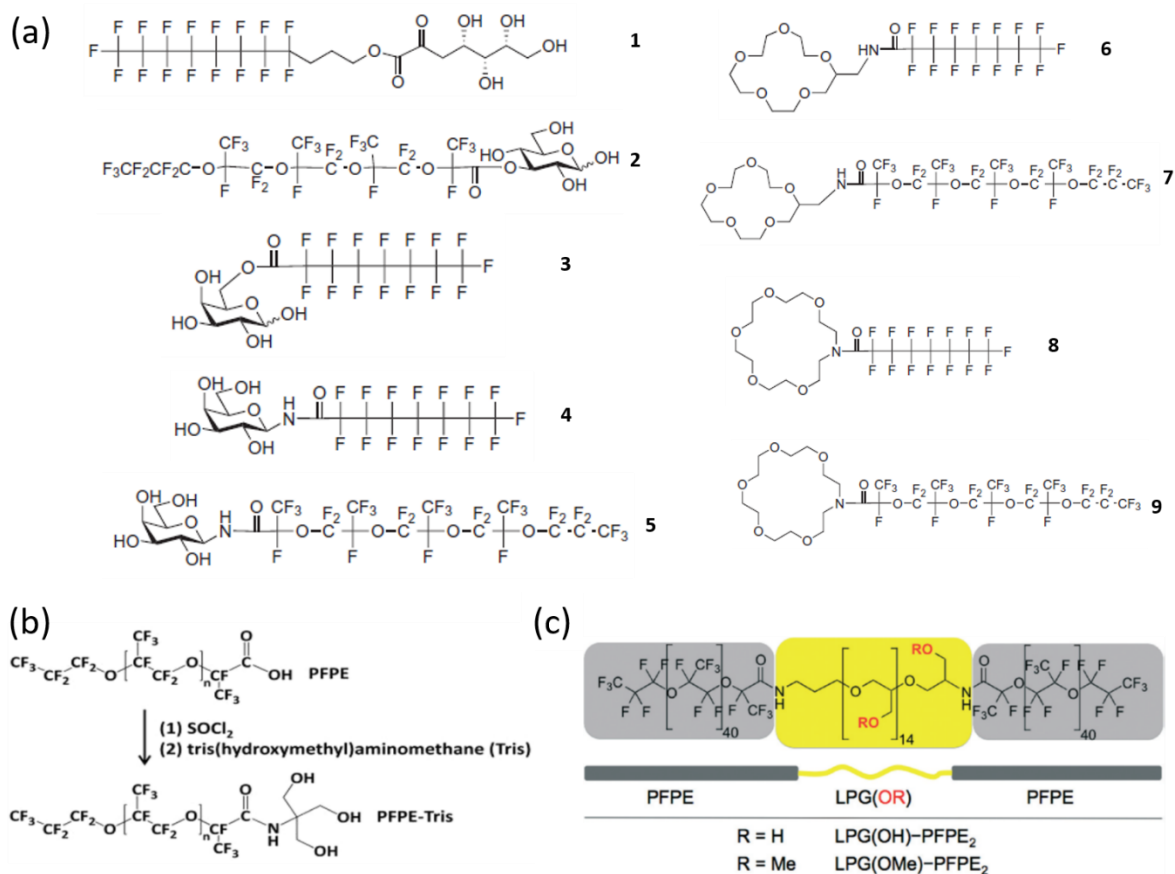
Figure 8. Fluorosurfactants with a variety of polar head groups. Reused with the permission from ref.[50, 58-59] Copyright 2010 Elsevier Inc. Copyright 2014 American Chemical Society. Copyright 2015 The Royal Society of Chemistry.

Holt *et al.* reported fluorosurfactants with four hydroxy groups containing linear and cyclic carbohydrate head groups, and they compared the performance of these surfactants with linear and cyclic penta- and hexaethylene glycol-based fluorosurfactants (Figure 8a).[58] Surprisingly, although the carbohydrate groups were more polar than the ethylene glycol oligomers, the carbohydrate-based surfactants were the worst performer of all.[58] However, when cyclic crown ethers were compared with their linear counterparts, the linear ethylene glycol oligomers showed better performance. Chiu *et al.* documented fluorosurfactant with tris head groups that had three hydroxy groups (Figure 8b).[50] They showed that the tris-based surfactants could make w/o/w double emulsion droplets while encapsulating mammlian cells in them.[50] While short-term incubation of the single emulsions loaded with bacterial cells showed good performance, long-term incubation of the double emulsions loaded with mammalian cells revealed polydisperse droplet size distributions.[50] Moreover, they did not show any data regarding release of the cultured cells from the inner droplets of the double emulsions. In

another study, to mimic the length and geometry of the most effective PEG600-based tri-block copolymer fluorosurfactants, Wagner *et al.* reported a linear polyglycerol-based tri-block copolymer fluorosurfactants with ~14 repeating units all having either hydroxy or methoxy pendent groups (Figure 8c).[59] Interestingly, the methoxy-containing surfactant was more robust than the highly polar hydroxy-containing surfactant.

In sum, the limited library of non-ionic fluorosurfactants with different polar head groups suggests that the performance of fluorosurfactants for droplet microfluidics is highly influenced by the geometry and type of the polar groups rather than the highly polar nature of the hydrophilic head groups. Therefore, novel polar head groups are needed to design fluorosurfactants and investigate their performance under stringent test conditions to reveal more about the structure-property relationships.

1.3.3 *Micro-capsule and/or Microgel templating*

Emulsion droplets prepared by PDMS-based droplet microfluidics benefit from the incredible control over the droplet size distribution. In this regard, fluorosurfactants play a major role to give stability to the generated droplets by preventing undesired coalescence, which makes the monodisperse droplets highly useful for quantitative assay design.

In the field of bioinformatics, there is a need to quantitatively map gene expression at the single-cell resolution which is the quantum limit of molecular biology to identify cell-to-cell heterogeneity.[55] Since a single cell can release ~500,000 mRNA, it is crucial to capture all of these to collect high value bioinformation.[60] By capitalizing on monodispersity and high stability of the emulsion droplets, Weitz and coworkers reported an elegant approach to generate primer functionalized monodisperse microgel beads for barcoding transcriptomes at the single-cell level (Figure 9a).[55] They showed that acrylamide monomers, initiators, and primer molecules with reactive functional groups for amide coupling all were co-encapsulated into droplets. The droplets were then incubated off-chip under a suitable reaction conditions to synthesize barcoded poly(acrylamide) microgels. Moreover, it was shown that following a washing step, the emulsion droplets could be broken to release the barcoded microgels that were further used for splitting and pooling to geometrically increase the barcode libraries (Figure 9b). Finally, they showed co-encapsulation of single-barcodes, single-cells, and cell-lysis buffer for a quantitative single-cell transcriptome analysis (Figure 9c).
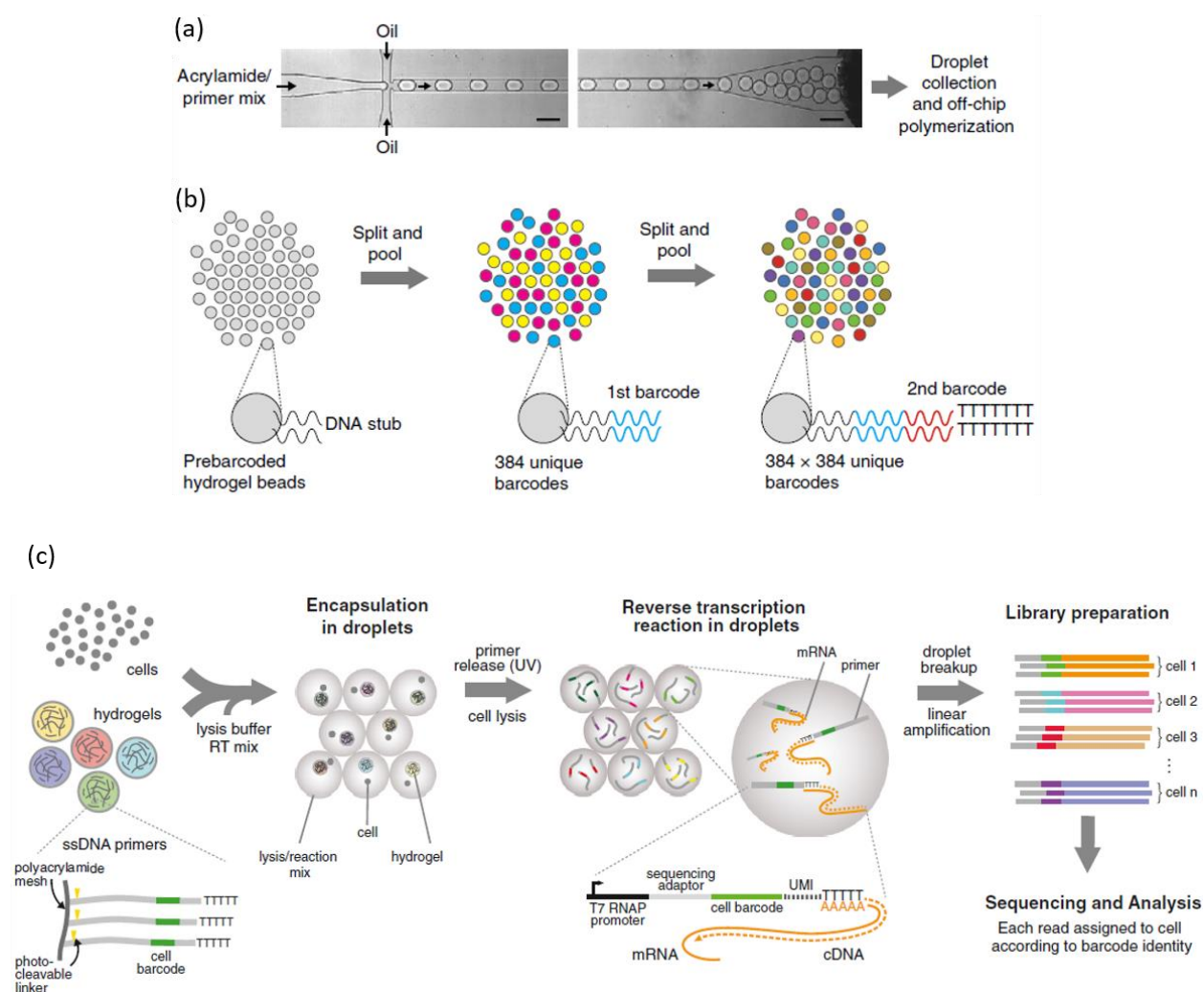
Figure 9. Fabrication of acrylamide-based microgle particles functionalized with primers for barcoding single-cell transcriptome. (a) Quantitative encapsulation of primers and acrylamide monomers with initiators for monodisperse functional microgel particle preparation. (b) Scheme showing the 'split-and-pool' approach to increase barcode diversity on microgel particles. (c) Co-encapsulation of single-cells, single-barcodes, and cell-lysis buffer into droplets. Primers from the microgels are released by photo-cleavage while cells are being lysed. Finally, cDNA is synthesized followed by PCR amplification and library preparation for single-cell sequencing. Reprinted with the permission from refs.[55, 61] Copyright 2016 Springer Nature (a-b). Copyright 2015 Elsevier Inc. (c).

If proper chemistry is applied, microgel particles can also be adaptible for many different applications, including emulsion polymerase chain reaction (ePCR), microgels delivery to different body organs (Figure 10).[62-63] They can be used as a single microgels, mixed with microgels comprised of different polymer compositions, or applied to bulk hydrogels to make composite materials.[63] Furthermore, for biomedical applications, microgels

can be interlinked to tune their mechanical properties and exterior porosity that have been proven to be crucial for cell-to-cell communications, cell proliferation, cell migration, and vascularization to engineer thicker tissues.[63] Besides, monodisperse thin-shell micro-capsules have been reported for therapeutic delivery of cells. Using PDMS-based droplet microfluidics platform, Mooney and coworkers have documented single-cell encapsulation into thin alginate microgels that were used to control both *in vitro* and *in vivo* cellular microenvironments.[64]
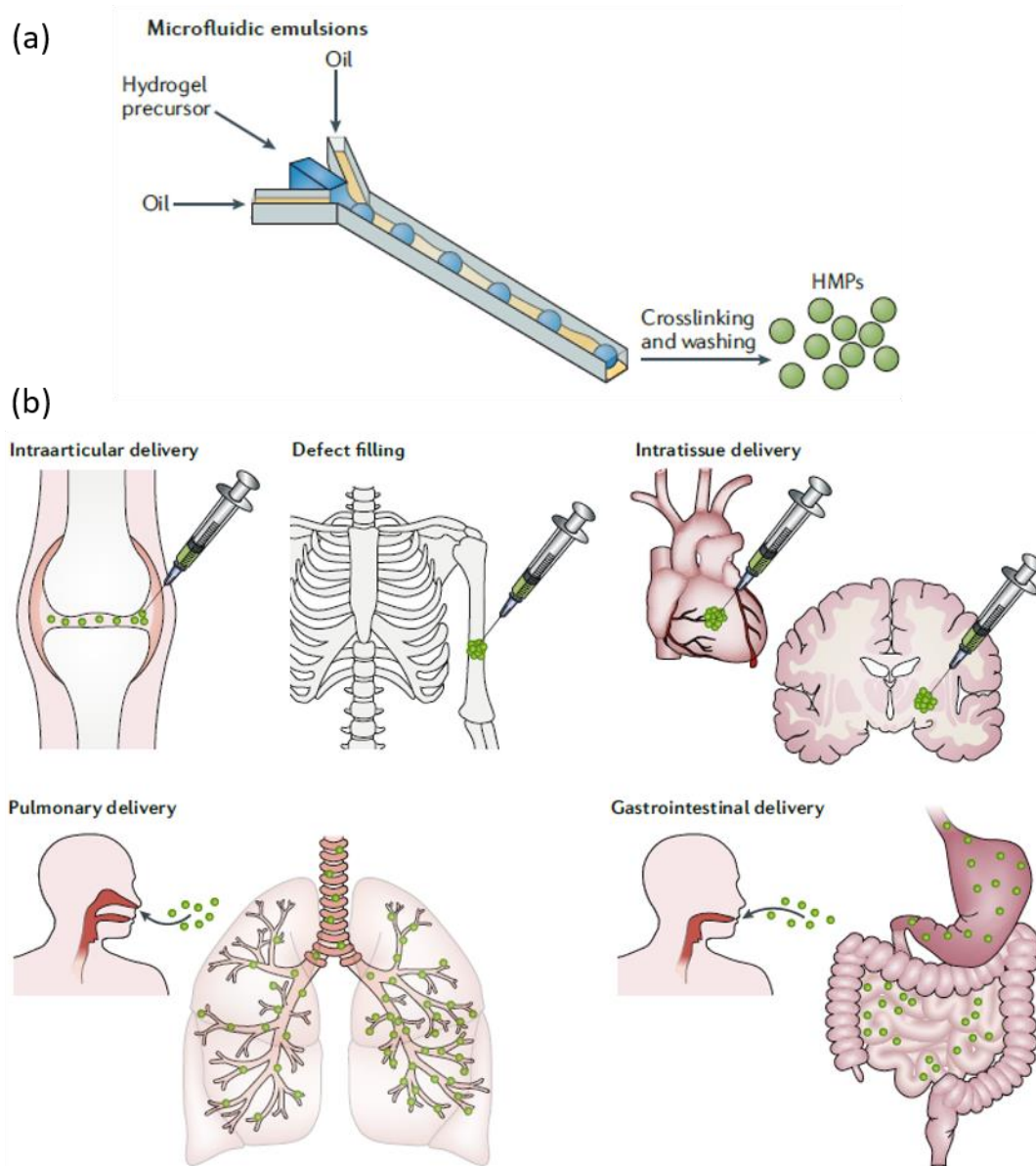
Figure 10. Preparation of microgels emulsions and their potential uses in biomedical fields. (a) General scheme illustrating encapsulation of precursors into micro-droplet for hydrogel microparticles (HMPs) fabrication. (b) Potential delivery of microgels with or without bio-cargos to different tissues in the human body. Reused with the permission from ref.[63] Copyright 2019 Springer Nature.

Undoubtedly, the potential of microfluidic emulsions-based microgels is enormous. Using a PDMS device, emulsion droplets can be made at 1-10 kHz rates with typical flow rates on the order of 1 mL h^{-1}, which can satisfy industrial level production volume ~1000 tons per year if massive parallelization of droplet-making channels is employed.[65] But, the key bottleneck of this technology platform is the efficient removal of fluorosurfactants after emulsion generation irrespective of the emulsion volumes. Therefore, a rational fluorosurfactant design is inevitable to address this issue and exploit the potential of microfluidic emulsions with an industrial potential.

1.3.4 Droplet-PCR

Today, the most successful commercial application of fluorosurfactants is droplet-PCR, generating almost $1 billion revenue for biotech industries. Unlike bulk emulsions, fluorosurfactants-stabilized microfluidic emulsions offer numerous possibilities to manipulate micro-droplets, including merging, splitting, re-loading, identifying, and sorting of droplets, all at kHz speeds.[4, 16] Furthermore, monodisperse emulsion droplets have been very attractive for droplet-PCR application. It is worth mentioning that without PCR the field of molecular biology is unthinkable and the advent of droplet-PCR has further enabled molecular biologists to reach the quantum limit of molecular biology that allows analyses of thousands of single DNA molecules in parallel at an ultrahigh-throughput manner using tiny amount of reagents, where only a few microliters of reagent is typically sufficient for analysis.[62, 66] Unlike typical PCR, droplet PCR (dPCR) allows miniaturization of single copy DNA into droplet that is amplified to multiple copies without competing with the amplicons carrying different genetic information. Thus, unlike calibration curve dependent analyses of PCR amplification products, after PCR, it is possible to digitally quantify a rare event in cell biology by analyzing each single drop that further helps to detect, for example, cancer cells carrying new mutation in their genome.[62, 67] Using dPCR, Pekin et al. demonstrated detection and quantification of a KRAS gene, a mutated biomarker for cancer cells, in genomic DNA in presence of a large excess of unmutated KRAS genes, where techniques for example dual probe TaqMan® assays fail when the target mutant's abundancy is less than ~1% in a sample of non-mutated amplicon.[67]

However, emulsion droplets containing PCR reagents are highly sensitive to high temperature PCR and a significant portion of them often coalesce after thermal cycling, questioning the single drop resolution data quality. Lan et al. reported significant coalescence of droplets of >50 µm diameter during PCR thermocycling even though a high concentration

of fluorosurfactant (5% w/w) was employed before thermocycling (Figure 11).[68] To remove the coalesced droplets, it is possible to use a filter in the microfluidic channel or, alternatively, a fractionation microfluidic device, but then a significant number of droplets wil be lost, which may contain the target information, forcing to trade-off with the efficiency and yield of the droplet-based assays.[68-69] By using excess of surfactant, although the droplet stability can be improved to some degree, it does not prevent the coalescence to satisfaction, but it adds extra cost for the assays.[70] Moreover, commercial surfactants often display batch to batch variations, yet they are highly expensive.[71] Also, if it is intended to use home-made PEG-based tri-block compolymer surfactants, the polydisperse nature of surfactant precursors becomes the limiting factor in synthesizing a highly pure fluorosurfactant. Besides, it is highly unlikely that all the molecular biology labs will have facility and expertise to synthesize surfactants. Hence, there is a need to synthesize fluorosurfactants that are readily available, biocompatible and robust, and that can address all the above mentioned issues arising during droplet PCR.
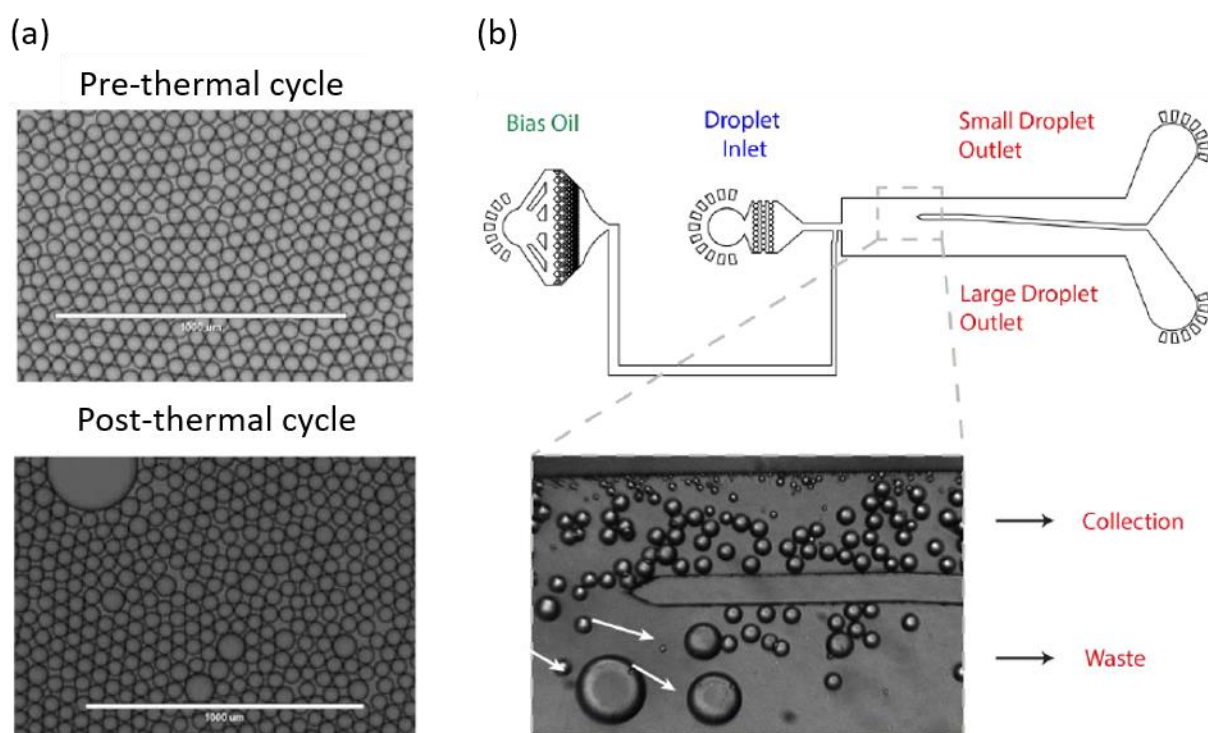

Figure 11. Micrographs showing pre- and post-PCR stability of the droplets (a) and filtration of the coalesced droplets using a fractionation microfluidic device (b). Reprinted from ref.[68]

1.3.5 Drug-screening

Prior to *in vivo* studies, screening of drug cytotoxiciy *in vitro* is one of the key steps in the process of drug development. This presents an opportunity to use pico- to nanoliter volume micro-droplets that can co-encapsulate single cells, drugs, and a wide variety of reagents to create a *in vivo* mimetic three-dimensional (3D) environment. Consequently, droplet-based drug screening has become an attractive cutting-edge platform technology that not only reduces the reagent consumption but also allows manipulation of cell-loaded droplets at the kHz rates.[4] Agresti *et al.* showed that a droplet-based screening platform can be several-million-fold cost-effective and 1000-fold time-saving compared to a robotic system.[72] Using the droplet microfluidics-based approach, Sarkar *et al.* evaluated activities of single drug-resistant cells, such as drug uptake dynamic and cytotoxicity in the presence of drug Doxorubicin (Dox).[73] They reported that the uptake of Dox by drug-sensitive cells was heterogeneous while it was uniformly low in case of drug-resistant tumor cells. Besides, they co-cultured both cell types in droplets and found a homotypic fusion between the cells led to high cell survival. It is of great concern that not just the cancer cells but also bacteria can readily acquire single drug resistance that necessitates trying multi-drug treatment to synergistically perturb different cell signalling pathways or other modes of cellular actions, and to provide a highly benefical therapy to the patients.[73-74] But, the screening of FDA approved drugs in several combinations will be a massive task that can benefit from droplet microfluidics-based high-throughput screening platform.[75] However, using emulsion droplets, although screening of one drug at a time for cytotoxicity test is feasible, screening multiple drugs or many combinations of drugs in parallel becomes irrational because droplets suffers from inter-droplet molecular leakage issue, which reduces the assay quality and makes the combinatorial drug discovery process inefficient under droplet microfluidics platform.[71] To study the inter-droplet leakage kinetics, Gruner *et al.* used less-leaky and more-leaky dyes as model compounds.[1] They showed that a less-leaky dye migrates from drop to drop at the time-scale of hours, whereas the migration occurs within minutes with a more-leaky dye (Figure 11). They proposed that both polarity of the cargo and surfactant, that is used to stabilize the emulsion droplets, play a crucial role to dictate the inter-droplet molecular transport. Hence, to capitalize the full potential of droplet-based screening platform, novel fluorosurfactants are needed that will address the inter-droplet leakage issue and make each independent micro-droplet to be truly functional equivalent of a chemist's reaction flask or a well on a microtiter plate that is free from cross-contamination.
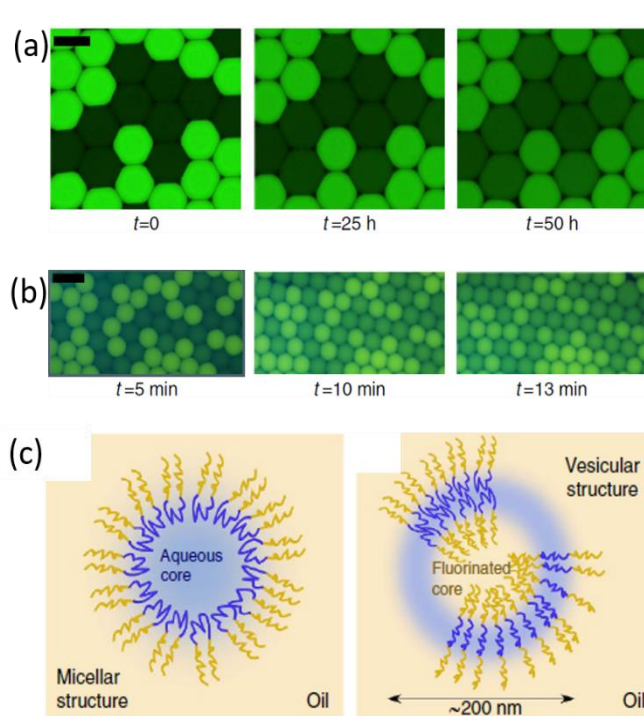
Figure 12. Micrographs showing inter-droplet cross-contamination and self-assembly of fluorosurfactants. A PFPE-PEG-PFPE surfactant in HFE7500 oil was used to stabilize the emulsion droplets and study the inter-droplet molecular transport phenomena. (a) Molecular transport of less-leaky fluorescein occurs over hours. (b) Molecular transport of more-leaky rhodamine 6G occurs over minutes. (c) The tri-block copolymer surfactant molecules assemble in HFE7500 oil to form not only a micellar shape but also a vesicular structure. The vesicular structure is attributed to be one of the reasons that allows inter-droplet excahnge of small molecules to readily occur. Reprinted from ref.[1]

1.3.6 Functional assay

Fluorosurfactants serve not just the primary purpose of stabilizing the emulsion droplets, they can do more. If a single-cell-based enzyme catalysis assay in micro-droplets is designed, to gain access to over-expressed enzymes inside the cell, it is often needed to lyse the cell that will release the enzymes from the cellular compartments and allow them to hydrolyze a fluorogenic substrate inside the droplets to yield a fluorescence signal for an optical read-out.[76] Based on the optical read-out, the active droplets where the enzymatic reaction took place can then be isolated to extract the complete genetic information of the cells. Thus, a high-throughput screening of a large mutant library for enzyme catalysis can be performed.[72] The cell lysis is often carried out using a cell-lysis buffer.[76] However, it has been shown that fluorosurfactants with ammonium salt or poly-L-lysine head groups can effectively lyse the encapsulated cells, showing the versatile usage of a surfactant.[77] It is worth mentioning that the cells were seeded on fluorosurfactant solution instead of encapsulating them into droplets. In another study, Platzman *et al.* demonstrated that a fluorosurfactant can also be functionalized with gold nanoparticles to capture thiol-containing biomolecules.[78] They showed that droplets stabilized with the functional surfactants could create articficial antigen-presenting cell (APC) analogues to selectively interact with T-cells allowing them to expand inside the droplets. However, the gold nanoparticle coupled surfactant was not robust enough to stabilize the droplets and maintain the monodispersity, which shrinks the possibility to establish a

quantitative assay for T-cell induction and expansion in micro-droplets (Figure 13). Therefore, unlike a pre-functionalized surfactant, a fluorosurfactant that can be functionalized in situ with biomolecules from the aqueous droplets is needed that might be more effective to keep maintain the monodispersity of the droplets, and take advantage of droplet-based quantitative assay design.
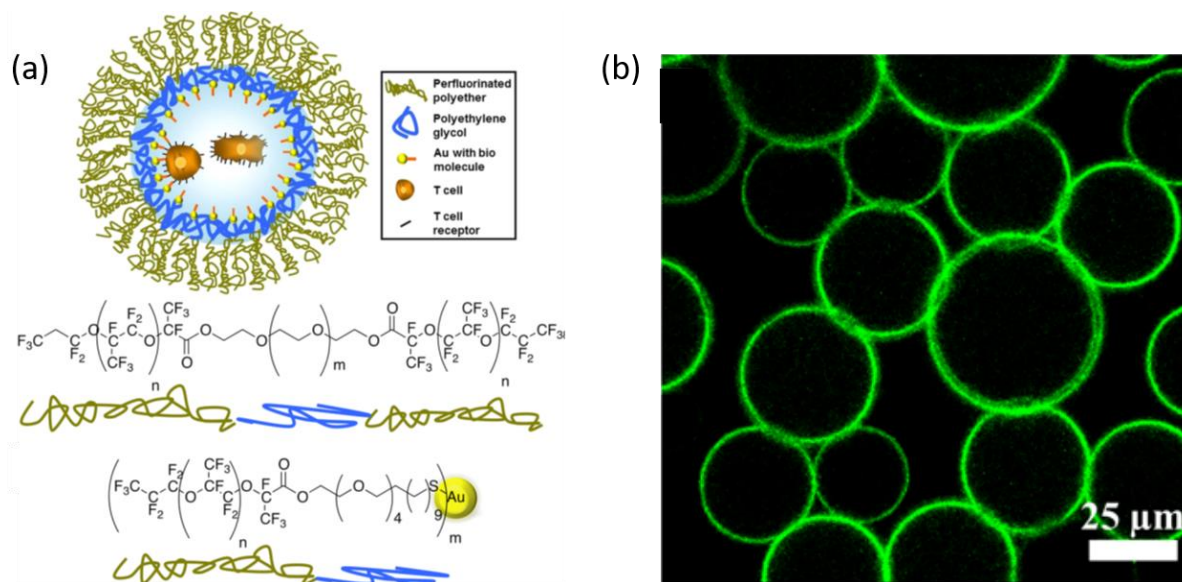
Figure 13. (a) Scheme showing antigen-presenting cell (APC) mimetic 3D micro-environment created by the gold-functionalized surfactants. (b) Micrographs showing stability and polydispersity of the droplets stabilized with GFP-linked functional surfactants. Reused from ref.[78]

1.4 Glycerol and thioglycerol building blocks

1.4.1 *Linear, dendritic, and cyclic oligoglycerols*

Glycerol oligomers are a class of precursor molecules with multiple hydroxy groups that can be readily tuned to design linear, dendritic, and cyclic architectures (Figure 14).[48, 79-81] Moreover, they can be used to make high molecular weight polymers through polymerization or polycondensation reactions.[82]
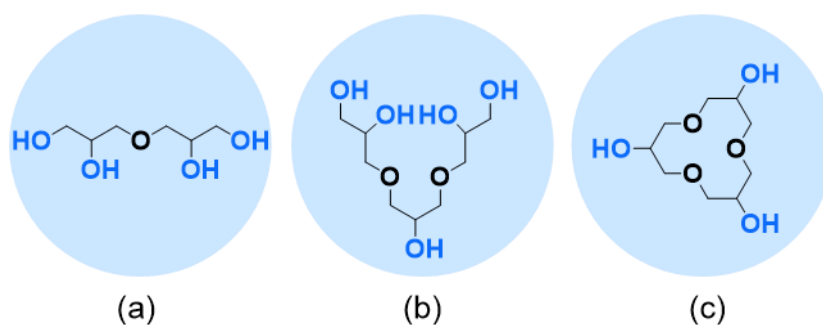
Figure 14. Oligoglycerols with different architechtures: linear oligoglycerol (a), dendritic oligoglycerol (b), and cyclic oligoglycerol (c). Reused from refs.[80, 82-83] Copyright 2020 Wiley-VCH, Weinheim (b). Copyright 2012 The Japan Institute of Heterocyclic Chemistry (c).

These ether-based oligoglycerols with different lengths, geometries, and degree of branching have been proven to be bioinert. These properties have successfully been exploited to design detergents for protein extraction, food-grade and biocompatible emulsifiers for w/o emulsions, and coating materials for anti-fouling surfaces.[48, 83-87] Additionally, oligoglycerols which are highly polar compounds were conjugated to proteins that demonstrated increased bioavailability and therapeutic efficacy of the proteins.[86]

To get access to different architectures of oligoglycerols, different synthetic strategies can be used, including chemo-enzymatic synthesis, Williamson ether synthesis, anionic ring-opening of epoxide.[82, 85, 88] If linear oligoglycerols with different lengths are desired, they can be achieved by changing the number of glycerol units. Linear oligoglycerols can be synthesized following these steps: first, protection of primary hydroxy groups in glycerols by acetylation; second, protection of secondary hydroxy groups by benzoylation; third, the deprotection of primary hydroxy groups and subsequent etherification to grow the number of glycerol repeating units.[82] If dentritic oligoglycerols of different generations are desired, then, both convergent and divergent methods can be employed to prepare them using solketal, methallyl dichloride, and epichlorohydrin as the precursors.[48, 79, 88-89] Similarly, different regioisomers of oligoglycerol dendrons can also be synthesized to exploit them under different circumstances where structure-activity relationship is crucial.[48-49]

1.4.2   *Features and advantages of oligoglycerols*

Oligoglycerols benefit from easily-sourced precursors, facile chemistry, and large-scale one-pot synthesis, and are thus highly attractive for industrial applications.[79, 88] They present a high degree of flexibility to tune their hydroxy functionality with a wide variety of reactive and functional groups, including clickable azide, clickable alkene, nucleophilic amine, negatively

charged sulfate.[80, 85, 90-91] Moreover, the presence of chiral centers in the precursors of oligoglycerols provides a powerful source to design many unique spatial architectures of glycerol oligomers that can be easily exploited in the field of supramolecular chemistry.[92] It is even more rewarding to have 1,2-diols at the terminus or at the branches of the oligoglycerol, which can be readily oxdized to form selectively either a ketone by boronic acid catalyst or an aldehyde by sodium metaperiodate, and thus present a new platform for a cytocompatible hydrazone- or oxime-based reversible chemistry for different applications, including protein bioconjugations, cross-linked macromolecular network.[80, 93-95] The 1,2-diols can also be used with a boronic acid precursor to create a boronic ester-based dynamic covalent chemistry for controlled drug delivery applications, for instance (Figure 15 a).[96-98] Besides, capitalizing on the selective chemistries available for primary and secondary hydroxy groups, Mittal *et al.* demonstrated that the glycerol oligomers can be functionalized with different compounds through both esterification and etherification (Figure 15 b).[99]
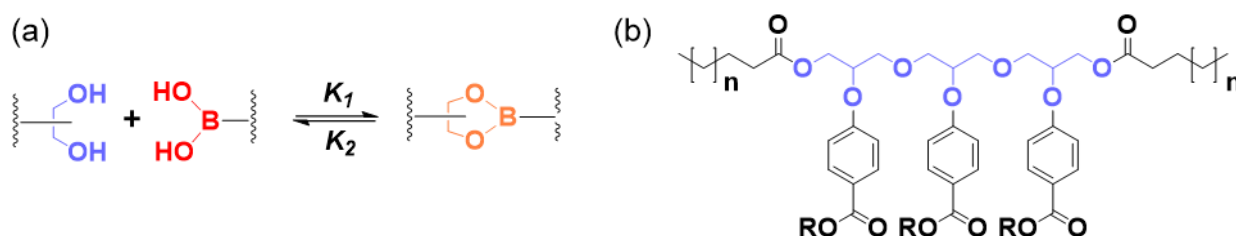
Figure 15. Schemes showing multifunctionality of primary vs. secondary hydroxy groups and 1,2-diols. (a) 1,2-diols participate in dynamic boronic ester formation. (b) The primary and secondary hydroxy groups are selectively coupled to different chemical moieties. Reprinted from refs.[98-99]

1.4.3   Features and advantages of thioglycerol

Like glycerol oligomers, thioglycerol can also benefit from its 1,2-diols for a wide range of chemistry discussed above. Additionally, the presence of a thiol group in thioglycerol makes it attractive not just for facial thiol-ene or thiol-yne click chemistry but also for designing thioether-based oxidation responsive materials.[45, 100-104] Since thiol-yne chemistry allows two thiols to react with one alkyne, using thioglycerol, a multi-functional chemical structure can be easily synthesized under mild reaction conditions.[102] Using thiol-yne click reaction, Chen *et al.* demonstrated a polyhydroxy-containing third generation (G3) dendrimer with 192 hydroxy groups, in which, starting with 12 hydroxy groups in the first generation, the number of hydroxy groups quadrupled in every next generation (Figure 16).[104] Also, thioglycerol due to its thiol functional group can potentially participate in thiol-Michael addition reaction under

physiological conditions to fabricate new materials and/or to improve aqueous solubility of the materials. Besides, thioglycerol has found its application in cell culture medium to improve the activation and proliferation of lymphocytes, justifying its biocompatibility.[105]
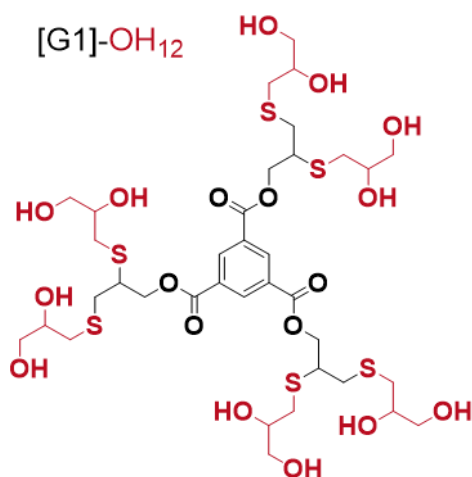
Figure 16. Chemical structure showing thioglycerol-based first generation dendrimer with 12 hydroxy groups. Reprinted with the permission from ref.[104] Copyright 2009 The Royal Society of Chemistry.

2 Scientific Goals

PDMS-based droplet microfluidics have expanded the landscape of bioanalytics and biomaterials design in pico- to nanoliter volume microdroplets. Here, fluorosurfactants play a crucial role by stabilizing these microdroplets. But the main limitations of the current PEG-based gold standard fluorosurfactant are the following: (i) it cannot make droplets that are robust for high temperature treatment; (ii) it cannot make droplets that are safe from cross-contamination; and (iii) it cannot make droplets that are multi-functional. Thus, commercially available gold standard PEG-based fluorosurfactant cannot be used in high-performance biochemical assays. The poor performance of the commercial surfactant is primarily attributed to its PEG-based head group and its linear tri-block geometry. Unlike PEG, oligoglycerols are promising candidates as polar head groups due to their multifunctional presentation of hydroxyl groups which make them highly water soluble, biocompatible, readily customizable, and capable to create intra- and intermolecular hydrogen bonds. Moreover, glycerol oligomers can provide interesting geometries with exquisitely precise length, degree of branching, and number of hydroxyl groups, making them attractive for a wide variety of potential applications.

To find a high-performance fluorosurfactant, the main aim of this thesis was to design, synthesize, and characterize fluorosurfactants comprising perfluoropolyethers (PFPEs) of different chain lengths and oligoglycerols with variable geometry, length, backbone (ether, thioether), functionality, and/or number of hydroxy groups.

In the first project, dendritic oligoglycerols with two and four hydroxy groups will be used as polar head groups to design a series of non-ionic fluorosurfactants with PFPE tails of low, medium, and high chain lengths. As discussed, when emulsion droplets are created by droplet microfluidics, fluorosurfactants dissolved in fluorous oil populate the entire oil-water interface and thus dictate the droplet stability by preventing their coalescence. So first, the novel non-ionic surfactants will be employed in PDMS-based droplet microfluidics to investigate their ability to make stable water-in-fluorinated oil (w/o) emulsion droplets. Oligoglycerols are highly polar because of the presence of multiple hydroxyl groups. Furthermore, they are a great source of multiple hydrogen bond donors and acceptors. Therefore, to reveal the effect of high polarity and hydrogen bond networks of the head groups on droplet stability at high temperature, and to evaluate the biocompatibility of the surfactants, reagents for polymerase chain reaction (PCR) will be encapsulated into the droplets, which will then be subjected to a high temperature treatment for PCR reactions. The stability of the pre-PCR and post-PCR

droplets will be analyzed. The inertness of the surfactants with the PCR reactions will be evaluated based on the success of the PCR reactions in the droplets. Because a high degree of hydrogen bonds will be present at the droplet interface, the surfactants should not allow any small molecules to leak out from the droplets. Therefore, inter-droplet leakage kinetics of a fluorescent probe will be monitored over several days. The surfactants shall also be tested to assess their suitability to stabilize viscous droplets bearing polymer precursors for gelation. Finally, the surfactants will be tested to investigate their biocompatibility with mammalian cells.

Polar head groups having different spatial geometry with same molecular weight can function differently, and they can give insights into a complex structure-property relationship. Therefore, in the second project, the facile access to glycerol oligomers with different spatial architectures (linear and dendritic), will be utilized for the synthesis of fluorosurfactants comprising linear and dendritic oligoglycerols with three to four hydroxy groups and a common PFPE of low chain length. In addition, their polarity indexes and interfacial tension values will be evaluated to learn how surface activity can be controlled by the polarity of the surfactants or, alternatively, by the geometry of the polar head groups. Furthermore, the long-term cargo retention capability of the microfluidic droplets stabilized by the fluorosurfactants with different geometry shall be investigated to understand effect of geometry or architecture of head groups. Typically, PEG-based gold standard surfactant cannot be post-modified due to the lack of functional groups. So, it is crucial to reveal whether the multifunctional oligoglycerol-based surfactants can be easily post-modified with high purity and yield. The post-functionalized surfactant shall also be tested to evaluate its capability to make robust and monodisperse droplets and for creating a reactive droplet interface. Therefore, a linear triglycerol-based surfactant will be post-modified with a clickable azide moiety by facile esterification. The functional surfactant will then be used to make droplets and covalently fish alkyne-bearing biomolecule complexes from the droplets via efficient strain promoted azide-alkyne cycloaddition (SPAAC) reaction.

Ether-based oligoglycerols are not responsive to eternal stimuli such as pH, reactive oxygen species, and enzymes. Therefore, stimuli responsive thioether-based oligoglycerols will be synthesized as a novel class of polar headgroups for the development of fluorosurfactants. Besides, the beauty of a thioether compound is its selectivity towards oxidation. Thus, capitalizing on the selectivity, either a sulfoxide or a sulfone can be generated which can dramatically increase the polarity of the thioether-based oligoglycerols. Hence, to design a highly water soluble fluorosurfactant without introducing any charged group, thioether-based

oligoglycerol can be used as it will allow the surfactant to preserve its non-ionic character, yet it will provide high water solubility after oxidation of the backbone thio-ethers.

Therefore, in the third project, a novel fluorosurfactant comprising a thio-ether-based acetal protected triglycerol and a low chain length PFPE will be synthesized and characterized. The acetal protected surfactant will then be oxidized with either sodium periodate or meta-chloroperoxybenzoic acid (mCPBA) to create either a sulfoxide or a sulfone derivative of the surfactant, respectively. Subsequently, the acetals will be deprotected to have 1,2 hydroxy functionalized fluorosurfactants containing thio-ether, sulfoxide, and sulfone groups in the dendritic head groups. Furthermore, the presence of polar functional groups like sulfone and sulfoxide, unlike ether or thioether, will encourage further to oxidize the cis-1,2-diols to generate a reactive aldehyde functionality bearing fluorosurfactant. Therefore, five surfactants with different functionalities will be synthesized from just one parent surfactant. All of them will be tested under droplet microfluidics condition for investigating following properties such as stabilizing w/o emulsion droplets, making reactive droplet interface to covalently fish alkyne-bearing biomolecule complexes from the droplets via efficient SPAAC reaction, and/or participating in dynamic covalent chemistry. Besides, they shall be used to stabilize drug-responsive single-cell loaded droplets with a view to understanding their biocompatibility with gene expression of the cells in presence of the drug doxycycline.

3 Publications and Manuscripts

In the following section, the scientific outcomes of this PhD thesis are listed, and the contributions of the authors are specified.

3.1 Dendronized fluorosurfactant for highly stable water-in-fluorinated oil emulsions with minimal inter-droplet transfer of small molecules

M. S. Chowdhury, W. Zheng, S. Kumari, J. Heyman, X. Zhang, P. Dey, D. A. Weitz, R. Haag

Author's contributions: In this publication the author contributed to the concept and design, and performed all the synthesis, most of the characterization, and data evaluation, as well as wrote the draft of the manuscript.

Dendronized fluorosurfactant for highly stable water-in-fluorinated oil emulsions with minimal inter-droplet transfer of small molecules

Mohammad Suman Chowdhury [1], Wenshan Zheng[2], Shalini Kumari[1], John Heyman [3], Xingcai Zhang [3], Pradip Dey [1], David A. Weitz[3]* & Rainer Haag [1]*

Fluorosurfactant-stabilized microfluidic droplets are widely used as pico- to nanoliter volume reactors in chemistry and biology. However, current surfactants cannot completely prevent inter-droplet transfer of small organic molecules encapsulated or produced inside the droplets. In addition, the microdroplets typically coalesce at temperatures higher than 80 °C. Therefore, the use of droplet-based platforms for ultrahigh-throughput combination drug screening and polymerase chain reaction (PCR)-based rare mutation detection has been limited. Here, we provide insights into designing surfactants that form robust microdroplets with improved stability and resistance to inter-droplet transfer. We used a panel of dendritic oligo-glycerol-based surfactants to demonstrate that a high degree of inter- and intramolecular hydrogen bonding, as well as the dendritic architecture, contribute to high droplet stability in PCR thermal cycling and minimize inter-droplet transfer of the water-soluble fluorescent dye sodium fluorescein salt and the drug doxycycline.

[1] Institut für Chemie und Biochemie, Freie Universität Berlin, Takustrasse 3, 14195 Berlin, Germany. [2] Department of Chemistry and Chemical Biology, Harvard University, Cambridge, MA 02138, USA. [3] School of Engineering and Applied Sciences, Department of Physics, Harvard University, 29 Oxford Street, Cambridge, MA 02138, USA. *email: weitz@seas.harvard.edu; haag@chemie.fu-berlin.de

26

Fluorosurfactant-stabilized, water-in-fluorinated-oil (w/o) droplets, with volumes of pico- to nanoliters, have facilitated a variety of powerful research techniques. Emulsions made with fluorosurfactant-containing fluorinated oil have been shown to be biologically inert and, due to fluorinated oil's capacity for dissolved oxygen, are suitable for cell culture. Accordingly, these emulsions have been exploited for numerous biological applications, including rapid parallel transcriptome profiling of thousands of cells with single-cell resolution[1,2], high-throughput drug screening[3–5], analysis of products secreted by individual cells[6], directed evolution of desired enzymes[7,8], and construction of synthetic cells[9]. Additionally, emulsion droplets are easily generated with highly monodisperse and reproducible droplet size, making them suitable to study different aspects of physics and chemistry[10–14]. These tiny reaction chambers are created, analyzed, and sorted at kHz rates, typically using poly-dimethylsiloxane (PDMS) microfluidic devices[4]. However, small organic molecules can exchange between adjacent droplets[4,12], limiting their utility for high-throughput screening applications. In addition, droplets are often unstable during thermal cycling, reducing reliability of the polymerase chain reaction, (PCR)[4,15], which is an extremely efficient method for nucleic acid amplification and is a critical step in most genetic analyses. The poor droplet integrity is often caused by the nature and type of the fluorosurfactant used to stabilize the droplet.

The non-ionic tri-block copolymer fluorosurfactant, PEG-PFPE$_2$ (EA surfactant from RAN Biotechnologies), made of poly (ethylene glycol) and perfluoropolyethers (PFPE), is widely used to stabilize the emulsion droplets within fluorinated oil[1,6,11,16,17]. However, during thermal cycling (PCR), a significant number of droplets merge. In addition, small molecules (~200 to ~500 Dalton) can easily pass between droplets[12,15]. The poor performance of PEG-PFPE$_2$ surfactant can partially be attributed to its synthesis limitations and to its structure. PEG molecules are also somewhat hydrophobic[18] and thermo-responsive[19–21], which can influence biological assays[18,20] and destabilize droplets that are subjected to temperature change, e.g., during PCR. In addition, due to the polydisperse nature of both PEG and PFPE, the exact molar amount of each molecule cannot be determined and the ratio of the molecules (1:2, respectively) during tri-block copolymer synthesis is often incorrect. Consequently, a mixture of di-block, tri-block, unmodified precursors, and ionically coupled surfactant molecules is created[11], generating batch-to-batch variation in the final product. Finally, surfactants with a tri-block structure can efficiently form micelles and bilayer vesicles, which can destabilize and act as carriers between drops.

Di-block surfactants do not suffer from these problems. Their synthesis can employ an excess of polar head group to ensure complete covalent coupling to the fluorinated tail. The unconjugated head group can then be removed by simple work-up, resulting in pure di-block surfactant, with no undesired products that may destabilize droplets. Structurally, because di-block surfactants cannot form bilayer vesicles, vesicle-mediated inter-droplet cargo transfer should not occur.

Although di-block fluorosurfactants have been synthesized with a variety of head groups, including carbohydrate-derivatives[22] and PEG of various lengths[23], these surfactants were inferior to the commonly used PEG600-PFPE$_2$ tri-block copolymer fluorosurfactant[11], justifying testing of alternative head groups. We hypothesize that use of dendritic head groups carrying hydroxy moieties, which readily form inter- and intramolecular hydrogen bonds[24], might lead to high-performance surfactants. However, we rule out linear head groups based on our previous studies showing that a linear polyglycerol-based tri-block copolymer fluorosurfactant, despite having thirteen hydroxy groups, was unable to stabilize droplets[15]. Instead,

different architectures of head groups are needed to design new and effective fluorosurfactants.

Here, we describe a systematic design and testing of dendronized fluorosurfactants containing mono- or tri-glycerol polar head groups and fluoro-tails of three different lengths. Our two best-performing surfactants combined a four hydroxy-group-containing polar head group with fluorinated tails of low- or medium length (2 or 4 kDa). For microdroplet PCR and small molecule droplet-retention, these surfactants were superior to surfactants made with a polar head group lacking hydroxy groups and to the PEG-PFPE$_2$ surfactant.

Results and discussion

Synthesis of dendronized fluorosurfactants. For the synthesis of the dendronized fluorosurfactants we use a facile amide coupling to covalently couple the dendritic tri-glycerol (dTG) moiety to the PFPE chains. By reacting the amine-functionalized oligo-glycerols with the activated carboxy terminus of the non-polar fluoro-chains, followed by deprotection of the acetal groups the fluorosurfactants were obtained in high yields of 75–85% (Fig. 1). It is worth mentioning that the unreacted protected oligo-glycerol derivatives are purely soluble in organic solvents such as dichloromethane (DCM), methanol, and tetrahydrofuran (THF). In addition, these organic solvents are immiscible with fluorinated solvents, including HFE7100 and HFE7500, and, due to their lower density, phase separate into a top layer. Thus, excess unreacted protected oligo-glycerol moieties can be easily be removed by washing with excess of DCM. Deprotected oligo-glycerol derivates are soluble in THF or methanol, and additional washing with these solvents results in pure di-block fluorosurfactant, with no undesired products. We synthesized three surfactants that are consisted of tri-glycerol-based dendritic polar heads (dTG), which have four hydroxy (–OH) groups, and PFPE polymer chains with three different fluorine chain lengths of high (H), medium (M), and low (L) molecular weights (MW), providing H-dTG, M-dTG, and L-dTG, respectively, are shown in Fig. 1 (bottom panel). We also synthesized two surfactants that carry only two –OH groups in their non-ionic heads using glycerol-amine. The combination of mono-glycerol (G) with medium and low MW PFPE chains created M–G and L–G surfactants, respectively, as illustrated in Fig. 1 (top panel). These five di-block dendronized surfactants allow us to systematically investigate the effect of polar head group geometries and the number of –OH groups on droplet stability and performance under demanding conditions. The successful preparation of the fluorinated surfactants was confirmed by the amide (-NH-CO-) stretching peak from 1710 to 1740 cm^{-1} in FT-IR spectroscopy. In contrast, an unmodified PFPE-COOH (Krytox) showed a strong IR band at 1775 cm^{-1} (Supplementary Fig. 1). We used deionized water and a 2% (w/w) surfactant in HFE7500 oil to prepare w/o emulsions by bulk-mixing. Surprisingly, all five surfactants produced stable emulsions irrespective of the length of PFPE chains and the number of glycerol units. Furthermore, long-term incubation of the emulsions, prepared by tri-glycerol based surfactants, for about 30 days at room temperature in small glass vials did not cause any noticeable merging of the droplets. In contrast, mono-glycerol based surfactants stabilized the droplets for about a week.

Emulsion droplet stability during PCR. We investigated the ability of all five di-block surfactants to stabilize the microfluidically generated large droplets, ~95 micrometer (μm) diameter (~500 pL) and test their stability during PCR reactions between 60 °C and 98 °C. We chose relatively large droplets because droplet stability decreases with droplet size and we
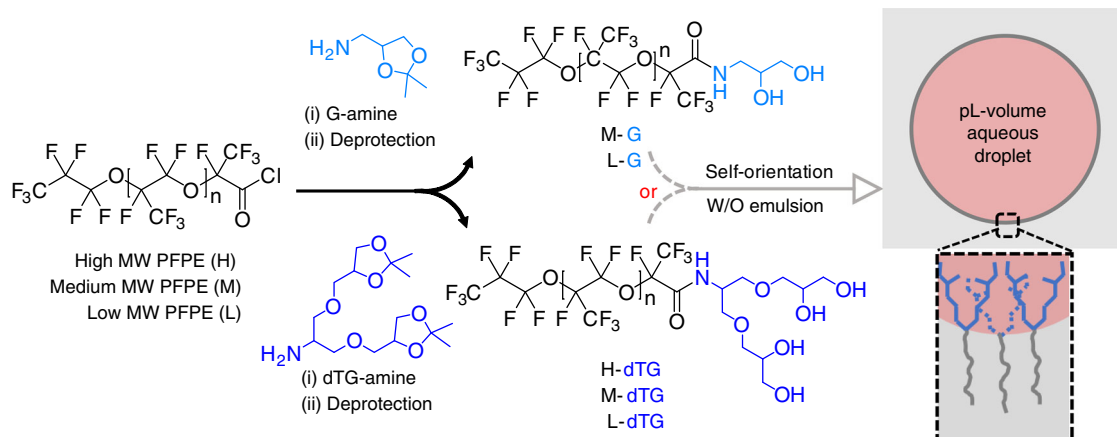
Fig. 1 Synthesis of fluorosurfactants with dendritic glycerol head groups. PFPE tails of two different fluoro-chain lengths (M, L) were conjugated to the mono-glycerol (G) polar head (upper drawing, light blue) to create surfactants M-G and L-G; PFPE tails of three different molecular weights (H, M, L) were conjugated to dendritic tri-glycerol (dTG) polar head to create surfactants H-dTG, M-dTG, and L-dTG (lower drawing, blue). These surfactants orient at the interface (deep gray) of water (light red) and fluorinated oil (gray) to stabilize picolitre-volume (pL) water-in-oil (W/O) emulsion droplets, as depicted in the picture

wanted a stringent test case, and we used the PEG-PFPE$_2$ surfactant as a reference standard. Moreover, complex droplet manipulations, for example in-droplet barcoding[1,25] and pico-injection[26,27] often use large droplets. Thus, using each of these six surfactants, at equal w/w concentrations (2%), we encapsulated PCR mix into monodisperse droplets of ~95 μm diameter that were stable at room temperature (Supplementary Fig. 2). After 35 cycles of PCR reaction between 60 °C and 98 °C, we found that all three surfactants containing the tri-glycerol dendron (dTG) as the polar head group effectively stabilized the drops during PCR reaction, irrespective of the PFPE chain lengths (Fig. 2b and Supplementary Fig. 3). Within this group, the L-dTG surfactant was superior to the H-dTG and M-dTG surfactants (Supplementary Fig. 4). We created droplets using these surfactants at roughly equimolar amounts, corresponding to 2% w/w H-dTG and 0.7% w/w L-dTG. Under these conditions, H-dTG droplets were more stable than L-dTG-stabilized droplets and the L-dTG-stabilized droplets coalesced upon collection and/or minimal external force applied to the droplet collection tubing, suggesting that the H-dTG longer fluorinated tails can provide more stability than shorter tails. Of note, droplets made with 2% w/w L-dTG were more stable than those formed with the PEG-PFPE$_2$ surfactant (Fig. 2d, Supplementary Figs. 3–4). However, droplets generated with 4% w/w PEG-PFPE$_2$ had superior post-PCR thermal stability than droplets stabilized with 2% w/w PEG-PFPE$_2$ (Supplementary Figs. 3–4). A quantitative analysis of the post-PCR droplet size distributions shows that dTG and PEG based reference surfactants ability to stabilize droplets follows this order: 2% L-dTG ≥2% M-dTG > 4% PEG-PFPE$_2$ ≥2% H-dTG > 2% PEG-PFPE$_2$ (Supplementary Figs. 3–4).

Droplets formed with the mono-glycerol (G)-based surfactants were also stable at room temperature. However, all the droplets merged during PCR, as illustrated in Fig. 2b, c and Supplementary Fig. 5b. Because the only structural difference between dTG and G polar groups is the number of hydroxy groups, 4 vs 2, respectively, this result clearly demonstrates the importance of inter- and intra-molecular hydrogen bonding. Furthermore, the head-group architecture also influences surfactant performance. Fluorosurfactants created with glucose derivatives, which also carry four hydroxy groups, whose primary difference from dTG-surfactants is a cyclic vs. a dendritic geometry, are unable to make stable emulsions[22]. We hypothesize that, mechanistically, the dTG's four hydrogen bond donors, and its dendritic architecture

collectively favors inter- and intramolecular H-bonding and provides greater emulsion stability.

We further characterized the performance of dTG-based surfactants by performing in-droplet click-chemistry to crosslink together the high-viscosity polymers dendritic poly(glycerol-sulfate) azide and homo-bifunctional PEG-cyclooctyne, generating spherical hydrogels. We prepared highly monodisperse droplets, carrying polymer precursors, at kHz rates with all three types of surfactant using a concentration of 2% (w/w) in HFE7500 oil (Supplementary Fig. 6). We incubated the emulsions to allow crosslinking, and then transferred the gels to aqueous solution. For all three surfactants, the isolated gels were monodisperse and no inter-microgel cross-linking was seen, proving that droplets did not merge during crosslinking and that the crosslinking was complete. This suggests that dTG-based surfactants, which have equally high performance when synthesized with PFPE tails of ~2, ~4, or ~6 kDa, tolerate a larger range of PFPE tail length than PEG-based fluorosurfactants, which function only if the PFPE chain is ~6–7.5 kDa[11,12,15,23].

These data show that, for a given fluorinated tail group, dTG containing surfactants can stabilize droplets better than the corresponding G containing surfactants. We attribute this to dTG's symmetrical architecture, its four H-bond donors and acceptors, and the flexibility provided by its two chiral centers. Tri-glycerol based dendronized surfactants' robust droplet-stabilizing activity prompted us to study its capacity to prevent small molecule inter-drop diffusion. This is of great interest, as it is extremely challenging to prevent leaching of small molecules to the neighboring microscopic droplets[4]. In addition, a surfactant that prevents substrate leakage will allow compartmentalization of small-molecule drugs, enabling in vitro high-throughput screening in very small volume droplets. Performing biological assays in picolitre-volume microscopic droplets instead of robot-assisted screening in microtiter plates would lead to dramatic cost savings due to low reagent consumption and, in cell-based assays, a significant reduction in number of cells required[7].

Minimized inter-droplet transfer. We studied the inter-droplet leakage of a small water-soluble dye, sodium fluorescein salt ($M_w = 376$ g mol^{-1}) by mixing populations of empty and dye-containing droplets and measuring the transfer of dye to the empty droplets. For each surfactant tested, we used a parallel drop
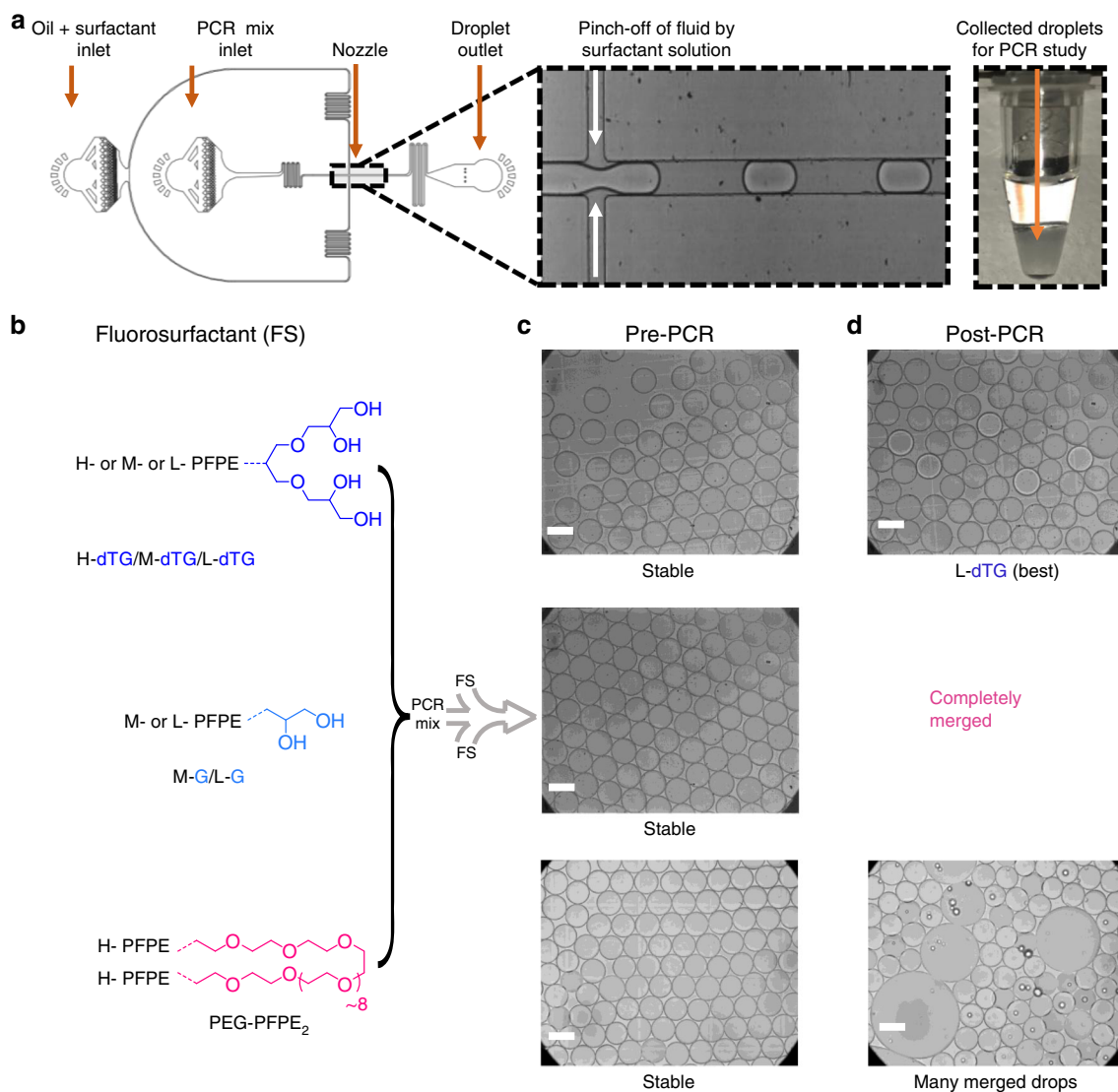
Fig. 2 Polar head group geometry dictates droplet stability. a Polydimethylsiloxane (PDMS) based microfluidic devices are used to prepare microdroplets containing PCR reagents. **b** The three tri-glycerol (dTG)-based surfactants (H-dTG, M-dTG, L-dTG), the two mono-glycerol (G)-based surfactants (M-G, L-G), and the PEG600-based fluorosurfactant, PEG-PFPE$_2$, were used to create droplets for stability testing (chemical structures in **b**). **c** Droplets produced using the tri-glycerol, the mono-glycerol, and the PEG600-based surfactants showed no merging during >24 h incubation at 4 °C (**c** showing pre-PCR droplets). **d** After 35 cycles of PCR, L-dTG-stabilized droplets showed almost no merging. In contrast, droplets generated using mono-glycerol (G)-based surfactants (M-G, L-G) merged completely during the PCR. Droplets stabilized with PEG-PFPE$_2$ surfactant showed substantial merging (**c** depicting post-PCR droplets). Scale bar, 100 μm

maker (Supplementary Fig. 7) to prepare and mix two populations of aqueous droplets: PBS + FITC droplets, containing 2 μM sodium fluorescein salt in PBS; and PBS-only droplets, containing only PBS. Each mixed droplet population was collected in an Eppendorf tube and incubated at 37 °C. Droplets created with H-dTG, M-dTG and L-dTG surfactants were more resistant to dye diffusion than those created with M-G and L-G (note: H-G surfactant was not synthesized as M–G and L–G surfactants did not perform better than dTG-based surfactants), indicating that the dTG head-group improves dye-retention better (Fig. 3 and Supplementary Fig. 8).

We also address the effect of tail length on inter-droplet dye exchange, finding that, for dendritic head groups, droplets produced with the longer chain surfactants are more resistant to leaching than those produced with the short chain (H-dTG = M-dTG > L-dTG; M–G > L–G). Quantitatively, after 24 h incubation, the fluorescence intensity of PEG-PFPE$_2$ surfactant-stabilized PBS-only drops was, respectively three times and 13 times the intensity measured in PBS-only droplets stabilized by our worst-performing surfactant, L–G (Supplementary Fig. 8c), and our best-performing surfactant, M-dTG (Fig. 3b). Not surprisingly, the fluorescence intensity of M-G surfactant-stabilized PBS-only drops was three times the intensity measured in PBS-only droplets stabilized by M-dTG surfactant (Fig. 3b), confirming the importance of a dense hydrogen bond network at the oil–water interface.

To directly address the contribution of hydrogen-donor activity of the hydroxyl groups in oligo-glycerol-based surfactants, we test if a high salt concentration, known to form ion–dipole interactions and disrupt inter-and intramolecular hydrogen bonding, decreases dye retention in droplets stabilized with the oligo-glycerol-based surfactant M-dTG. Indeed, in presence of 5 M NaCl we see inter-droplet leakage of water-soluble fluorescein dye after 24 h (Supplementary Fig. 9).
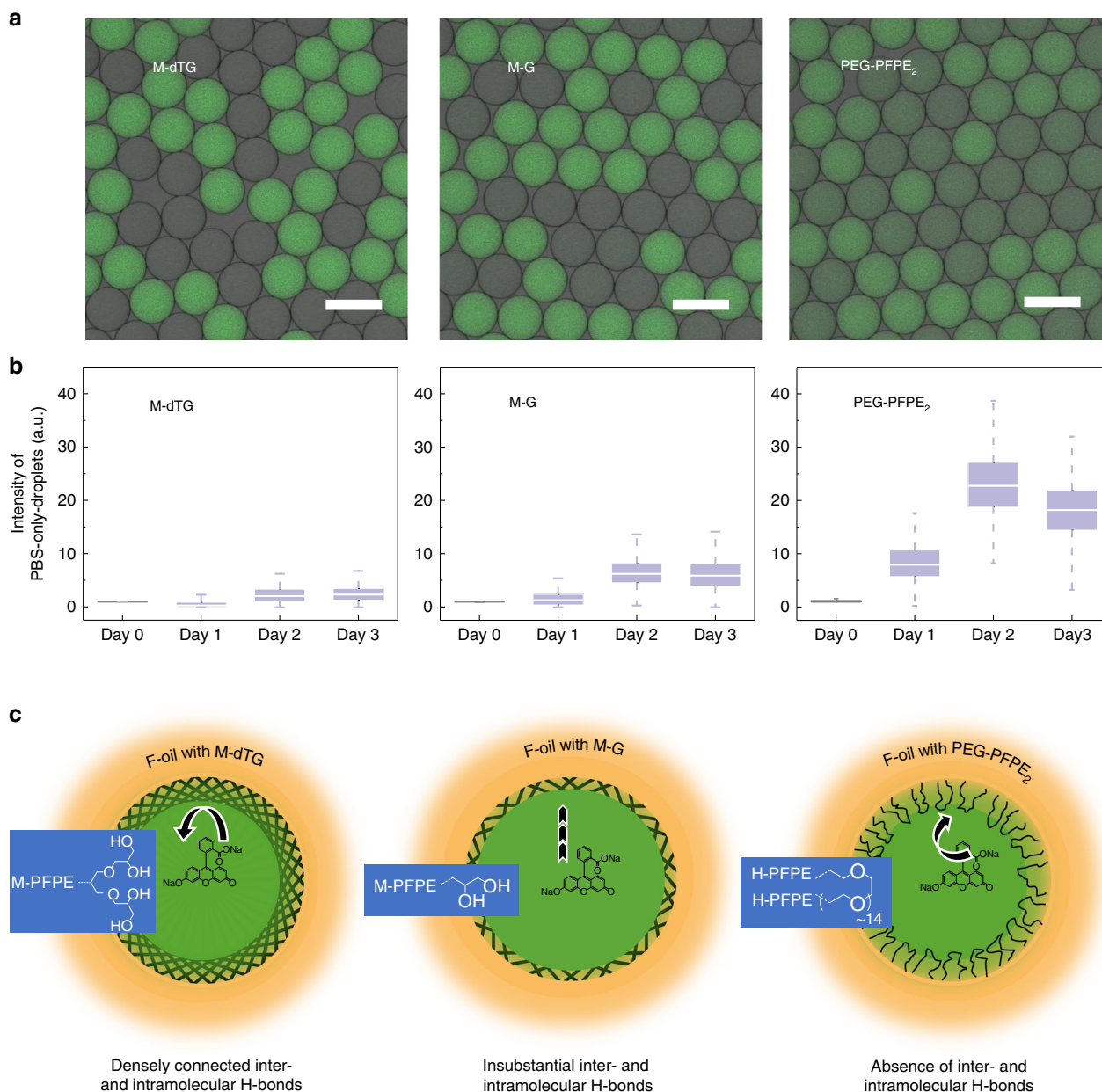
Fig. 3 Influence of dense hydrogen bond network on inter-droplet diffusion. **a** For each surfactant, we used parallel drop maker to create a mixture comprising equal amounts of PBS-only-droplets and PBS + sodium fluorescein salt-containing droplets. Confocal fluorescent imaging of droplets after 72 h incubation at 37 °C is shown in top panel. **b** We incubated these mixtures, took fluorescence images at the indicated time points, and then performed quantitative analysis of the fluorescence intensity of the 10 randomly selected PBS-only droplets. Box-plot demonstrates that dye was almost completely retained in droplets stabilized by M-dTG, while some transfer was detected in M-G droplets. PEG-PFPE$_2$ surfactant-stabilized droplets showed substantial transfer (left to right). The box plots represent the median (center line), the interquartile range (box) and the non-outlier range (whisker). **c** A model representing the plausible inter- and intramolecular hydrogen bonding from M-dTG, M-G, and PEG-PFPE$_2$ surfactants (left to right). The lines denote hydrogen bonding at the interface of oil and water. For PEG-PFPE$_2$ surfactant, as there is no hydrogen bond donor, there is no inter- and intramolecular hydrogen bond present. Scale bars = 100 μm; a.u. = arbitrary units. Source data of Fig. 3b (middle panel) are provided as a Source Data file

Further, to better define the improved performance of the M-dTG surfactant relative to PEG-based surfactants, we tested retention of the small molecule dye resorufin ($M_w = 235$ g mol^{-1}). In our experiments with droplets stabilized with 4% (w/w) PEG-PFPE$_2$ surfactant, almost 50% of the dye is transferred from droplets containing 2 μM resorufin + PBS to PBS-only-droplets after 30 min. However, in droplets stabilized with 2% (w/w) M-dTG surfactant, the inter-droplet transfer of ~50% resorufin dye occurs after 330 min, indicating that inter-droplet transfer between M-dTG stabilized droplets is 11 times slower

than between PEG-PFPE$_2$ stabilized droplets (Supplementary Fig. 10).

The high performance of the tri-glycerol dendron-containing (dTG-based) surfactants suggests that the symmetrical geometry, multiple hydrogen bond donors, and flexible ether groups collectively help the dTG polar group form densely connected inter- and intramolecular H-bonds, which act as a strong web-like network at the oil–aqueous interface (see model in Fig. 3, bottom panel). This is supported by our results showing that high-salt concentrations reduce dye retention.

In addition, we believe that the hydrogen-donor activity of dTG-head groups may enhance retention of cargo molecules containing hydrogen-bond accepting atoms, e.g., oxygen (O) and nitrogen (N). When these molecules approach the H-bond-dense water–oil interface, dTG-based surfactants will donate hydrogen bonds to the cargo, increasing its aqueous solubility[28].

G-head groups, due to their limited number of hydroxy groups and lower number of flexible chiral centers, make insufficient inter- and intra-molecular H-bonds and do not significantly interact with cargo containing hydrogen-bond accepting atoms as depicted schematically in Fig. 3c. In contrast, PEG forms neither inter- or intramolecular hydrogen bridges and does not act as hydrogen bond donor to increase dye solubility at the aqueous–oil interface. This may partially explain the relatively poor dye retention of droplets stabilized with the PEG-PFPE$_2$ surfactant. In addition, the PEG-PFPE$_2$ surfactant, as a tri-block copolymer, can form bilayer vesicles to mediate transport between droplets[12,29].

Cell-based reporter system. Our findings suggest that M-dTG is the best of the dTG- and G-based surfactants for drop-stability and retention of water-soluble small molecules (fluorescein) and more leaky small molecules (resorufin). To be truly valuable for droplet-based drug-screening, a surfactant must also prevent inter-drop transfer of encapsulated small, non-polar compounds and it should be biocompatible. We developed a cell-based assay, much more sensitive than dye-transfer monitoring, in which reporter gene activity is used to characterize leakage of a drug, doxycycline (DOX), between M-dTG-stabilized droplets. We used a hyperactive piggyBac transposase (hyPBase)[30] and XLone-GFP[31] plasmid constructs to create a Tet-On 3 G DOX-inducible GFP expressing stable cell line, DOX-GFP-HEK 293 (reporter cells) (Supplementary Fig. 11). In the absence of DOX, GFP expression is negligible, whereas 48 h incubation with 500 nM DOX results in easily-detected GFP signal in 73.5% of the cells (Fig. 4a). We then determined that the cell-stream of our parallel drop maker loads cells into droplets roughly according to Poisson prediction (Fig. 4b, c). At five cells per droplet volume, 83% of the droplets contain one or more cells. We further demonstrated that droplet size remains constant over a 72 h incubation (Fig. 4d).

In addition, to test the biocompatibility of the M-dTG surfactant and the PEG-PFPE$_2$ surfactant (a reference standard), we generated cell-containing droplets equivalent to those used for cell culturing experiments (see Fig. 4b, c) and incubated for 24, 48, and 72 h incubation time points. We used perfluoro-octanol to release the cells from the droplets and tested viability using Calcein AM and Ethidium Homodimer-1 dyes based live/dead cell viability assay kit (Invitrogen). At each time point, cell survival is roughly 85–90% (Fig. 4e). By comparison, the cell survival is about 95% when cells were cultured under standard conditions in well plates. This demonstrates that dTG-based surfactant, M-dTG, is not cytotoxic to cells and is suitable for cell-based assays.

We used the DOX-GFP-HEK 293 cells to test DOX transfer between droplets within populations stabilized by either M-dTG or PEG-PFPE$_2$ surfactant. We used the surfactants at roughly equimolar concentrations, 4% PEG-PFPE$_2$ and 2% M-dTG. We created a mixture of cell-containing droplets and droplets containing 1 μM DOX, incubated for the indicated times, and then released the cells from the droplets. In positive control sample, cells were encapsulated and cultured in droplets with DOX at the indicated concentrations. To compare GFP expression level of cells grown in droplets with GFP expression level of cells grown in bulk (standard culture plates), we cultured cells in six-well plates. When cells were cultured in bulk with DOX

(positive control in bulk), almost 60% of them were GFP+ after day 1, 73.5%, were GFP+ after day 2, and 69% after day 3. In-droplet control experiments showed that cell response to DOX is roughly equivalent in droplets stabilized with M-dTG or PEG-PFPE$_2$ surfactant. After 1 day a high percentage of cells encapsulated with 500 nM DOX, 52.3% and 53.9% respectively, were GFP+; 31.3% and 25.5%, respectively, were GFP+ when incubated with 200 nM DOX (Fig. 5 and Supplementary Fig. 12).

In the experiments to test transfer of DOX from DOX-only droplets (1 μM) to cell-only droplets, we see that GFP expression in droplets stabilized with M-dTG is lower than in droplets stabilized with PEG-PFPE$_2$, 37.1% vs 44.5% (compare Fig. 5 column 4 with supplementary Fig. 12 column 3). When cells incubated for one day are compared, the inter-droplet transfer from M-dTG stabilized droplets containing 1 μM DOX induces cells to express GFP at roughly the same level as seen for cells incubated for one day in control droplets containing 200 nM DOX. Our results also show that, for a given concentration of DOX, cells incubated in bulk conditions yield more GFP+ cells than cells incubated in droplets (Fig. 5, compare columns 2 and 3). This is not surprising, as the effective concentration of cells cultured in droplets is ~10 times that of cells cultured in standard conditions.

These studies of inter-droplet transfer clearly suggest that M-dTG-stabilized droplets, relative to those stabilized with PEG surfactant, are significantly better at retaining the water-soluble dye fluorescein sodium salt, and are measurably superior at retaining other small molecules such as resorufin and doxycycline. Thus, dTG-based surfactants, which are synthesized from easily-sourced building blocks, have great potential as robust and economical droplet stabilizers and will be powerful reagents for droplet-based single cell analysis even under PCR conditions and for drug screening applications.

In addition, we provide insights into surfactant design through systematic analysis of two different polar head groups with three fluorinated tail groups. We found that polar groups can interact through inter- and intramolecular hydrogen bonds and provide the emulsified droplets high-temperature tolerance and high retention of encapsulated small molecules. Further, the hydroxy moieties of the polar head groups can easily be functionalized, enabling surfactant optimization for specific chemical environments. We expect our surfactants to be of immediate use in droplet-based experiments requiring high droplet integrity.

Methods

Materials. We purchase the monocarboxylic acid-terminated perfluoropolyethers, brand name Krytox, of three different chain lengths that are Krytox 157-FSH ($M_w = 7000$–7500 g mol^{-1}), Krytox 157-FSM ($M_w = 3500$–4000 g mol^{-1}), and Krytox 157-FSL ($M_w = 2000$–2500 g mol^{-1}) from LUB SERVICE GmbH (Germany). We buy HFE 7100 and HFE 7500 oils from 3 M. We obtain 2,2-Dimethyl-1,3-dioxolane-4-methanamine (acetal-protected mono-glycerol-NH$_2$, G-NH$_2$) from Merck (Germany). We purchase tri-block copolymer fluor-osurfactant PEG-PFPE$_2$ (EA surfactant) from RAN Biotechnologies (Beverly, MA). The EA surfactant has two perfluoropolyether tails (each having a MW ~6000 g mol^{-1}) coupled to a homo-bifunctional PEG600-amine head group[1]. All other chemicals we purchase are reagent grade. These chemicals are either from Acros Organics (Belgium) or from Merck (Germany) unless otherwise stated. They are used as received without further purification. All moisture sensitive reactions are conducted in flame-dried glassware under dry conditions. The acetal-protected tri-glycerol dendron-amine (dTG-NH$_2$) is synthesized following previously reported synthetic routes with slight modifications indicated below[15,32]. For the fluor-osurfactants' synthesis the protocol by Holtze et al.[11], Baret et al.[12], and Wagner et al.[15], is used. The surfactant solution is prepared in the HFE-7500 oil, a biocompatible oil phase, at 2% and 4% by weight. To make microgels, two polymer precursors, homo-bifunctional polyethylene glycol-cyclooctyne (PEG-DIC) and dendritic polyglycerol sulfate azide (dPGS-N$_3$) are reacted according to previously reported synthetic schemes[33].

Analytical methods. NMR spectra are recorded on an ECX400 spectrometer (Jeol Ltd., Japan), or an AMX 500 spectrometer (Bruker, Switzerland). Proton NMR chemical shifts are reported as δ values in ppm. Deuterated solvent peak is used to
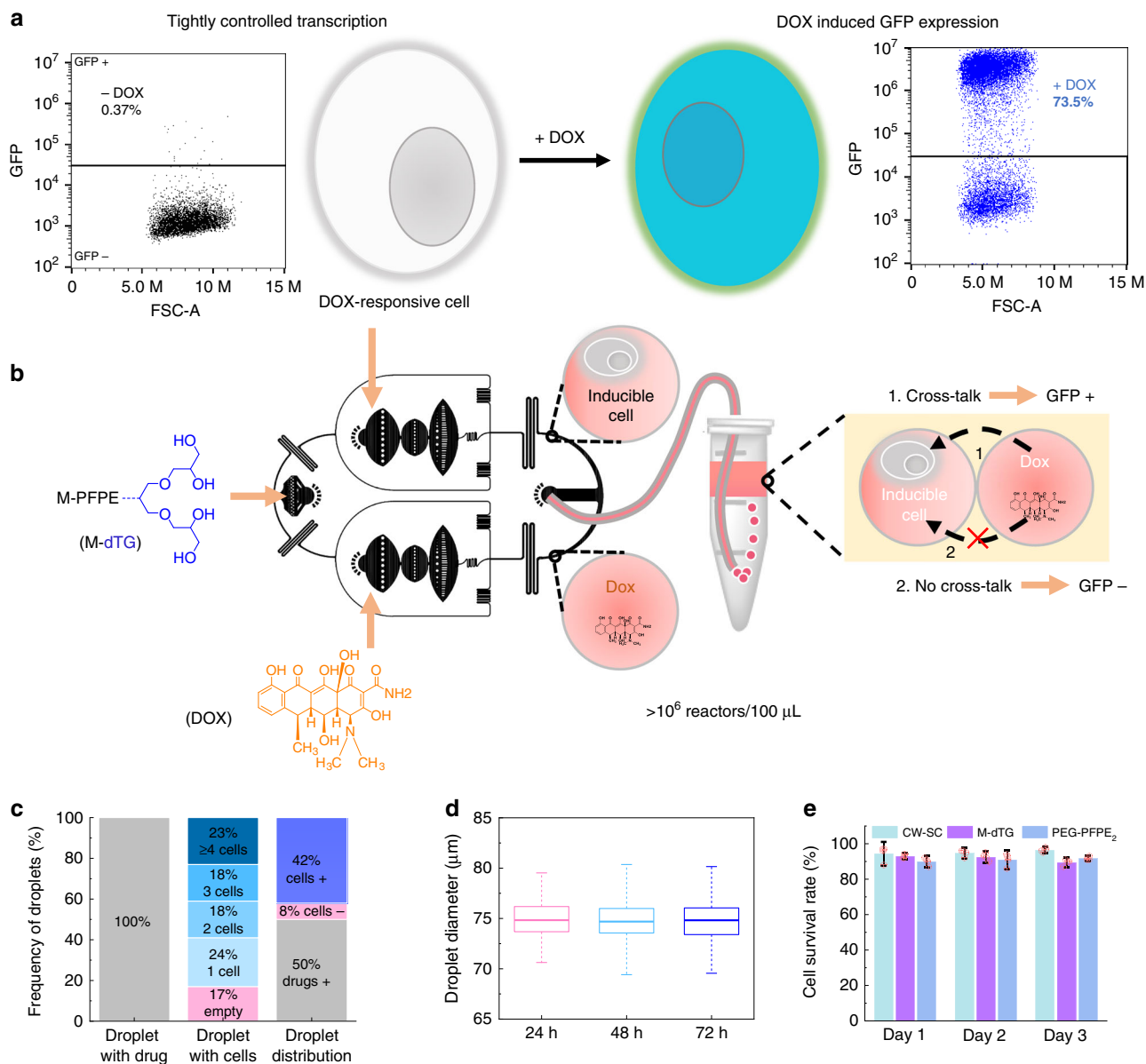
Fig. 4 Cell-based reporter system to test inter-droplet drug diffusion. **a** HEK 293 cells stably transfected with a doxycycline responsive GFP reporter construct (reporter cells) show no GFP expression in the absence of drugs and become highly fluorescent after 48 h incubation in the presence of 500 nM DOX-solution. **b** Homogeneous population of DOX-containing droplets and Reporter-cell-containing droplets was generated using a parallel drop maker that creates an equal number of droplets from two independent aqueous streams. **c** Cell-loading into droplets roughly follows Poisson predictions. We imaged 533 droplets immediately after cell encapsulation to determine cell occupancy. We used an input density of five cells per droplet volume and found that 83% of the droplets contained one or more cells. Therefore, with cells at this concentration, the parallel drop maker generates a mixed droplet population in which 42% droplets contain one or more cells, 50% contain only doxycycline, and 8% are empty. **d** Box-plot of droplet size distribution after 24, 48, and 72 h incubation at 37 °C demonstrates that the mean average droplet diameter remained constant (~75 μm) over the time course ($n = 204$–226 droplets for each time point). The box plots represent the median (center line), the interquartile range (box) and mean ± 1.5 x s.d. (whisker). **e** Viability of cells cultured in wells or in droplets. As a positive control we cultured cells at standard concentration in culture wells (CW–SC) ($1 × 10^6$ cells/ml). We used M-dTG and PEG-PFPE$_2$ surfactants to generate cell encapsulated droplets and incubated droplets at 37 °C for the indicated times. We isolated cells from the droplets to perform live/dead assay using Calcein AM and Ethidium Homodimer-1 dyes based live/dead cell viability assay kit (Invitrogen). We counted ~500–2000 cells to estimate the cell survival rate at the indicted time points. Data are presented as mean ± s.d., $n = 4$ images from distinct areas. Source data of c–e are provided as a Source Data file

calibrate the recorded peak. To record IR spectra, Nicolet AVATAR 320 FT-IR 5 SXC (Thermo Fisher Scientific, USA) is used with a DTGS detector from 4000 to 650 cm^{-1} wavenumbers. Bright field and fluorescence imaging are obtained with Zeiss Axio Observer (Germany) and Leica confocal microscope (TCS SP8, Germany). To record green fluorescence signals, 488 nm excitation wavelength is used, and the emission signals are detected by a 520/55 nm band pass filter. A high-speed Phantom MIRO ex2 camera (Vision Research, USA) is employed for brightfield imaging during microfluidic droplet preparation. FACSAriaIII (USA) cell sorter and BD Accuri™ C6 Plus (USA) flow cytometer are used for cell sorting

and to analyze the GFP expressing cells, respectively. Flow cytometry data is analyzed using FlowJo v10. Homemade MATLAB scripts are used to analyze droplet size distribution by finding droplet circles and extracting the corresponding diameters that are adjusted to final diameter according to the actual pixel size of the image. OriginPro 2019b (Academic) was used to prepare Boxplots and bar charts.

Synthesis of acetal-protected dTG-NH$_2$. Acetal-protected tri-glycerol dendron-hydroxy (dTG-OH) is dried under high vacuum at 60 °C overnight. Thereafter,
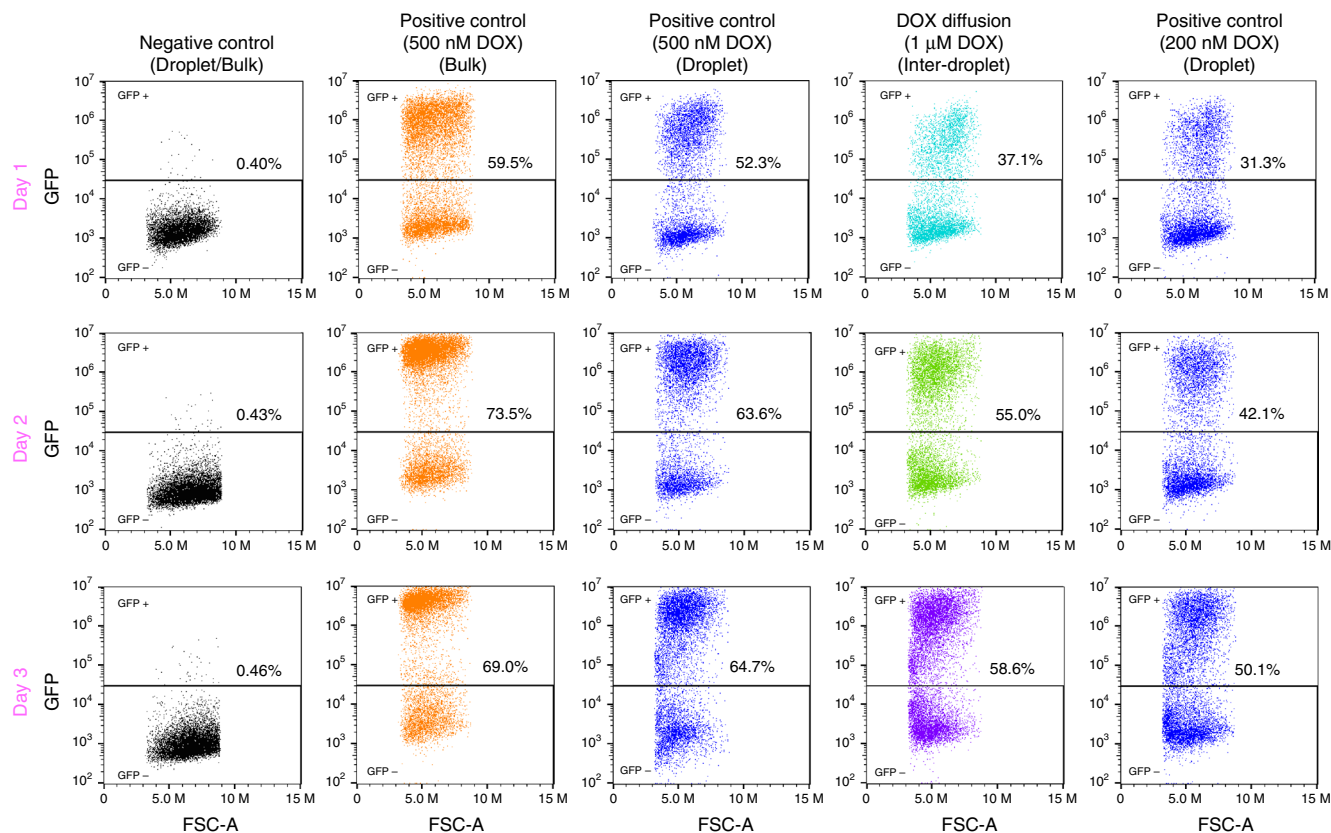
Fig. 5 DOX-inducible GFP-reporter cells to quantify drug transfer. We used the parallel drop maker to generate homogenous mixtures in which 50% of the droplets contained DOX (at the indicated concentrations), 42% contained ≥1 cell, and 8% were empty. We incubated droplets at 37 °C for the indicated times, isolated the cells from the droplets, and quantified the GFP+ cells using flow cytometer. GFP intensity is plotted against forward scatter-area (FSC-A). For the positive control in bulk, we cultured the DOX-GFP-HEK 293 cells with DOX in six well plates using standard cell culture methods. For the Positive Control (Droplet), all droplets, including those with cells, contained DOX at the indicated concentration

dTG-NH$_2$ is prepared in a three-step process. In the first step, the hydroxy groups are mesylated using 1.5 equivalents of methane sulfonyl chloride (MsCl) and 2 equivalents of triethyl amine. This reaction is performed in DCM at 0 °C to RT overnight under inert conditions while stirring. The mesylated acetal-protected tri-glycerol (dTG-OMs) is extracted in dichloromethane (DCM) against water, the solution is dried over Na$_2$SO$_4$ salt, and then the volume is concentrated under reduced pressure. To substitute the mesyl group by azide, dTG-OMs in dimethylformamide (DMF) is dissolved and NaN$_3$ salt (3 eq.) is added into it. The reaction mixture is heated with continuous stirring for 3 days at 75 °C under argon. Then the solvent is evaporated, and the compound is extracted in DCM followed by drying over Na$_2$SO$_4$ salt, and filtering through cotton wool. After removing the solvent, the acetal-protected dTG-N$_3$ is obtained in quantitative conversion of mesyl to azide groups. Finally, to convert azide to amine functionalities, 10% (w/w) a palladium catalyst (10% Pd on Charcoal) is used with respect to the weight of acetal-protected dTG-N$_3$ for hydrogenation. The substrate is dissolved in dry ethanol in a hydrogen reactor and pressurized to ~5 bar hydrogen atmosphere at RT for 3 days under vigorous stirring. Then the Pd/Charcoal is filtered using a well-packed bed of cellite®545 on a fritted glass filter (pore size 4). After concentrating the solution, the acetal-protected dTG-NH$_2$ is obtained in almost quantitative yield.

Synthesis of di-block dendronized surfactants. The diblock-dendronized fluorosurfactants are synthesized in a three-step process. In the first step, oxalyl chloride is used to activate the acid group in Krytox, producing acyl chloride terminated Krytox[11,12,15]. The reaction is performed in a one-neck round bottom Schlenk flask equipped with a magnetic stirrer bar. Krytox (1 eq.) is dried at 100 °C under HV for 3 h and after cooling down the flask to RT, it is dissolved in dry HFE7100. Then a catalytic amount of DMF is injected into the Krytox solution under argon atmosphere. Then oxalyl chloride (10 eq.) is added and the formed toxic gases are removed via a Schlenk line. After 30 min, the reaction is continued overnight at RT under argon atmosphere with vigorous stirring. Then all the volatile gases and the solvent are removed under high vacuum (HV) using an additional cold trap. Krytox 157 FSH, Krytox 157 FSM, and Krytox 157 FSL as high, medium, and low molecular weight fluorinated blocks, respectively are used in the same way for all three types. In the second step, 1.3 equivalents of dry

acetal-protected G-NH$_2$ or dTG-NH$_2$ are used to react with the activated-Krytox. DCM is used to dissolve the acetal-protected oligo-glycerol-amine precursor and then added dropwise into the activated-Krytox solution in HFE7100 under argon atmosphere. Subsequently triethylamine (3 eq.) is added as an organic base into the reaction mixture. For a better miscibility of these different solvents, a ratio of 1:1 or 1:0.75 of DCM and HFE7100 is used. Then the reaction mixture is refluxed for 2 days at 50 °C and the crude reaction mixture transferred into a one-neck round bottom flask to remove the solvents and acid vapors under reduced pressure. The dried compound is dissolved in HFE7100 and methanol and stirred vigorously for ~20 min. HFE7100 has a density of 1.52 g/ml, whereas methanol has a density of 0.79 g/ml. Due to such a high-density gradient the two solvents phase separate. Then the top clear organic phase of methanol (10×) is removed. This washing step removes the base, salt, and the excess unreacted dendron molecules, providing purely the di-block dendronized fluorosurfactants. Finally, acidic methanol, 0.5–1.0 ml of 37% (w/w) HCl solution in 20 ml of methanol for a 10 g batch, is added into the acetal-protected oligo-glycerol containing fluorosurfactant, dissolved in HFE7100 to deprotect the acetal groups from the oligo-glycerol molecules overnight at 50 °C, generating water soluble polar group in the fluorosurfactant. After repeated washing with methanol (20×), the different fluorosurfactants are obtained in 75–85% isolated yield after HV drying.

PDMS device fabrication. The PDMS microfluidic devices are fabricated according to the methods described in Mazutis et al.[34], with minor modifications and details specific to our experiments. SU8-on-Si wafer is prepared using spin coated SU-8 2050 photoresist (MicroChem, MA) layer of a desired thickness that is UV etched using the photomask. PDMS is baked at 65 °C for 3 h after pouring onto the SU-8 master. To remove the debris after hole punching, we sonicate the PDMS slab in an isopropanol bath, dry with pressurized air, then bake at 75 °C to ensure all isopropanol is evaporated. After plasma bonding of PDMS slab to glass, the PDMS-on-glass device is heated on a 75 °C hot plate for ~10 min and then incubated at 65 °C overnight in an oven to enhance bonding. To make the channel surfaces hydrophobic, PTFE-syringe-filtered Aquapel (PPG Industries) is injected into the channel, incubated ~60 s at room temperature, and then blown out of the channels using pressurized nitrogen. To remove traces of Aquapel, PDMS device is incubated at 60 °C for ~2 h.

PCR experiments. Microfluidic drop making devices are used to create ~95 μm diameter monodisperse droplets stabilized by the indicated surfactants (2% w/w) in HFE7500 carrier oil. Each emulsion of droplets is created from 40 μl PCR mix comprising 25.2 μl water, 8 μl 5x Phusion HF detergent-free Buffer (F520L, Thermo Fisher), 0.8 μl 10 mM dNTPs (diluted from 25 mM dNTP mix, Thermo Fisher, R1121), 1.6 μl 2 μM forward primer (5′ TCGTCGGCAGCGTCAGATGTG 3′, ordered from IDT), 1.6 μl 10 μM reverse primer (5′ GTCTCGTGGGCTCGGAG ATGT 3′, ordered from IDT), 0.4 μl Phusion High-Fidelity DNA Polymerase (F530L, Thermo Fisher), 0.4 μl 20 mg/mL bovine serum albumin (BSA, B14, Thermofisher), 0.4 μl 10% tween-20 (diluted from Tween-20, Sigma-Aldrich, P9416-50 mL), and 1.6 μl template (4 μl 2.5 μg/mL Lambda Phage genome is fragmented and tagged by 6 μl reagents from Nextera kit from Illumina following its protocol, FC-121-1031, then diluted 100 times by water). The PCR program is 98 °C for 30 s; then 35 cycles of 98 °C for 7 s, 60 °C for 30 s, and 72 °C for 20 s; then a final step of 72 °C for 10 min. After PCR thermocycling, droplets are broken by adding perfluorooctanol (PFO; 370533, Sigma) to the droplets (five volumes of PFO to one volume of the droplet aqueous contents). 5 μl aqueous phase of each sample is electrophoresed on a 2% agarose using 1x TAE buffer. In total 6 μl GeneRuler 100 bp DNA ladder (Thermo Fisher, SM0241) is used as reference. Gel is stained post-electrophoresis with gel red (41002, Biotium) and imaged using a UV light box and camera (Supplementary Fig. 5c).

Release of microgel particles. After droplet preparation, the emulsion droplets are incubated at 37 °C for ~30–60 min to allow strain-promoted azide-alkyne cycloaddition (SPAAC) reaction generating cross-linked networks. To release the microgel templates, we first pipet to remove excess oil underneath the droplet emulsion and then the droplet emulsion is washed 5–10 times. For each wash, a volume of HFE7500 oil equivalent to five times that of the droplet emulsion is added to the droplets and mixed by gentle inversion of the Eppendorf tube. This oil is then removed from underneath the droplets. After washing, a volume of PBS medium equivalent to five times that of the droplet emulsion is added to the droplets. This causes the droplets to coalesce during gentle inversion and release the microgel particles into the access aqueous phase.

Parallel drop maker. The parallel flow-focusing drop maker uses one oil stream and two aqueous inlets to create two distinct populations of same-size droplets that are mixed in incubation line before reaching the outlet of the channel and then collected into an Eppendorf tube (Supplementary Fig. 7). The flow-focusing nozzle is 55 μm × 55 μm. Flow rates of 1200 μl/h for the HFE7500 continuous phase oil and 300 μl/h for each of the two aqueous streams creates droplets of ~90 μm diameter. Syringe pumps (Harvard Apparatus, USA) are used to control the flow of different liquid streams.

Dye diffusion experiment. A parallel drop maker (Supplementary Fig. 7) is used to prepare two populations of ~90 μm diameter droplets, which are mixed on-chip before collection in an Eppendorf tube. One droplet population contains PBS + sodium fluorescein dye and the other droplet population contains only PBS. The mixed droplet population is incubated at 37 °C and imaged by microscopy at days 0, 1, 2, and 3. The green fluorescence intensity of the PBS-only-droplets is quantified using the line profile tool of Leica software. The mean fluorescence value of day zero PBS-only droplets was assumed to be the background and was subtracted from the day 1, 2, and 3 measurements.

DOX-inducible HEK293 stable cell line generation. Human embryonic kidney 293 cells (HEK293, passage#6, ATCC® CRL-1573™) are cultured in Dulbecco's modified Eagle's medium (DMEM) under standard cell culture conditions. The growth medium is supplemented with 15% (v/v) fetal bovine serum (FBS) and 1% (v/v) penicillin-streptomycin (P-S). To generate a stable Tet-On 3 G DOX-inducible green fluorescence protein (GFP)-expressing reporter-cell line, HEK-293 cells are transfected with hyperactive piggyBac transposase (pCMV-hyPBase, a kind gift from the Sanger Institute, UK)[30] and XLone-GFP (a gift from Xiaojun Lian; Addgene plasmid # 96930)[31] plasmid constructs (Supplementary Fig. 11). Lipofectamine 3000 (Thermofisher) is used to transfect the plasmids, 5 μg of the XLone-GFP and 2.5 μg of the pCMV-hyPBase, into the cells in 6-well plates according to the supplier's instructions. After 72 h of transfection, Blasticidine S is used at 10 μg/ml in DMEM with 5% FBS and 1% P-S for 10 days to select the stably transfected cells. Cells are treated with 4 μM DOX for 24 h to turn on the GFP expression and then FACS is used to isolate a pure population of cells having maximum GFP fluorescence intensity. Stable monoclonal cell lines of high DOX sensitivity were generated using limiting dilution method and expanded under Blasticidine S selection. Cells are maintained with selection pressure for all downstream experiments. Reporter-cells are repeatedly tested for mycoplasma by PCR.

Flow cytometry analysis for inducible GFP expression. Prior to flow cytometry analysis, encapsulated cells are released from the emulsion droplets. Initially, excess oil underneath the droplet emulsion is removed by pipetting and then the droplet emulsion is washed five times. For each wash, a volume of HFE7500 oil equivalent to five times that of the droplet emulsion is added to the droplets and mixed by gentle inversion of the Eppendorf tube. This oil is then removed from underneath

the droplets. After washing, volume of 20% PFO in HFE7500 oil equivalent to five times that of the droplet emulsion is then added and mixed by gentle inversion. This causes the droplet to coalesce into a single aqueous fraction. Fresh HFE7500, equivalent to five times the aqueous volume is then added to dilute the remaining PFO. This HFE7500/PFO mixture is removed and then three aqueous volumes of DPBS, containing 0.5 mM EDTA and pre-heated to 37 °C, is added to the cell-containing medium to allow the cells dissociate into single cells for 5 min. The cell suspension is gently mixed by pipetting to fully disperse cells and immediately used to quantify the GFP expression by flow cytometer. FlowJo is used to analyze these recorded data. Flow cytometry gating is performed based on corresponding DOX-untreated control reporter-cell population. Singlet cell population gating and a comparison of GFP expression in presence and absence of DOX are displayed in the Supplementary Fig. 13.

Reporting summary. Further information on research design is available in the Nature Research Reporting Summary linked to this article.

Data availability

Data supporting the findings of this work are available within the paper and its Supplementary Information files. A reporting summary for this Article is available as a Supplementary Information file. The datasets generated and analyzed during the current study are available from the corresponding author upon request. The source data underlying Figs. 3b (middle panel), 4c, d, e and Supplementary Figs. 4a–e, 5c, and 8a–c are provided as a Source Data file.

Code availability

The homemade MATLAB scripts are available from the corresponding author upon reasonable request.

References

1. Klein, A. M. et al. Droplet barcoding for single-cell transcriptomics applied to embryonic stem cells. *Cell* **161**, 1187–1201 (2015).
2. Wong, I. Y., Bhatia, S. N. & Toner, M. Nanotechnology: emerging tools for biology and medicine. *Genes Dev.* **27**, 2397–2408 (2013).
3. Kulesa, A., Kehe, J., Hurtado, J. E., Tawde, P. & Blainey, P. C. Combinatorial drug discovery in nanoliter droplets. *Proc. Natl Acad. Sci. USA* **115**, 6685–6690 (2018).
4. Shembekar, N., Chaipan, C., Utharala, R. & Merten, C. A. Droplet-based microfluidics in drug discovery, transcriptomics and high-throughput molecular genetics. *Lab Chip* **16**, 1314–1331 (2016).
5. Sarkar, S., Cohen, N., Sabhachandani, P. & Konry, T. Phenotypic drug profiling in droplet microfluidics for better targeting of drug-resistant tumors. *Lab Chip* **15**, 4441–4450 (2015).
6. Eyer, K. et al. Single-cell deep phenotyping of IgG-secreting cells for high-resolution immune monitoring. *Nat. Biotechnol.* **35**, 977–982 (2017).
7. Agresti, J. J. et al. Ultrahigh-throughput screening in drop-based microfluidics for directed evolution. *Proc. Natl Acad. Sci. USA* **107**, 4004–4009 (2010).
8. Kintses, B. et al. Picoliter cell lysate assays in microfluidic droplet compartments for directed enzyme evolution. *Chem. Biol.* **19**, 1001–1009 (2012).
9. Weiss, M. et al. Sequential bottom-up assembly of mechanically stabilized synthetic cells by microfluidics. *Nat. Mater.* **17**, 89–96 (2018).
10. Rakszewska, A., Tel, J., Chokkalingam, V. & Huck, W. T. S. One drop at a time: toward droplet microfluidics as a versatile tool for single-cell analysis. *NPG Asia Mater.* **6**, e133 (2014).
11. Holtze, C. et al. Biocompatible surfactants for water-in-fluorocarbon emulsions. *Lab Chip* **8**, 1632–1639 (2008).
12. Gruner, P. et al. Controlling molecular transport in minimal emulsions. *Nat. Commun.* **7**, 10392 (2016).
13. Chiu, Y. L. et al. Synthesis of fluorosurfactants for emulsion-based biological applications. *ACS Nano* **8**, 3913–3920 (2014).
14. Riechers, B. et al. Surfactant adsorption kinetics in microfluidics. *Proc. Natl Acad. Sci. USA* **113**, 11465–11470 (2016).
15. Wagner, O. et al. Biocompatible fluorinated polyglycerols for droplet microfluidics as an alternative to PEG-based copolymer surfactants. *Lab Chip* **16**, 65–69 (2016).
16. Sidore, A. M., Lan, F., Lim, S. W. & Abate, A. R. Enhanced sequencing coverage with digital droplet multiple displacement amplification. *Nucleic Acids Res.* **44**, e66 (2016).
17. Lan, F., Haliburton, J. R., Yuan, A. & Abate, A. R. Droplet barcoding for massively parallel single-molecule deep sequencing. *Nat. Commun.* **7**, 11784 (2016).

18. Cao, Z. Q. & Jiang, S. Y. Super-hydrophilic zwitterionic poly(carboxybetaine) and amphiphilic non-ionic poly(ethylene glycol) for stealth nanoparticles. *Nano Today* **7**, 404–413 (2012).

19. Badi, N. Non-linear PEG-based thermoresponsive polymer systems. *Prog. Polym. Sci.* **66**, 54–79 (2017).

20. Kameta, N., Dong, J. & Yui, H. Thermoresponsive PEG-coated nanotubes as chiral selectors of amino acids and peptides. *Small* **14**, e1800030 (2018).

21. Muraoka, T. et al. A structured monodisperse PEG for the effective suppression of protein aggregation. *Angew. Chem. Int. Ed. Engl.* **52**, 2430–2434 (2013).

22. Holt, D. J., Payne, R. J., Chow, W. Y. & Abell, C. Fluorosurfactants for microdroplets: interfacial tension analysis. *J. Colloid Interface Sci.* **350**, 205–211 (2010).

23. Etienne, G., Kessler, M. & Amstad, E. Influence of fluorinated surfactant composition on the stability of emulsion drops. *Macromol. Chem. Phys.* **218**, 1600365 (2017).

24. Kumar, S. et al. Introducing chirality into nonionic dendritic amphiphiles and studying their supramolecular assembly. *Chemistry* **22**, 5629–5636 (2016).

25. Weitz, D. A. Perspective on droplet-based single-cell sequencing. *Lab Chip* **17**, 2539 (2017).

26. Abate, A. R., Hung, T., Mary, P., Agresti, J. J. & Weitz, D. A. High-throughput injection with microfluidics using picoinjectors. *Proc. Natl Acad. Sci. USA* **107**, 19163–19166 (2010).

27. Brouzes, E. et al. Droplet microfluidic technology for single-cell high-throughput screening. *Proc. Natl Acad. Sci. USA* **106**, 14195–14200 (2009).

28. Theberge, A. B. et al. Microdroplets in microfluidics: an evolving platform for discoveries in chemistry and biology. *Angew. Chem. Int. Ed. Engl.* **49**, 5846–5868 (2010).

29. Thiam, A. R., Bremond, N. & Bibette, J. From stability to permeability of adhesive emulsion bilayers. *Langmuir* **28**, 6291–6298 (2012).

30. Yusa, K., Zhou, L., Li, M. A., Bradley, A. & Craig, N. L. A hyperactive piggyBac transposase for mammalian applications. *Proc. Natl Acad. Sci. USA* **108**, 1531–1536 (2011).

31. Randolph, L. N., Bao, X., Zhou, C. & Lian, X. An all-in-one, Tet-On 3G inducible PiggyBac system for human pluripotent stem cells and derivatives. *Sci. Rep.* **7**, 1549 (2017).

32. Wyszogrodzka, M. & Haag, R. A convergent approach to biocompatible polyglycerol "click" dendrons for the synthesis of modular core-shell architectures and their transport behavior. *Chemistry* **14**, 9202–9214 (2008).

33. Dey, P. et al. Mimicking of chondrocyte microenvironment using in situ forming dendritic polyglycerol sulfate-based synthetic polyanionic hydrogels. *Macromol. Biosci.* **16**, 580–590 (2016).

34. Mazutis, L. et al. Single-cell analysis and sorting using droplet-based microfluidics. *Nat. Protoc.* **8**, 870–891 (2013).

Acknowledgements

Author contributions

M.S.C. designed the research, analyzed the data and wrote the manuscript; W.Z. performed the PCR experiment and analyzed the data. S.K. and M.S.C. jointly contributed to scale up of DNA plasmid constructs and worked on transfected stable cell lines generation. J.H. analyzed the data and contributed to the writing. X.Z. assisted in writing. P.D. synthesized polymer precursors for microgel template preparation. D.W. and R.H. supervised the study, analyzed the data and wrote the manuscript.

Competing interests

Freie Universität Berlin and Harvard University have filed an international patent (PCT/EP2018070036) on these dendronized fluorosurfactants. M.S.C., R.H. and D.W. are affiliated with these organizations and the patent. The remaining authors declare no competing interests.

Additional information

Supplementary information is available for this paper at https://doi.org/10.1038/s41467-019-12462-5.

Correspondence and requests for materials should be addressed to D.A.W. or R.H.

Peer review information *Nature Communications* would like to thank Samuel Kim and other, anonymous, reviewers for their contributions to the peer review of this work. Peer review reports are available.

Reprints and permission information is available at http://www.nature.com/reprints

Publisher's note Springer Nature remains neutral with regard to jurisdictional claims in published maps and institutional affiliations.

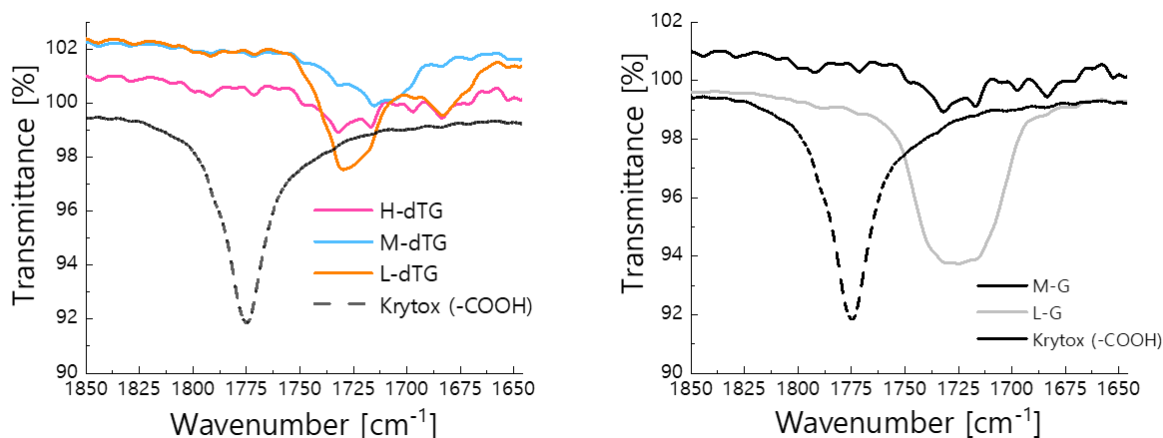**Supplementary Information (SI)**

Dendronized fluorosurfactant for highly stable water-in-fluorinated oil emulsions with minimal inter-droplet transfer of small molecules

Chowdhury et al.

Supplementary Figure 1. Characterization of the synthesized surfactants. We record FTIR spectra from viscous products of dendritic tri-glycerol (dTG)-based surfactants (left) and mono-glycerol (G)-based surfactants (right). When dTG- or G-precursor is used to functionalize Krytox of either high (H), medium (M), or low (L) molecular weight (MW), then either H-dTG, M-dTG, L-dTG, M-G or L-G is created. The unmodified carboxylic acid band of low molecular weight Krytox precursor shows strong peak at 1775 cm^{-1} on both figures (left and right) depicted by dotted lines (gray). The amide (-NH-CO-) stretching peaks, H-dTG (solid red line), M-dTG (solid green line), L-dTG (solid yellow line), M-G (solid black line), and L-G (solid gray line), from 1710-1740 cm^{-1} confirm the functionalization of low, medium, and high molecular weight Krytox terminuses with either dTG- or G-polar group.
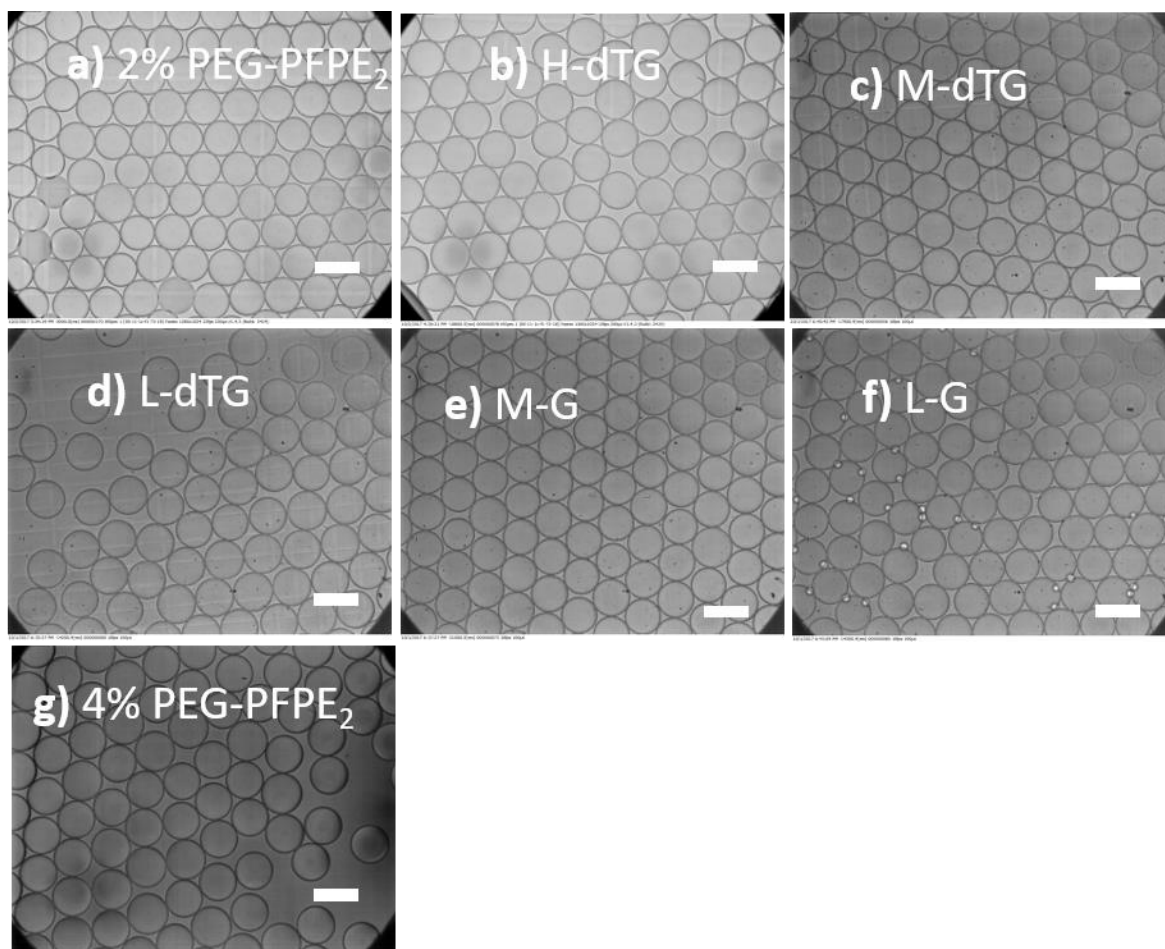
Supplementary Figure 2. Thermostability of the droplets before PCR thermocycle (pre-PCR). We use polydimethylsiloxane (PDMS) based microfluidic device to generate PCR-reagents carrying monodisperse droplets that are stabilized with 2% PEG-PFPE$_2$ surfactant (**a**), H-dTG surfactant (**b**), M-dTG surfactant (**c**), L-dTG surfactant (**d**), M-G surfactant (**e**), L-G surfactant (**f**), and 4% PEG-PFPE$_2$ surfactant (**g**). PEG-PFPE$_2$ is a reference surfactant in this study that uses PEG600 as a polar head group, which is a commercially available tri-block copolymer surfactant, EA surfactant, unlike our dendronized di-block surfactants. Droplets produced using the dTG, the G, and the PEG600-based surfactants showed no merging during >24h incubation at 4°C. Scale bar, 100 μm.
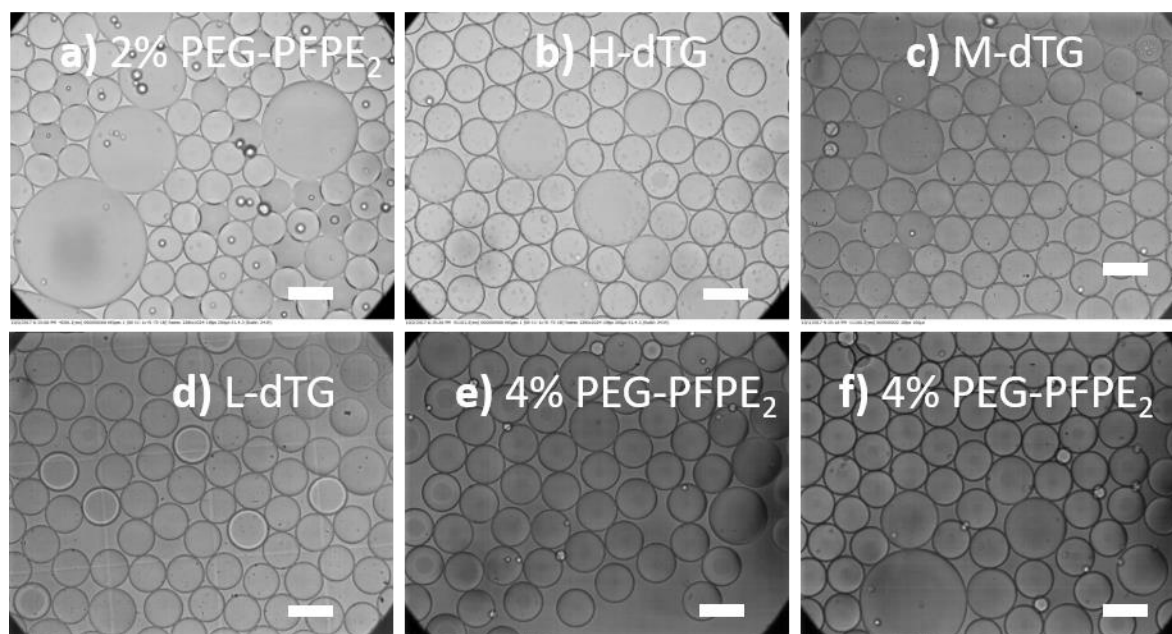
Supplementary Figure 3. Thermostability of the droplets after PCR thermocycle (post-PCR). We run a total of 35 cycles of PCR, which involves repeated thermal cycling from ~60°C to 98°C, enabling nucleic acid amplification. During PCR, droplets stabilized with commercially available PEG600-based surfactant (2% PEG-PFPE$_2$) showed substantial merging (**a**). H-dTG and M-dTG surfactants stabilized droplets showed some merging (**b** and **c** respectively). Surprisingly, the L-dTG surfactant stabilized droplets showed almost no merging (**d**). However, droplets stabilized with a higher concentration (4%) of PEG-PFPE$_2$ surfactant, performed as well as the H-dTG surfactant stabilized droplets (**e-f**). In contrast, droplets generated using mono-glycerol (G)-based surfactants (M-G, L-G) merged completely during the PCR, suggesting the lack of more polar hydroxy groups. Scale bar, 100 μm.
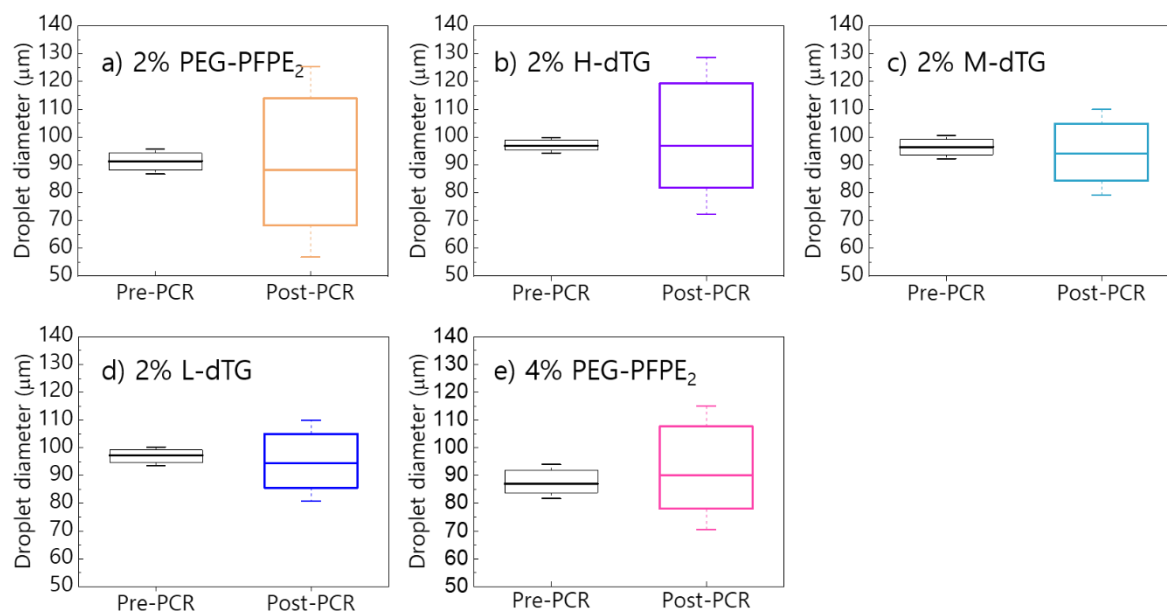
Supplementary Figure 4. Box-plot of droplet size distribution pre-and post-PCR. We run a total of 35 cycles of PCR, image a fraction of the droplets, and use a purpose-written Matlab script to analyze droplet size distribution. n = ~100 droplets for Pre-PCR size distribution analysis and n= ~200-400 droplets for Post-PCR size distribution analysis. The box plots represent the median (center line), mean ± s.d. (box), and mean ± 1.5 x s.d. (whisker). Source data of Supplementary Figures 4a-4e are provided as a Source Data file.
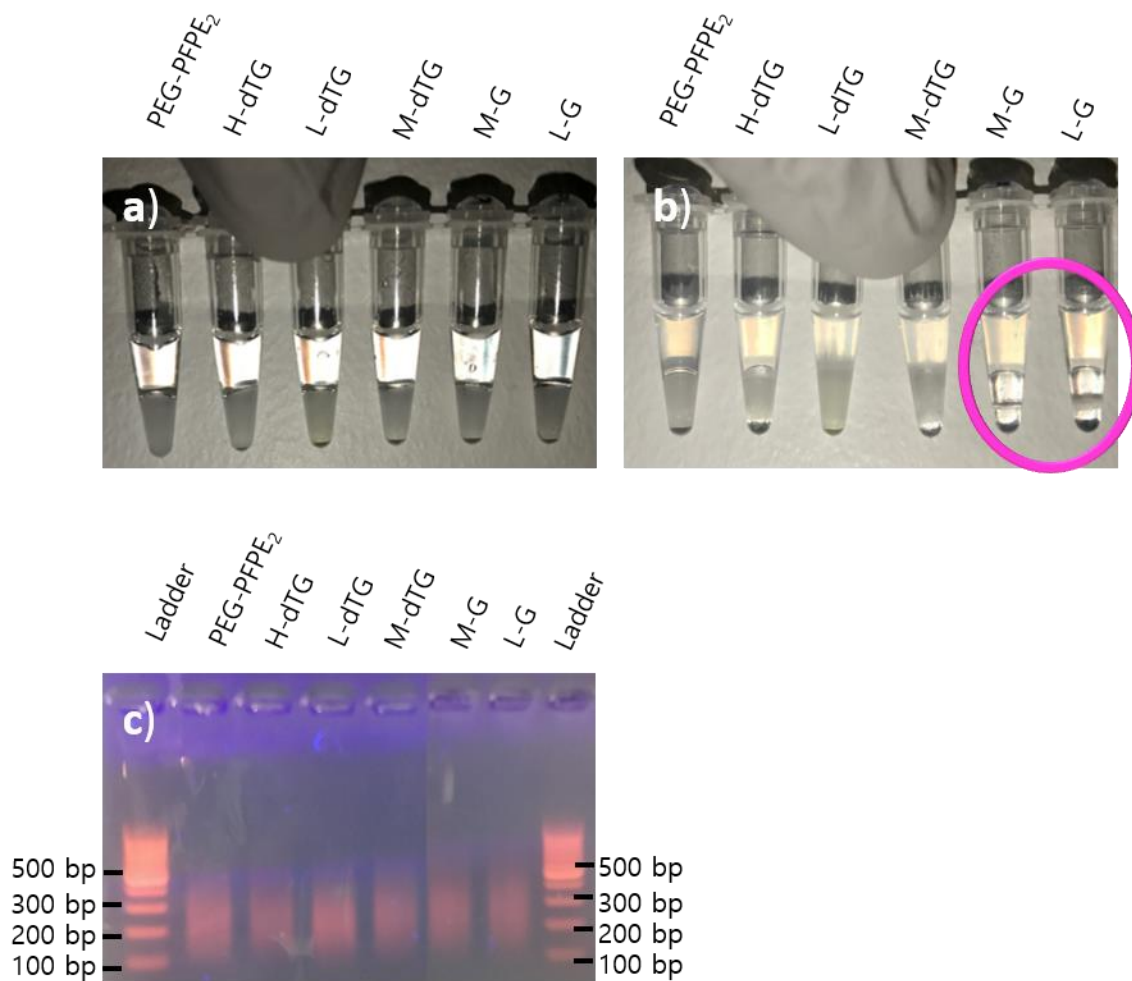
Supplementary Figure 5. Emulsion droplet integrity pre- and post-PCR, and analysis of PCR amplification product. a, For PCR thermocycling, we generate PCR-mix-containing droplets stabilized by six different surfactants (from left to right: 2% PEG-PFPE$_2$, H-dTG, L-dTG, M-dTG, M-G, L-G). We collect the emulsion droplets (gray bottom phase) in Eppendorf tubes and then add heavy mineral oil (bright phase) to prevent evaporation during PCR cycling. Prior to cycling, droplet emulsions are stable, as indicated by homogeneous droplet layer underneath the layer of mineral oil. **b,** Analysis of the post-PCR emulsions reveals that droplets made with M-G and L-G surfactants are not stable, as indicated by the water layer, resulting from merged droplets, below the mineral oil (see tubes regions circled in red). PEG-PFPE$_2$, H-dTG, and M-dTG surfactants performed better in PCR, as shown by the small water layer

between the mineral oil and emulsion droplet layers. Notably, no droplet merging is seen in the L-dTG stabilized emulsion droplets, indicating suitability of L-dTG surfactants in thermal-cycling applications. **c,** We electrophorese 10 µl of the 40 µl aqueous phase collected from breaking the droplets on 2% agarose gel to confirm that surfactants are free from PCR-inhibitors. 0.5 µg of 100 bp ladder was loaded into the first and last lanes. None of the surfactants inhibited PCR, as indicated by the strong amplification product in each sample lane. The products are a mixture of molecular weights because the phage genomic DNA is sheared randomly by Nextera Tagmentation and amplified using primers to the added tag DNA sequence. Each 40 µl PCR contained 16 pg of input DNA; thus, the unamplified product is not visible on this type of gel (data not shown). Source data of Supplementary Figure 5c is provided as a Source Data file.
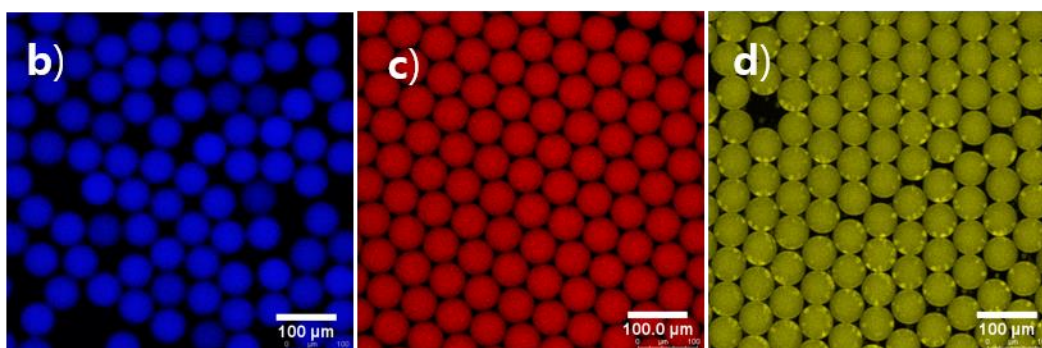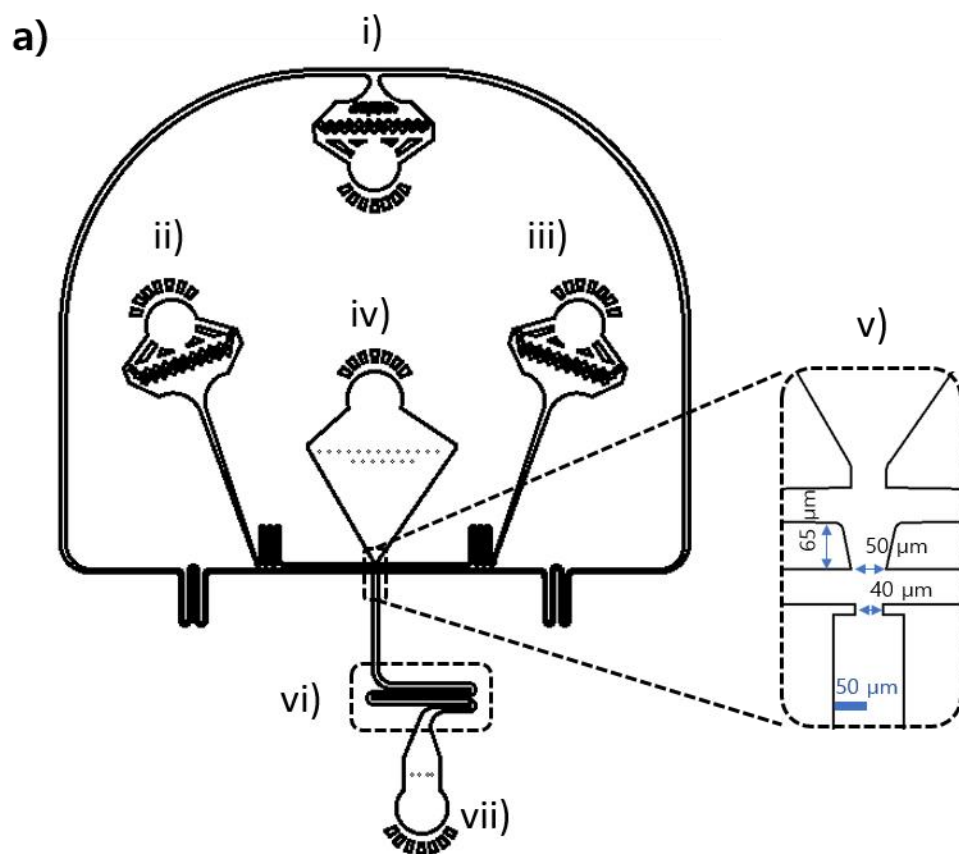
Supplementary Figure 6. Single drop making microfluidic device for click-chemistry based microgel template preparation in droplets stabilized by dendritic tri-glycerol (dTG)-based surfactants. a, This device produces monodisperse droplets. Inlet for surfactant-containing HFE7500 oil continuous phase (i). Inlets for different polymer precursor solutions (ii and iii). Additional inlet to encapsulate cells or to inject aqueous medium carrying different solutes (iv). Flow focusing junctions to make micrometer sized microgel droplets. The cross-section of the flow-focusing nozzle at

the pinch-off area is 40 μm x 50 μm (v). Delay line keeps droplets spaced while surfactant molecules orient at oil-water interface (vi). Outlet for the polymer precursors containing droplets (vii). This PDMS device allows us to fabricate microgels with 20% (w/v) polyanionic dendritic polyglycerol sulfate azide (dPGS-N$_3$), 20% (w/v) homobifunctional PEG dicyclooctyne (PEG-DIC), and 1% (w/v) of mono-fluorophore functionalized PEG-DIC that undergo SPAAC reaction in droplets, creating cross-linked networks[1,2]. Flow rates of 750 μl/h for the surfactant-containing HFE7500 continuous phase oil, 67 μl/h for the dPGS-N$_3$ aqueous phase, 133 μl/h for the PEG-DIC aqueous phase, and 40 μl/h for an additional aqueous phase containing only PBS medium create droplets of ~50 μm diameter. The overall polymer concentration in the aqueous phase is ~17% (w/v). We click-label the microgels with blue (3-azido-7-hydroxycoumarin, Jena Bioscience), red (Sulfo-Cy5-Azide, Jena Bioscience), and yellow (5/6-Sulforhodamine B-PEG$_3$-Azide, Jena Bioscience) fluorophores when the droplets are stabilized with H-dTG (**b**), M-dTG (**c**), and L-dTG (**d**) surfactants respectively. Long-term or short-term incubation of the droplets shows no inter-microgels cross-linking, suggesting that dendritic tri-glycerol (dTG)-based H-dTG, M-dTG, and L-dTG surfactants can stabilize viscous aqueous droplets and allow formation of cross-linked polymer networks.
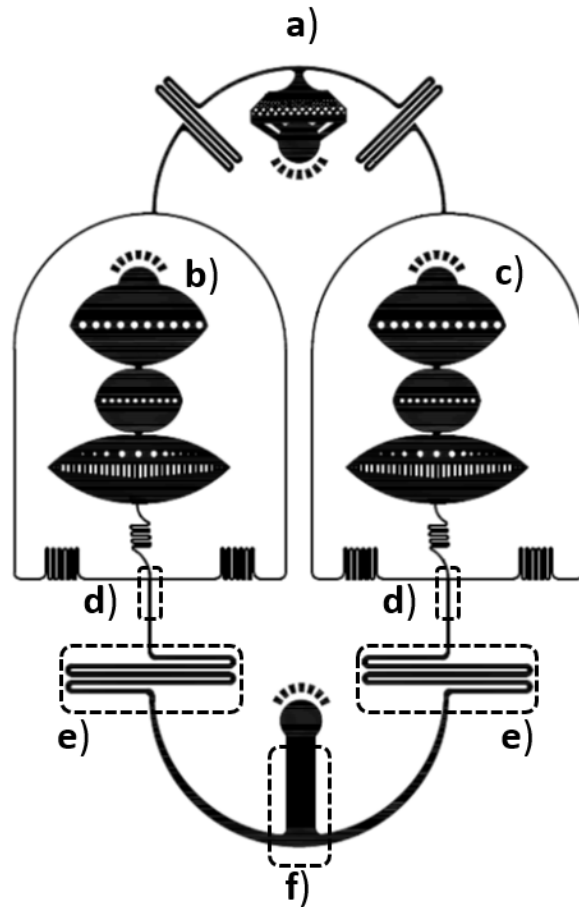
Supplementary Figure 7. Design of parallel drop making microfluidic device. This device produces a mixture comprising equal amounts of two different populations of droplets. **a,** Inlet for surfactant-containing HFE7500 oil continuous phase. **b,** and **c,** Inlets for different aqueous phases. **d,** Flow focusing junctions to make micrometer sized aqueous droplets. **e,** Delay line keeps droplets spaced while surfactant molecules orient at oil-water interface. **f,** The two different droplet populations join and mix in this broad channel prior to exiting the device.
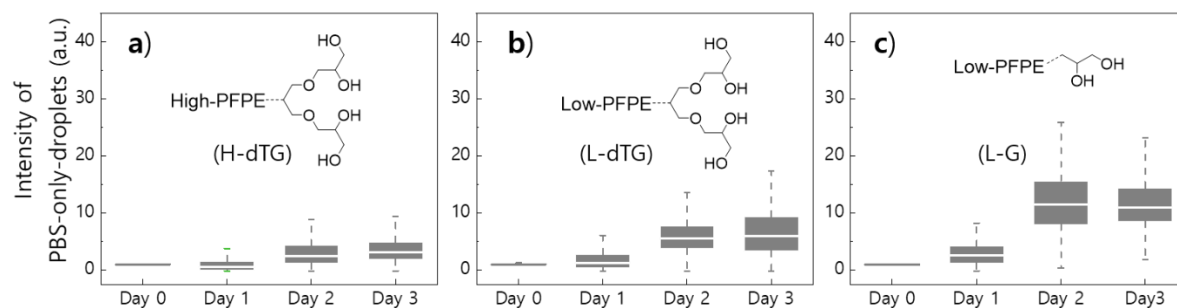
Supplementary Figure 8. Influence of long and short fluorinated tails and dense hydrogen bond network on inter-droplet diffusion. For each surfactant, we use a parallel drop maker (Supplementary Figure 7) to create a mixture comprising equal amounts of PBS-only-droplets and PBS+sodium fluorescein salt-containing droplets. We incubate these mixtures, take confocal images at the indicated time points, and then perform quantitative analysis of the fluorescence intensity of the 10 randomly selected PBS-only droplets. Box-plot shows that in droplets stabilized by H-dTG, there is almost no increase in green signal intensity after 24h incubation (**a**), while some increase was detected in L-dTG stabilized droplets (b), indicating that the loner fluorinated tail of H-dTG contributes to improved resistance to inter-droplet diffusions. To assess the effect of head groups capable of forming a dense hydrogen bond network, we compare L-dTG and L-G.   Quantitatively, after 24h incubation, the fluorescence intensity of PBS-only drops stabilized by L-G, was, 1.5 times the intensity measured in PBS-only droplets stabilized by L-dTG surfactants, indicating that a dense hydrogen bond network at the oil-water interface also reduces leakage of small water-soluble molecules (compare panels **b** and **c**). In droplets stabilized by H-dTG, having long fluorinated tails and head groups capable of forming a dense hydrogen bond network, the fluorescent signal in PBS-only droplets was one third that seen for droplets stabilized by L-G, which has short fluorinated tails and head groups capable of only limited hydrogen-bonding. This indicates that long fluorinated tail groups and head groups capable of forming a dense hydrogen bond network can function together within the same surfactant molecule. The box plots represent the median

(center line), the interquartile range (box) and the non-outlier range (whiskers). Source data of Supplementary Figures 8a-8c are provided as a Source Data file.
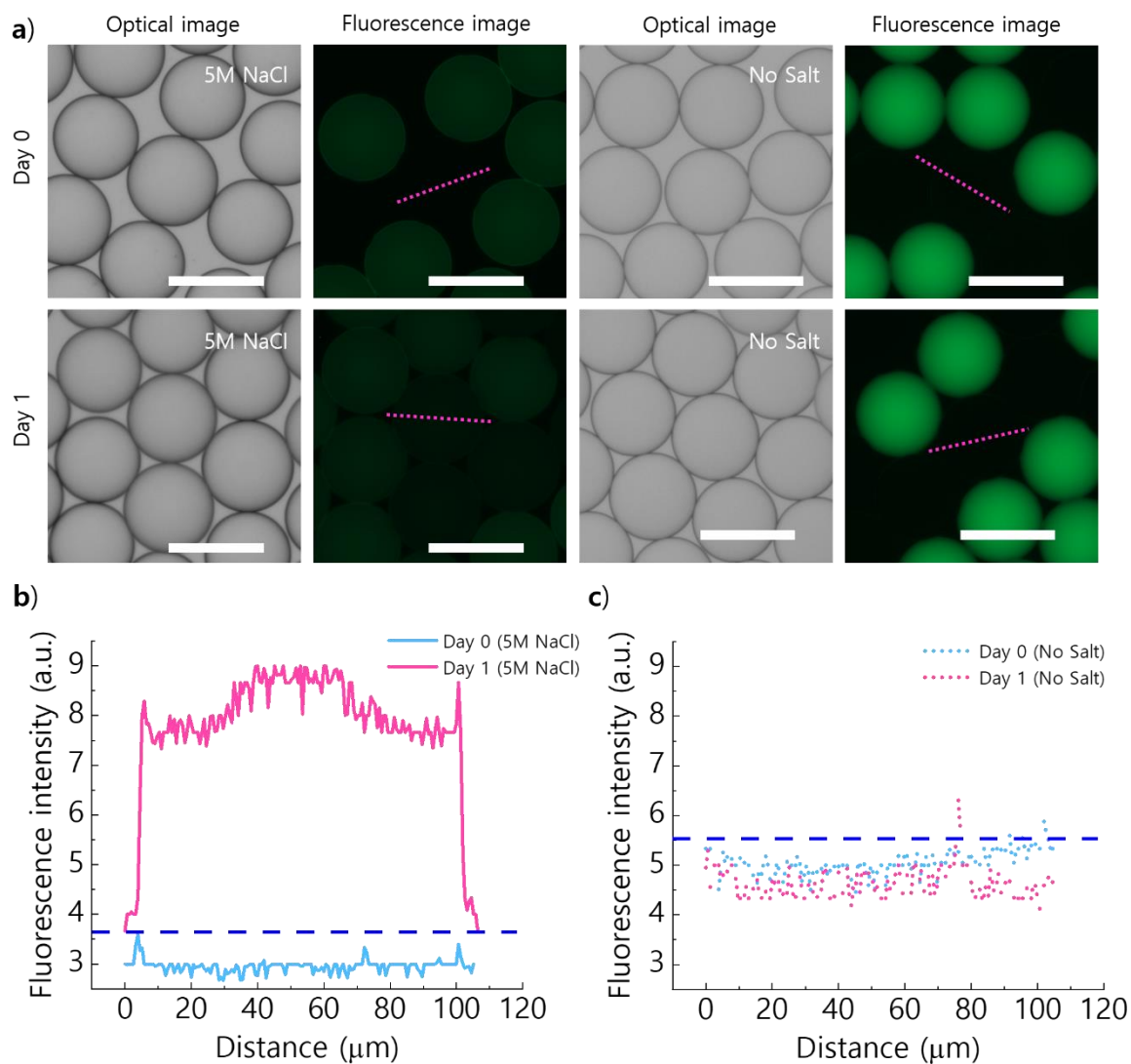
Supplementary Figure 9. Characterization of inter- and intra-molecular hydrogen bonds from dendritic tri-glycerol head groups. To test the contribution of hydrogen-donor activity of the hydroxyl groups in oligo-glycerol-based surfactants, we test if a high salt concentration, known to form ion-dipole interactions and disrupt inter-and intramolecular hydrogen bonding, decreases dye retention in droplets stabilized with the oligo-glycerol-based surfactant M-dTG. We use a parallel drop
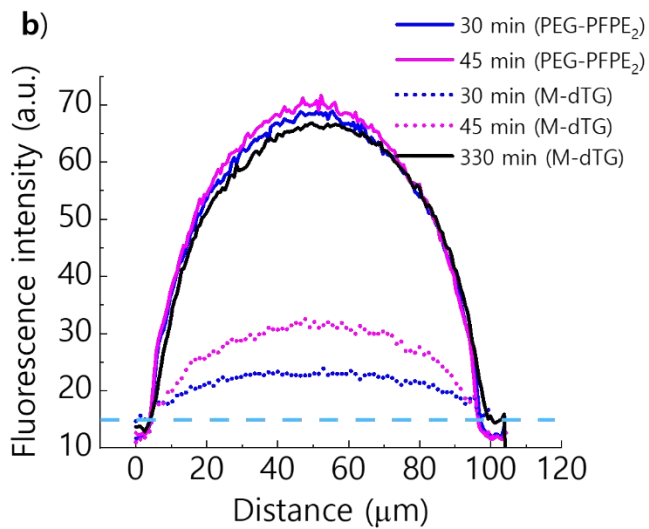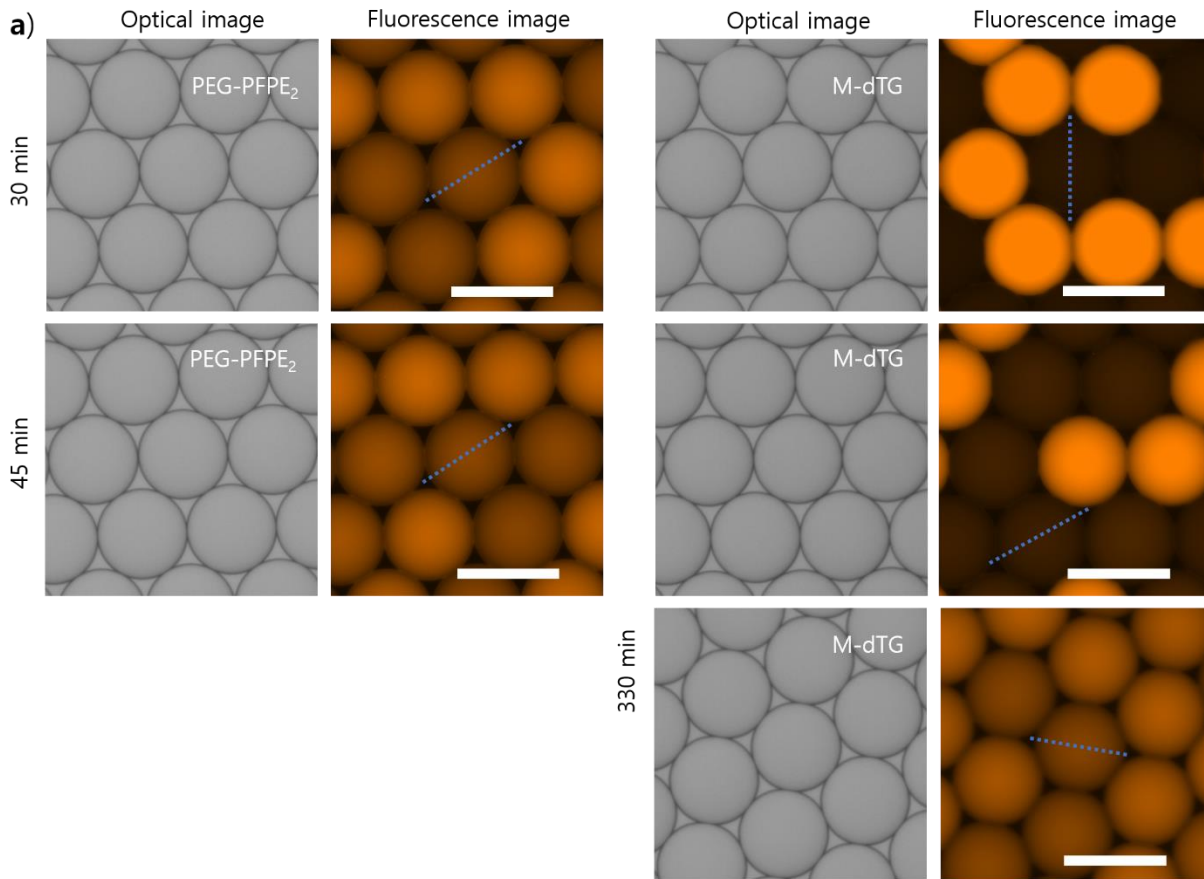
maker (Supplementary Figure 7) to create a mixture comprising equal amounts of PBS-only-droplets and PBS+sodium fluorescein salt-containing droplets (No salt droplets), and a mixture comprising equal amounts of PBS+5M NaCl droplets and PBS+5M NaCl+sodium fluorescein salt-containing droplets (5M NaCl droplets). We incubate these mixtures, take fluorescence images at the indicated time points, and then use Image J Plot Profiling to perform quantitative analysis of the fluorescence intensity of the PBS-only droplets and PBS+5M NaCl droplets **(a-c)**. Scale bar, 100 μm. Note, the fluorescence emission intensity of sodium fluorescein salt is known to be reduced in the presence of high salt. Thus, our No Salt droplets have much higher overall intensity than the 5M NaCl droplets. However, this does not affect the interpretation of the data, as we separately compare the increase in fluorescence of the empty droplets from day zero to day one.

Supplementary Figure 10. Inter-droplet diffusion of resorufin dye is minimized by surfactant having head group capable of forming a dense hydrogen bond network. We use M-dTG surfactant, as we have shown that droplets stabilized with this surfactant retain sodium fluorescein dye better than droplets stabilized with other

oligo-glycerol based surfactants (see Fig. 3a in the main text). For comparison, we use droplets stabilized with commercially available PEG-PFPE$_2$ at 4% w/w, as this gives roughly equimolar concentration to 2% M-dTG. For each surfactant, we use a parallel drop maker (Supplementary Figure 7) to create a mixture comprising equal amounts of PBS-only-droplets and PBS+resorufin-containing droplets. We incubate these mixtures at room temperature, take fluorescence images at the indicated time points, and then use the Image J Plot Profiling tool to perform quantitative analysis of the fluorescence intensity of the PBS-only droplets. **a,** Micrographs of the resorufin-containing droplets demonstrates that resorufin transfer between M-dTG-stabilized droplets is much less than resorufin transfer between PEG-PFPE$_2$ stabilized droplets. Scale bar, 100 μm. **b,** Intensity profile of PBS-only droplets stabilized with PEG-PFPE$_2$ and M-dTG surfactants at the indicated time points. The corresponding fluorescence images can be seen in Supplementary Figure 10(a).

(a)　　　　　　　　　　(b)　　　　　　　　　　(c)
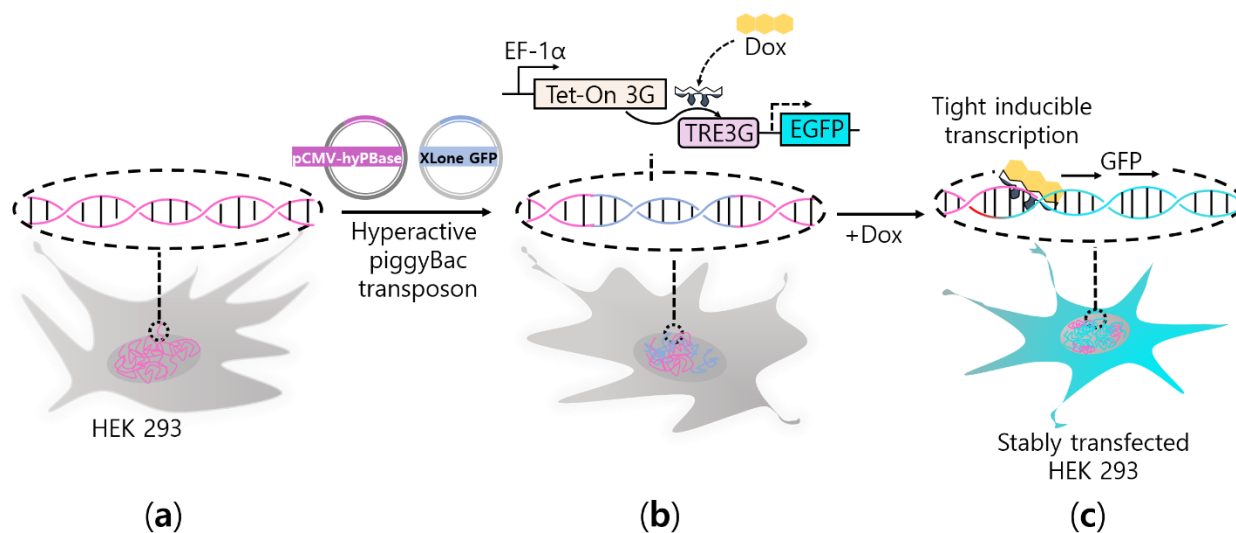
Supplementary Figure 11. Schematic representation of DOX-inducible stable cell line generation. a, HEK 293 cell line with native genome (red). **b,** Transposase from pCMV-hyPBase stably integrates XLone-GFP plasmid construct into the cell genome (light blue), generating DOX-sensitive reporter cell line (DOX-GFP-HEK 293) **c,** When DOX (yellow) binds to a trans-activator protein, cell produces green fluorescence protein (GFP).
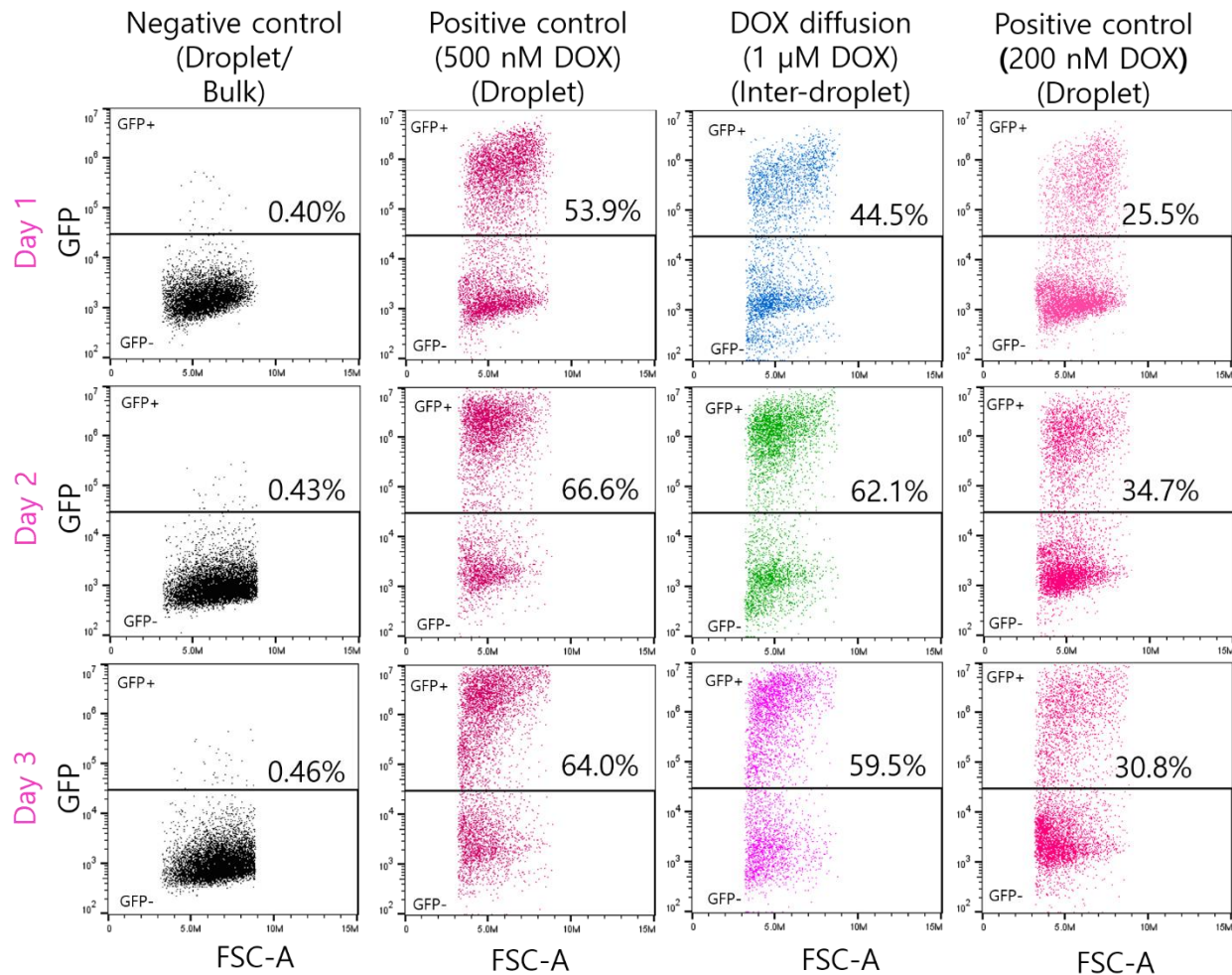
Supplementary Figure 12. DOX-inducible GFP-reporter cells to quantify drug transfer between PEG-PFPE$_2$ surfactant-stabilized droplets. We used 4% (w/w) PEG-PFPE$_2$ as a reference surfactant dissolved in HFE7500 oil and the parallel drop maker to generate homogenous mixtures in which 50% of the droplets contained DOX (at the indicated concentrations) and 50% contain no DOX. Due to Poisson distribution during cell encapsulation, ~40% of droplets that lack DOX contained at least one cell and the remaining ~10% of the droplets were empty. We incubated droplets at 37°C for the indicated times, isolated the cells from the droplets, and quantified the GFP+ cells using flow cytometry. GFP intensity is plotted against forward scatter-area (FSC-A). For the Positive Control (Droplet), all droplets, including those with cells, contained DOX at the indicated concentration.
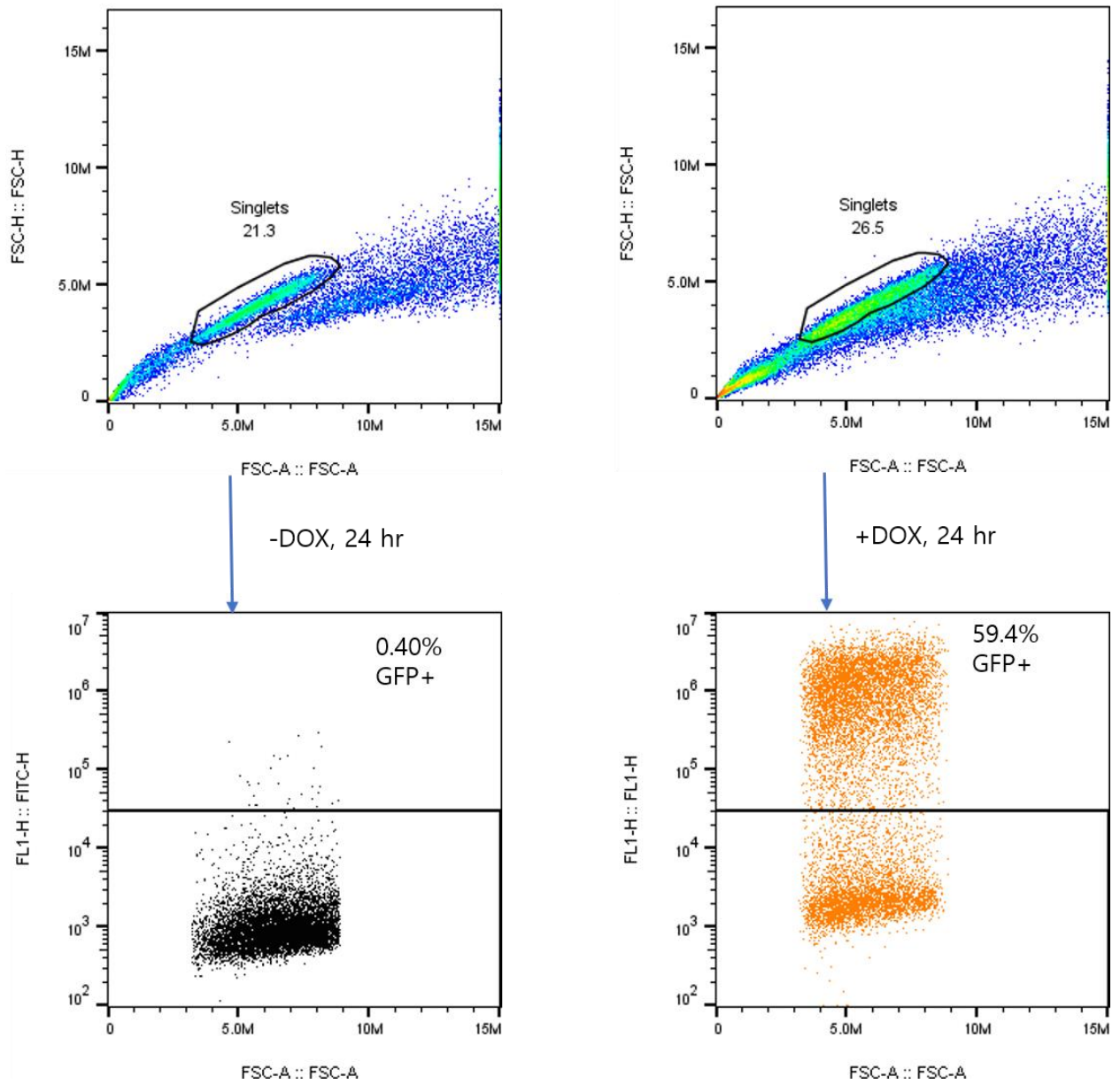
Supplementary Figure 13. Singlet cell population gating and comparison of GFP expression with and without DOX. Singlet cell population was selected from FSC-H/FSC-A gate to plot GFP intensity against forward scatter-area (FSC-A).

References

1. Dey P, Schneider T, Chiappisi L, Gradzielski M, Schulze-Tanzil G, Haag R. Mimicking of Chondrocyte Microenvironment Using In Situ Forming Dendritic Polyglycerol Sulfate-Based Synthetic Polyanionic Hydrogels. *Macromol. Biosci.* **16**, 580-590 (2016).

2. Steinhilber D, Rossow T, Wedepohl S, Paulus F, Seiffert S, Haag R. A microgel construction kit for bioorthogonal encapsulation and pH-controlled release of living cells. *Angew. Chem., Int. Ed. Engl.* **52**, 13538-13543 (2013).

3.2 Linear triglycerol-based fluorosurfactants show high potential for droplet-microfluidics-based biochemical assays
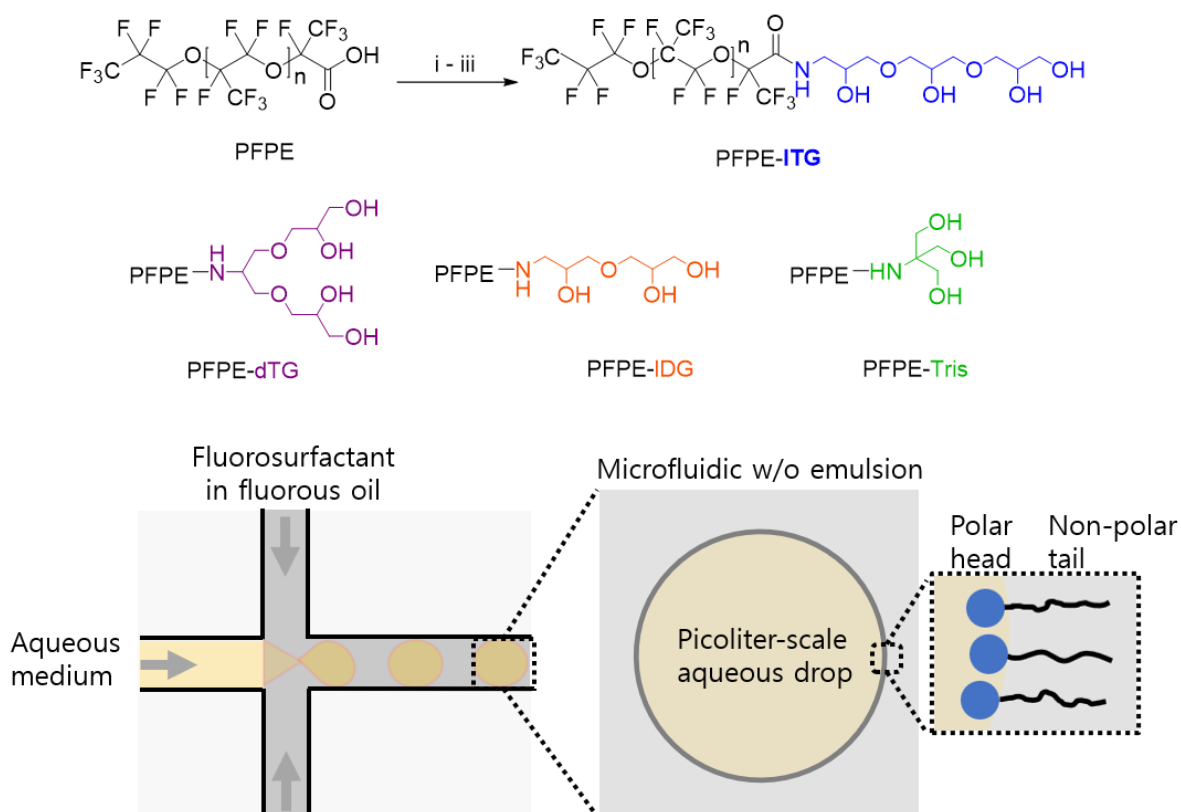
M.S. Chowdhury, W. Zheng, A. K. Singh, I. L. H. Ong, Y. Hou, J. Heyman, A. Faghani, E. Amstad, D. A. Weitz, R. Haag

Submitted to Soft Matter

Author's contributions: In this publication the author contributed to the concept and design, and performed all the synthesis, most of the characterization, and data evaluation, as well as wrote the draft of the manuscript.

Linear triglycerol-based fluorosurfactants show high potential for droplet-microfluidics-based biochemical assays

Mohammad Suman Chowdhury,[a] Wenshan Zheng,[b] Abhishek Kumar Singh,[a] Irvine Lian Hao Ong,[c] Yong Hou,[a] John A. Heyman,[d] Abbas Faghani,[a] Esther Amstad,[c] David A. Weitz,[d] Rainer Haag*[a]

[a] M.S. Chowdhury, Dr. A.K. Singh, Dr. Y. Hou, Dr. A. Faghani, Prof. R. Haag
Institut für Chemie und Biochemie
Freie Universität Berlin
Takustrasse 3, 14195 Berlin, Germany
E-mail: haag@chemie.fu-berlin.de
[b] Dr. W. Zheng
Department of Chemistry and Chemical Biology
Harvard University
Cambridge, Massachusetts 02138, USA
[c] Dr. I. L. H. Ong, Prof. E. Amstad
Soft Materials Laboratory, Institute of Materials
École Polytechnique Fédérale de Lausanne
1015 Lausanne, Switzerland
[d] J. A. Heyman, Prof. D. A. Weitz
School of Engineering and Applied Sciences, Department of Physics
Harvard University
29 Oxford Street, Cambridge, MA 02138, USA

Supporting information for this article is given via a link at the end of the document.

Abstract: Fluorosurfactants have expanded the landscape of high-value biochemical assays in microfluidic droplets, but little is known about how spatial geometries and polarity of head group contribute to fluorosurfactant performance. To decouple this, we design, synthesize, and characterize two linear and two dendritic glycerol- or tris-based surfactants with a common perfluoropolyether tail. To reveal the influence of spatial geometry, we choose inter-droplet cargo transport as a stringent test case. Using surfactants with linear di- and triglycerol, we show that inter-droplet cargo transport is minimal compared with their dendritic counterparts. We also demonstrate that the post-functionalization of PFPE-lTG having a linear geometry and four hydroxy groups enables 'from-droplet' fishing of biotin-streptavidin protein complex without trading off between fishing efficiency and droplet stability. Thus, our approach to design user-friendly surfactants reveals aspects of spatial geometry and facile tunability of the polar head groups that have not been captured or exploited before.

Droplet microfluidics has gained a momentum in bioanalytics where millions of pico- to nanoliter-volume drops are created, monitored, and sorted at kHz rates.[1] These drops are often metastable, leading to premature coalescence, and to enhance, their metastability fluorosurfactant is employed.[2] Typically, the fluorosurfactant is dissolved in a compatible bio-inert-fluorinated oil that contains a high amount of dissolved oxygen and is immiscible with aqueous and organic solvents, making it an ideal platform for immersing biomolecule captured droplets in it.[3,4] This feature has galvanized many exciting micro-droplets based research and product developments in chemistry and biology,[2] including synthesis of small organic molecules,[5] single-cell barcoding,[6] single-cell ChIP-seq,[4] directed enzymatic evolution,[7] therapeutic antibody discovery,[8] combinatorial drug screening,[9] digital ELISA.[10] To produce the water-in-fluorinated oil (w/o) emulsion droplets, typically, poly(dimethyl siloxane) (PDMS)-based microfluidic devices are used that provide an unprecedented control over droplet size, droplet scalability, and droplet analyses, covering a broad spectrum of miniaturized applications requiring a high-throughput platform.[11]

A commercially available PEG-PFPE$_2$, poly(ethylene glycol)-perfluoropolyether tri-block fluorosurfactant, is widely used to make monodisperse emulsion droplets.[12] Although it enables many droplet-based applications, it primarily suffers from four key issues: rapid inter-droplet molecular transport, low droplet stability, synthesis complexity due to polydisperse polymer chains used, and batch-to-batch variation, which limits its use in high-throughput drug-screening and directed enzymatic evolution.[13-17] Ultimately, the droplets stabilized with this surfactant do not resemble a sealed micro-reactor that should not suffer from these limitations. To address these issues, we recently reported a dendronized di-block fluorosurfactants that clearly outperformed the PEG-PFPE$_2$ surfactant in many aspects.[14] Even though other small polar molecules, such as oligo(ethylene glycol), monosaccharides, and poly(ethylene glycol), have been used to generate di-block PFPE surfactants, they often suffer from droplet instability.[18,19] However, fluorosurfactant with hexaethylene glycol was found to be more effective than its cyclic crown ether counterpart.[18] Remarkably, an earlier study shows that, although both linear and dendritic small compounds can have the same molecular weight, their spatial geometries can profoundly influence the anti-fouling properties of a 2D surface modified with self-assembled monolayer (SAM),[20] justifying the importance of different spatial geometries of small molecules in different respects.

Furthermore, fluorosurfactants that can be readily post-modified to customize the droplet interface are scarce. Although heterobifunctional PEG-based di-block copolymer fluorosurfactants have been reported, they are not user friendly due to either tedious synthesis protocols of the effective head groups before surfactant synthesis, lack of controllable coupling reaction, purification complexity as PEG-based surfactants
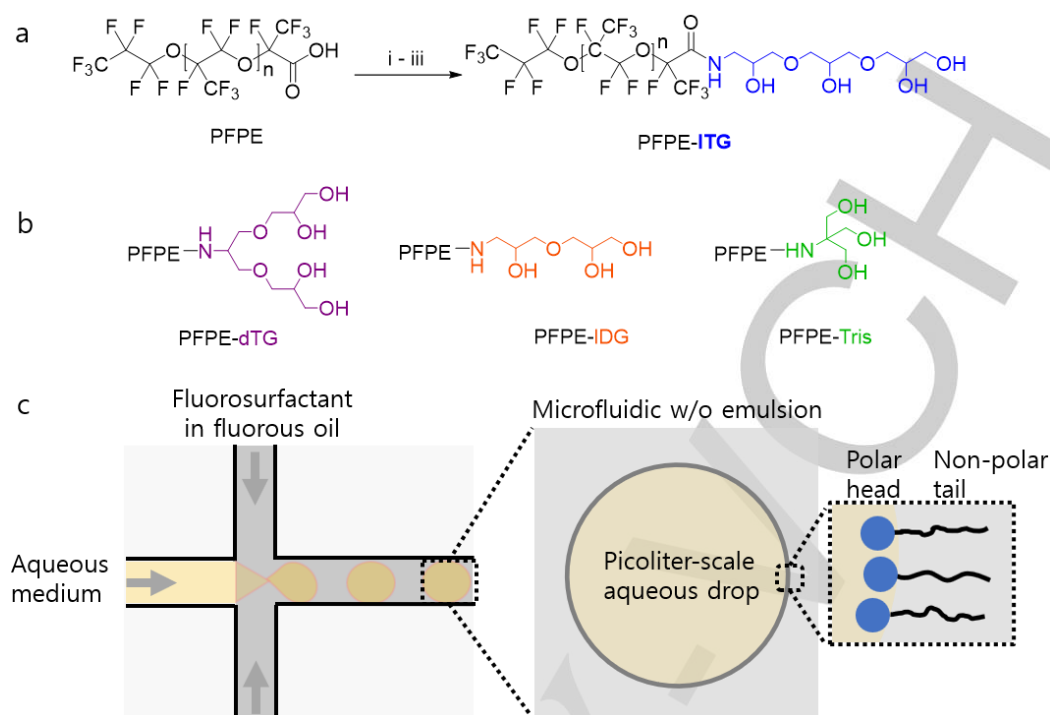
Figure 1. (a) Synthetic approach to linear triglycerol fluorosurfactant through amide coupling: (i) (COCl)$_2$, HFE7100, cat. DMF, rt, overnight; (ii) acetal protected linear triglycerol-NH$_2$, TEA, rt, overnight; (iii) H$^+$, CH$_3$OH-HFE7100, reflux, overnight. (b) Schematic illustration of the surfactants with different head groups. (c) A microfluidic approach for droplet generation (left). Surfactant orientation at the interface of water and oil (right).

readily form emulsion with organic solvents, or they often compromise with the stability of the droplets, their monodispersity, and, most importantly, with the number of functional groups at the droplet interface.[21,22] Hence, a fluorosurfactant that can be readily post-modified with a wide variety of chemical functionalities using a facile and user-friendly chemistry, and easily purified in a high yield is advantageous. Therefore, novel polar groups that can meet these requirements are needed to design and synthesize a tunable fluorosurfactant and to cover a broad spectrum of bioanalytics in microfluidic droplets.

Here, we contribute to the goal of rational surfactant design and report four surfactants containing either a linear or a dendritic spatial geometry with either three or four hydroxy groups and a common fluoro-tail. Using thin layer chromatography, we measured their polarity indexes to explore how different polarity can potentially alter their physicochemical functions. In addition, we evaluated their surface tension values to demonstrate whether a polar head group with different spatial geometries can alter surface activity of the surfactants and influence downstream applications. When these surfactants were tested to stabilized micro-droplets and minimize inter-droplet small-molecule transfer, we detected that although they could stabilize the droplets, their performance in cargo retention varied significantly. This is particularly important because a high cargo retention capability can greatly increase the data quality of drug-screening assays. Besides, we chose PFPE-lTG, the best-performing surfactants among all, for a post-modification. We found that it can be easily customized under mild conditions. Most importantly, the functional surfactant could generate robust

water-in-oil emulsions and provide a reactive droplet interface to fish biomolecules from droplets, in addition to offering an easy purification and a high-yield isolation. We thus systematically exploit the aspects of these surfactants with respects to inter-droplet molecular transport, and from-droplet fishing, in addition to giving some fundamental insights.

To synthesize linear and dendritic di-block fluorosurfactants, we freshly prepared activated perfluoropolyether (PFPE) tails, bearing acyl chloride at the terminus, which further reacted with acetal-protected amine-containing head groups in order to generate a stable amide bond between the tail and the head groups. Following a facile acetal deprotection under mild acidic conditions, the head groups became highly polar, which created a di-block fluorosurfactant, typically, in high yields of 70-80%. We employed an excess of the head group components to achieve full conversion of the activated fluorous tail. As fluorous solvents such as HFE7100 and HFE7500 are immiscible in organic solvents,[3] multiple post-reaction washing with an excess of either methanol or dimethylformamide (DMF) removes the unreacted head groups and other possible impurities. We synthesized two triglycerol-based surfactants, both having four hydroxy (-OH) groups and a commercial PFPE tail, but one being a linear triglycerol, lTG, and the other being a dendritic triglycerol, dTG. Both produce a linear and a dendritic diblock surfactants: PFPE-lTG and PFPE-dTG, respectively (**Figure 1**). Also, we synthesized two surfactants that were composed of three -OH groups containing linear diglycerol or tris and a PFPE tail, creating PFPE-lDG or PFPE-Tris, respectively (**Figure 1**).

2

Both the less polar PFPE-IDG and PFPE-Tris surfactants help us demonstrate three crucial things: how the interfacial tension (IFT) may vary due to lack of one -OH, the minimum number of -OH groups needed to obtain an optimal droplet stability, and cross-check the impact of three-hydroxy-carrying linear or dendritic spatial geometries with the four-hydroxy-carrying linear or dendritic one, respectively.
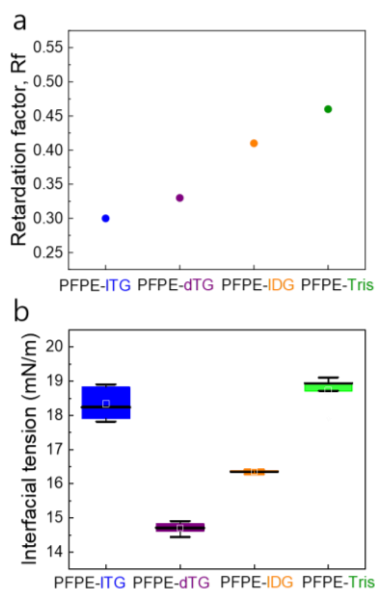

Figure 2. (a) Rf values on silica indicating the polarity of fluorosurfactants (left). A mixture of 20% methanol (v/v) and HFE-7100 was used as the elution solvent. (b) Interfacial tension (IFT) of the fluorosurfactants measured under identical test conditions (right) by the hanging drop method. Deionized water and 1% (w/w) surfactant containing HFE-7500 oil were used to measure the IFT between water drop and HFE-7500 oil at 25 °C.

Although different spectroscopic methods can be used to characterize the surfactants, for instance, NMR, IR,[21] we analyzed them using thin layer chromatography on silica plates (TLC) to investigate the polarity index of all four surfactants by means of a retardation factor (Rf), which would otherwise be extremely difficult by the available spectroscopic means due to solubility issues. We found that the PFPE-dTG and PFPE-ITG showed marginally different Rf values: ~0.33 and ~0.3, respectively, despite having an equal number of hydroxy groups. By contrast, PFPE-Tris had the maximum Rf of ~0.46 among all four surfactants, whereas its counterpart PFPE-IDG had Rf ~0.41 **(see Figure 2a and Figure S1)**. We attribute this polarity variation between equal hydroxy-containing surfactants to the ratio of primary vs. secondary hydroxy groups in the head groups, reflecting their different interactions with the polar silica surface. Additionally, we found no unreacted PFPE-COOH in the surfactant bands, qualitatively, suggesting no PFPE acid impurity was left and the amide coupling between the polar head and the non-polar tail was successful.

To understand the influence of the -OH group number and spatial geometry of the head on interfacial tension (IFT), we tested the surface tension of all four surfactants. We used 1% surfactant by weight in HFE7500 oil to measure the IFT in MQ water. We found that the PFPE-dTG reduces the IFT more than the other three surfactants do, where IFTs of PFPE-ITG and

PFPE-Tris show significantly higher values, indicating different surface interactions (**Figure 2b**).

Although the difference of IFT values between PFPE-ITG and PFPE-dTG surfactants was at the minute level, this result encouraged us to investigate the inter-droplet molecular transport behavior by these surfactants to justify a known concept that a higher IFT is advantageous to reduce the inter-droplet molecular transport.[23] Besides, this stringent test helped us to understand how the linear or dendritic spatial geometry of four-hydroxy-containing surfactants PFPE-ITG or PFPE-dTG, respectively, influence the inter-droplet molecular transport.
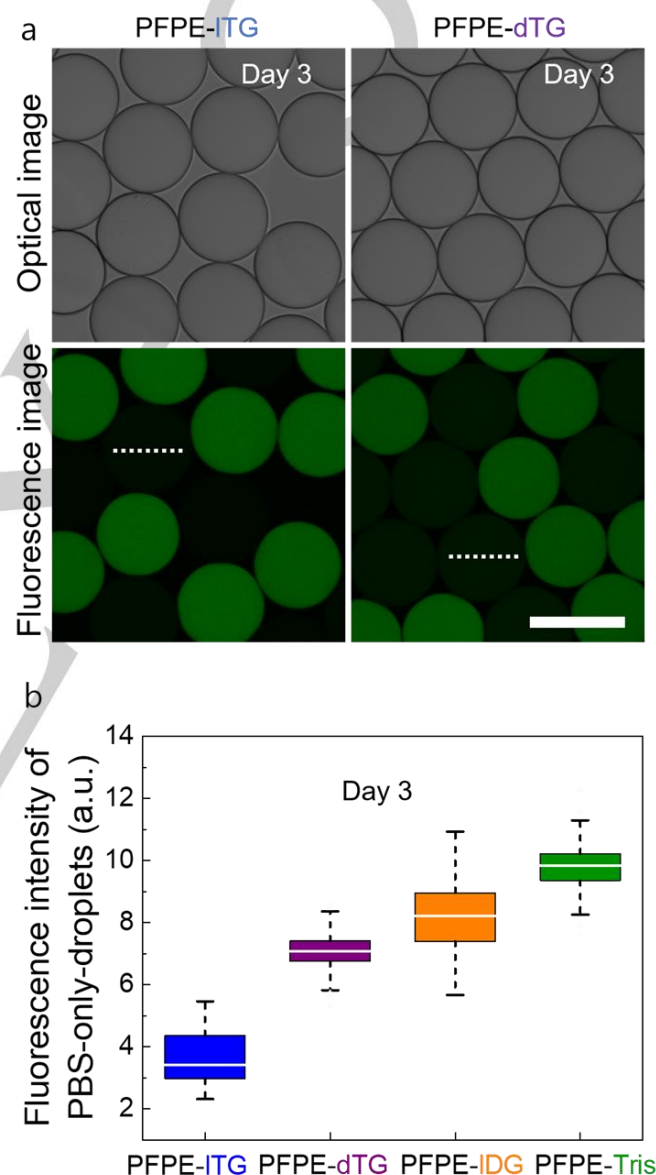
Figure 3. (a) Micrographs showing the inter-droplet diffusion of a fluorescence dye sodium fluorescein salt after 72 h where two populations of empty and dye-containing droplets were stabilized with PFPE-ITG or PFPE-dTG. Two representative initially empty droplets are marked by the dotted lines characteristic for intensity measurements. (b) A quantitative fluorescence intensity analysis of five randomly selected PBS-only-droplets using Image J plot profiling tool where the droplets were stabilized with either PFPE-ITG, PFPE-dTG, PFPE-IDG, or PFPE-Tris after three days **(see Figure S2)**. Scale bar, 100 µm**.**

3

To test the inter-droplet molecular transport, we used 3 µM sodium fluorescein salt as a water-soluble and less-leaky dye. By using a parallel droplet maker,[14] we produced a mixture comprising an equal proportion of PBS-only and PBS+fluorescein dye droplets (**Figure 3a**). We collected the water-in-oil emulsion droplets in an Eppendorf tube and incubated them at 37 °C.

Surprisingly, droplets stabilized with the linear PFPE-lTG surfactant were more preventive to inter-droplet dye diffusion than those had been stabilized with its dendritic counterparts, PFPE-dTG. Quantitatively, on day 3, the green fluorescence signal of PFPE-dTG stabilized PBS-only drops was ~3 times the signal detected in PBS-only drops stabilized by PFPE-lTG, which suggested, although both the surfactants were featuring four -OH groups, both the spatial geometry and a slightly different surface tension were playing a pivotal role to display different transport behaviors (**Figure 3b**). Additionally, we assume that the marginal polarity variation due to different spatial geometry and ratio of primary vs. secondary -OH groups in the polar heads could also impact the cargo retention phenomena. Furthermore, when we tested the three -OH group containing surfactants, we found that the linear diglycerol-based surfactant, PFPE-lDG, performed ~3 times better than its dendritic counterpart PFPE-Tris even though there was no big difference in their surface tension values measured, justifying the undeniable influence of head group polarity (**Figure 3b**). Clearly, this data suggests a higher surface tension alone was not the deciding factor to control the inter-droplet leaching, rather the number of -OH groups, ratio of primary vs. secondary -OH groups, the overall polarity, and the head group's spatial geometry, collectively, play a major role in controlling the inter-droplet transport kinetics. Overall, we think a linear polar head group with a minimum of four hydroxy groups is needed to design a more effective surfactant when leakage of small molecule is concerned. However, when PBS droplets produced

with PFPE-lTG, PFPE-dTG, PFPE-lDG, or PFPE-Tris and incubated at 37 °C over a week, droplets remained monodisperse, but a long-term storage of the droplets over a month showed the following droplet stability order: PFPE-lTG=PFPE-dTG>>PFPE-lDG>PFPE-Tris. This suggests three -OH groups containing surfactants can also be used for applications that are insensitive to leakage and do not require a high droplet stability, such as microgel preparation. However, different aqueous media can profoundly influence the droplet stability,[14] indicating testing them at different conditions.

Hence, the high performance of PFPE-lTG and its spatial geometry motivated us to exploit it further by post-functionalization for more sophisticated applications such as from-droplet fishing of a protein complex. It is worth mentioning that a PEG-based di-block copolymer fluorosurfactant can also be used for post-modification, but since it cannot make robust and monodisperse droplets, for quantitative analyses, it is unattractive to use the PEG-based di-block copolymer surfactants.[19, 21] We, therefore, investigated the post-modification of the linear triglycerol surfactant with bromoacetic acid followed by substitution of the bromine with azide **(Figure 4a)**. The covalently coupled azido moiety in the linear triglycerol head could be clearly confirmed by the strong azide signal at ~2100 cm^{-1} in FT-IR spectroscopy (**Figure 4b**). Besides, the FT-IR data also confirmed a newly formed ester bond by displaying the ester signal ~1750 cm^{-1}. Moreover, when the functional surfactant reacted with slightly excess of cyclooctyne containing DBCO-PEG4-Biotin, the azide peak ~2100 cm^{-1} disappeared, and the ester peak remained, confirming that the click reaction was successful. Although azido acetic acid is commercially available, we wanted to demonstrate that a multi-step post-modification could be easily conducted which is not feasible with the widely used commercial PEG-based tri-block copolymer surfactant PEG-PFPE$_2$, because there is no reactive site in its main chain.
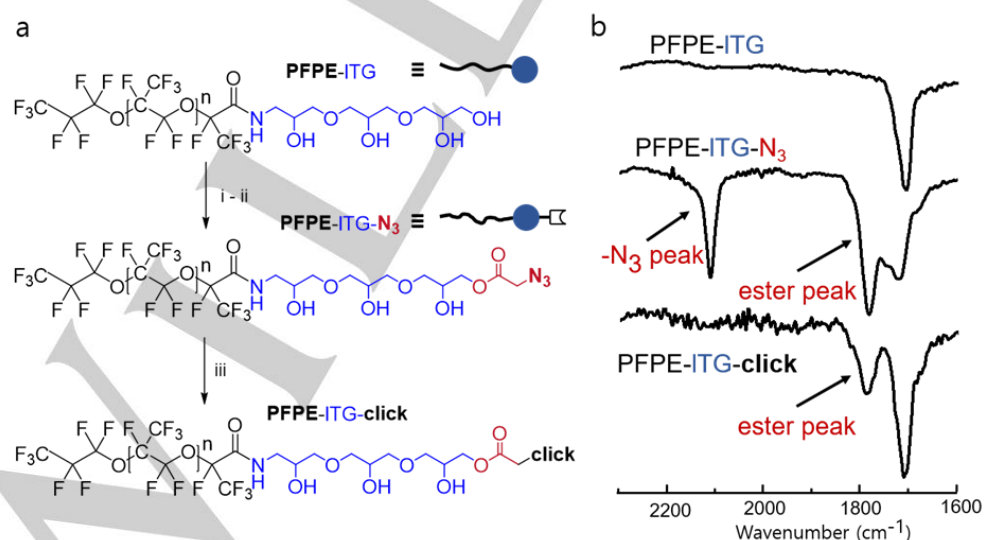

Figure 4. (a) Post-modification of PFPE-lTG by esterification: (i) bromoacetic acid, EDC·HCl, HOBt, DMF-HFE7500; (ii) NaN$_3$, DMF-HFE7500; (iii) DBCO-PEG4-biotin, CH$_3$OH-HFE7100. (b) FT-IR spectra showing the presence of azide and ester in the modified PFPE-lTG-N$_3$ surfactant, absence of both in the pristine surfactant, and disappearance of azide signal after the click reaction.

4

We used a single-drop maker-device to generate droplets of ~70 micron-sized with the azide-coupled linear surfactant PFPE-ITG-N_3. We employed one equivalent of bromo acetic acid to react with statistically one -OH per head group, incorporating one azide functionality per surfactant molecule. Using the PFPE-ITG-N_3, we first encapsulated strained cyclooctyne-containing DBCO-Sulfo-Cy-3 fluorophore in the aqueous core of the droplet. We found that under this tested condition this functional surfactant effectively fishes from 5 - 10 µM DBCO-Sulfo-Cy-3 within 10 minutes via azide-cyclooctyne click reaction **(Figure S3)**. Next, we tested a more complex system that consisted of biotin and streptavidin. It is worth mentioning that the protein complex of biotin and streptavidin is widely used in many biosensing applications, where the streptavidin carries four biotin binding sites, offering multivalency for many applications, including robust crosslinking,[24] antibody-drug conjugation,[25] capturing antibodies, and antigen.[26] However, the biotin-streptavidin interaction is highly sensitive to its surroundings, such as linker chemistry, ionic concentration, pH, hydrogen-bonding, making the assay highly tricky, unless the reaction conditions are optimized.[27,28] Therefore, we used Milli-Q water and freshly prepared the protein complex using one equivalent of Cy5-streptavidin (MW ~ 60000 g mol^{-1}) and eight equivalents of DBCO-PEG4-Biotin, providing two biotins for each biotin-binding site in the streptavidin. In this way, we found that using the PFPE-ITG-N_3 surfactant, from-droplet fishing of the biotin-streptavidin protein complex could also be conducted effectively within 5-10 minutes after encapsulation (**Figure 5b**).
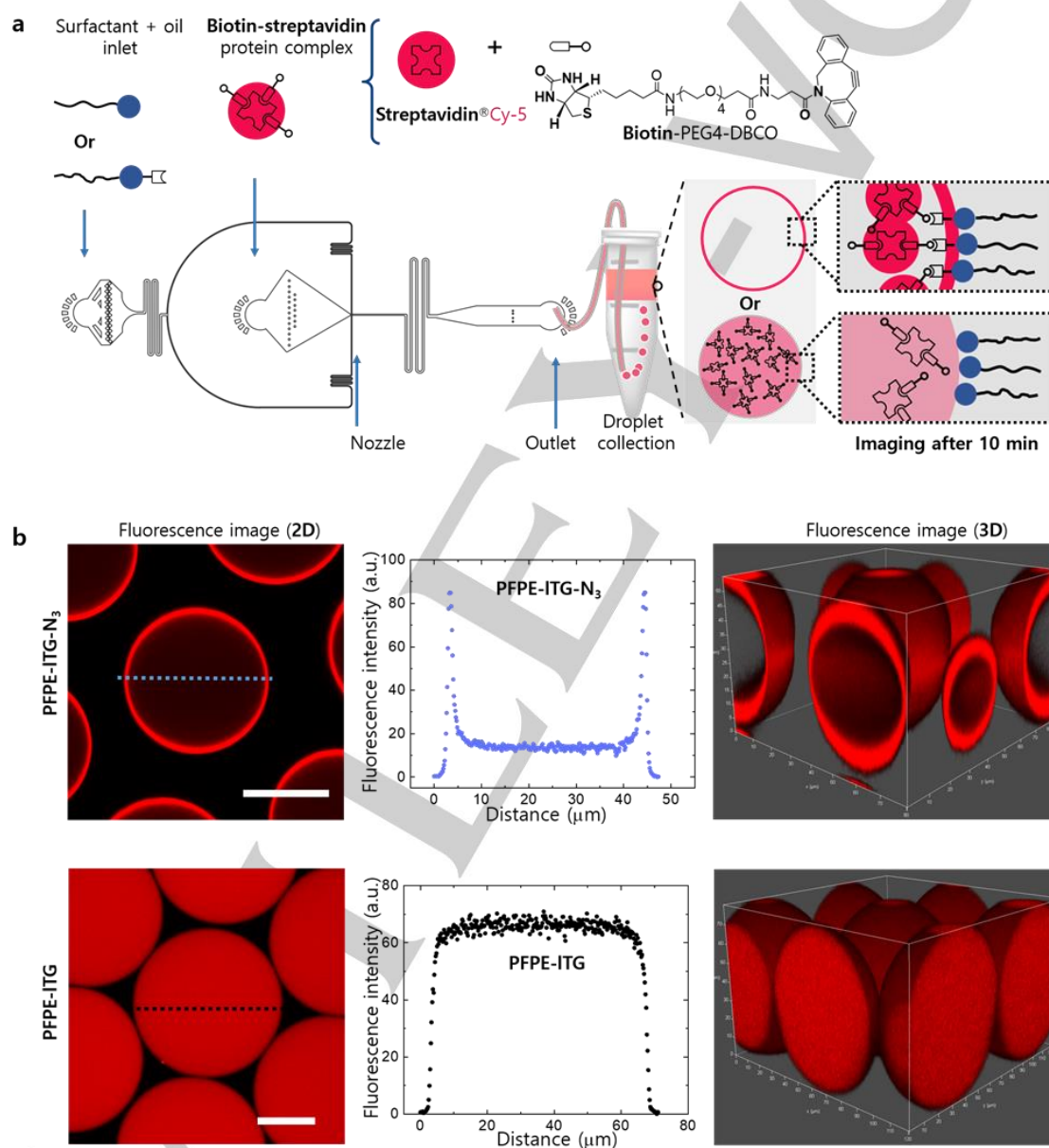
Figure 5. (a) Schematics of a PDMS-based, single-drop maker device to encapsulate biotin-streptavidin protein complex mixture in microdroplets, and a water-in-oil emulsion droplet stabilized with either PFPE-ITG-N_3 or PFPE-ITG surfactant, illustrating the from-droplet fishing ability by each surfactant individually. Here, the protein complex is comprised of DBCO-PEG4-Bbiotin and streptavidin®Cy-5. (b) 2D and 3D confocal fluorescent images of the protein complex encapsulated droplets stabilized with either PFPE-ITG-N_3 (top row) or PFPE-ITG (bottom row) surfactant. Unlike PFPE-ITG, PFPE-ITG-N_3 enabled from-droplet fishing via azide-cyclooctyne click reaction between surfactant and protein complex, which was clearly shown by the strong fluorescence intensity at the droplet interface. Images were taken after 10 minutes of droplet generation. Scale bars, 25 µm.

5

Undoubtedly, the from-droplet biomolecules fishing approach is a big step forward for droplet-based bioanalytical assay, requiring capture and immobilization of target molecules at the droplet interface, that would benefit from this readily tunable functional surfactant in many respects.

Relative to dendritic triglycerol, and those lacking hydroxyl groups, triglycerol with a linear spatial geometry appears to be the most effective polar head group for a minimal inter-droplet leakage of a water-soluble fluorescein dye. Consequently, we envision that linear triglycerol-based fluorosurfactants have high potential as robust and easily sourced water-in-oil emulsion stabilizers. Most importantly, they are extremely useful to improve the data quality of assays such as droplet-based high-throughput drug screening which should not suffer from inter-droplet leakage.

Additionally, we have shown that a multi-step post-modification of the linear triglycerol-based surfactant can be easily performed to alter its chemical functionality by grafting a small functional group to the hydroxy group. Thus, when azido moiety was linked to the linear triglycerol head, the post-functionalized surfactants effectively stabilized the droplets, created a reactive droplet interface, and enabled from-droplet fishing, in addition to providing biocompatibility. Which hints, to alter the chemical environment of the droplet interface, other biomolecules or small molecules with diverse functional groups could also be easily coupled to the linear triglycerol-based fluorosurfactants without trading off with the stability of the droplets and their monodispersity. This new linear triglycerol-based fluorosurfactant imposes no limitations to a broad range of user-defined biochemical assays in microfluidic droplets.

Acknowledgements

[1] E. K. Bowman, H. S. Alper, *Trends Biotechnol.* **2020**, *38*, 701.
[2] A. B. Theberge, F. Courtois, Y. Schaerli, M. Fischlechner, C. Abell, F. Hollfelder, W. T. S. Huck, *Angew. Chem. Int. Ed.* **2010**, *49*, 5846.
[3] I. Lim, A. Vian, H. L. van de Wouw, R. A. Day, C. Gomez, Y. Liu, A. L. Rheingold, O. Campàs, E. M. Sletten, *J. Am. Chem. Soc.* **2020**, *142*, 16072.
[4] A. Rotem, O. Ram, N. Shoresh, R. A. Sperling, A. Goren, D. A. Weitz, B. E. Bernstein, *Nat. Biotechnol.* **2015**, *33*, 1165.
[5] S. Mashaghi, A. Abbaspourrad, D. A. Weitz, A. M. van Oijen, *Trends Anal. Chem.* **2016**, *82*, 118.
[6] A. M. Klein, L. Mazutis, I. Akartuna, N. Tallapragada, A. Veres, V. Li, L. Peshkin, D. A. Weitz, M. W. Kirschner, *Cell* **2015**, *161*, 1187.
[7] B. Kintses, C. Hein, M. F. Mohamed, M. Fischlechner, F. Courtois, C. Lainé, F. Hollfelder, *Chem. Biol.* **2012**, *19*, 1001.
[8] K. Eyer, R. C. L. Doineau, C. E. Castrillon, L. Briseño-Rao, V. Menrath, G. Mottet, P. England, A. Godina, E. Brient-Litzler, C. Nizak, A. Jensen, A. D. Griffiths, J. Bibette, P. Bruhns, J. Baudry, *Nat. Biotechnol.* **2017**, *35*, 977.
[9] A. Kulesa, J. Kehe, J. E. Hurtado, P. Tawde, P. C. Blainey, *Proc. Natl. Acad. Sci. U.S.A.* **2018**, *115*, 6685.
[10] L. Cohen, N. Cui, Y. Cai, P. M. Garden, X. Li, D. A. Weitz, D. R. Walt, *ACS Nano* **2020**, *14*, 9491.
[11] T. S. Kaminski, O. Scheler, P. Garstecki, *Lab Chip* **2016**, *16*, 2168.
[12] L. Mazutis, J. Gilbert, W. L. Ung, D. A. Weitz, A. D. Griffiths, J. A. Heyman, *Nat. Protoc.* **2013**, *8*, 870.
[13] P. Gruner, B. Riechers, B. Semin, J. Lim, A. Johnston, K. Short, J.-C. Baret, *Nat. Commun.* **2016**, *7*, 10392.
[14] M.S. Chowdhury, W. Zheng, S. Kumari, J. Heyman, X. Zhang, P. Dey, D. A. Weitz, R. Haag, *Nat. Commun.* **2019**, *10*, 4546.
[15] N. Shembekar, C. Chaipan, R. Utharala, C. A. Merten, *Lab Chip* **2016**, *16*, 1314.
[16] O. Wagner, J. Thiele, M. Weinhart, L. Mazutis, D. A. Weitz, W. T. S. Huck, R. Haag, *Lab Chip* **2016**, *16*, 65.
[17] Y.-L. Chiu, H. F. Chan, K. K. L. Phua, Y. Zhang, S. Juul, B. R. Knudsen, Y.-P. Ho, K. W. Leong, *ACS Nano* **2014**, *8*, 3913.
[18] D. J. Holt, R. J. Payne, W. Y. Chow, C. Abell, *J. Colloid Interface Sci.* **2010**, *350*, 205.
[19] C. Holtze, A. C. Rowat, J. J. Agresti, J. B. Hutchison, F. E. Angilè, C. H. J. Schmitz, S. Köster, H. Duan, K. J. Humphry, R. A. Scanga, J. S. Johnson, D. Pisignano, D. A. Weitz, *Lab Chip* **2008**, *8*, 1632.
[20] M. Wyszogrodzka, R. Haag, *Langmuir* **2009**, *25*, 5703.
[21] I. Platzman, J.-W. Janiesch, J. P. Spatz, *J. Am. Chem. Soc.* **2013**, *135*, 3339.
[22] S. Ursuegui, M. Mosser, A. Wagner, *RSC Adv.* **2016**, *6*, 94942.
[23] G. Etienne, A. Vian, M. Biočanin, B. Deplancke, E. Amstad, *Lab Chip* **2018**, *18*, 3903.
[24] Y. Hu, A. S. Mao, R. M. Desai, H. Wang, D. A. Weitz, D. J. Mooney, *Lab Chip* **2017**, *17*, 2481.
[25] D. Xu, A. J. Heck, S. L. Kuan, T. Weil, S. V. Wegner, *Chem. Commun.* **2020**, *56*, 9858.
[26] A. S. Cheung, D. K. Y. Zhang, S. T. Koshy, D. J. Mooney, *Nat. Biotechnol.* **2018**, *36*, 160.
[27] L. Cohen, D. R. Walt, *Bioconjugate Chem.* **2018**, *29*, 3452.
[28] G. O. Reznik, S. Vajda, T. Sano, C. R. Cantor, *Proc. Natl. Acad. Sci. U.S.A.* **1998**, *95*, 13525.

the Table of Contents
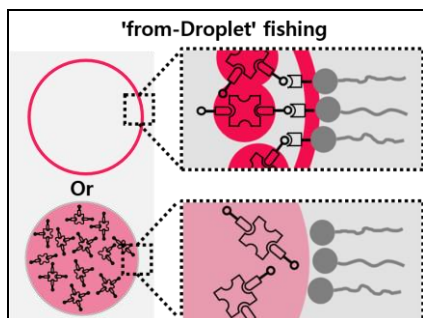
Despite having an equal number of hydroxyl groups, triglycerol with a linear spatial geometry rather than a dendritic geometry appears to be the most effective polar head group to design a fluorosurfactant for a minimal inter-droplet cargo leakage. To create a reactive droplet interface and enable from-droplet fishing of biomolecules, unlike commercial fluorosurfactants, a multi-step post-modification of the linear triglycerol-based surfactant can be easily performed.

Linear triglycerol-based fluorosurfactants show high potential for droplet-microfluidics-based biochemical assays

Mohammad Suman Chowdhury, Wenshan Zheng, Abhishek Kumar Singh, Irvine Lian Hao Ong, Yong Hou, John A. Heyman, Abbas Faghani, Esther Amstad, David A. Weitz, Rainer Haag*

Abstract: Fluorosurfactants have expanded the landscape of high-value biochemical assays in microfluidic droplets, but little is known about how spatial geometries and polarity of head group contribute to fluorosurfactant performance. To decouple this, we design, synthesize, and characterize two linear and two dendritic glycerol- or tris-based surfactants with a common perfluoropolyether tail. To reveal the influence of spatial geometry, we choose inter-droplet cargo transport as a stringent test case. Using surfactants with linear di- and triglycerol, we show that inter-droplet cargo transport is minimal compared with their dendritic counterparts. We also demonstrate that the post-functionalization of PFPE-lTG having a linear geometry and four hydroxy groups enables 'from-droplet' fishing of biotin-streptavidin protein complex without trading off between fishing efficiency and droplet stability. Thus, our approach to design user-friendly surfactants reveals aspects of spatial geometry and facile tunability of the polar head groups that have not been captured or exploited before.

Table of Contents

1.   **Experimental Section**

1.1   Materials

Krytox 157-FSL (MW = ~2200 g mol-1) with monocarboxylic acid at the terminus was purchased from LUB SERVICE GmbH (Germany). Both HFE 7100- and HFE 7500-fluorinated oils were obtained from 3M. Dibenzylcyclooctyne (DBCO)-Sulfo-Cy3 and dibenzylcyclooctyne (DBCO)-PEG4-Biotin were bought from Jena Bioscience (Germany). All other chemicals we purchased were reagent grade. These chemicals are from Acros Organics (Belgium) and/or from Merck (Germany) unless otherwise stated. They were used as received with no further purification. Prior to conducting moisture sensitive reactions, the glassware was flame-dried, and reactions were performed under inert conditions. The fluorosurfactant solution was made at 2% by weight in the bioinert HFE-7500 oil.

1.2   Instrumentation

Either an ECX400 spectrometer (Jeol Ltd., Japan) or an AMX 500 spectrometer (Bruker, Switzerland) was used to record the NMR spectra. δ values in ppm were used to present the proton NMR chemical shift. To calibrate the recorded peak, the deuterated solvent peak was used. To record IR spectra, Nicolet AVATAR 320 FT-IR 5 SXC (Thermo Fisher Scientific, USA) with a DTGS detector from 4000 to 650 cm−1 wavenumbers was employed. Fluorescence images were taken using Leica confocal microscope (TCS SP8, Germany). During water-in-oil emulsion droplet generation by microfluidic flow focusing, a high-speed Phantom MIRO ex2 camera (Vision Research, USA) was used for brightfield imaging. OriginPro 2019b (academic version) was used to generate Boxplots and bar charts. The fluorescence intensity of dye-encapsulated and dye-free droplets was analyzed by Image J.

1.3   Synthesis of four acetal-protected head groups
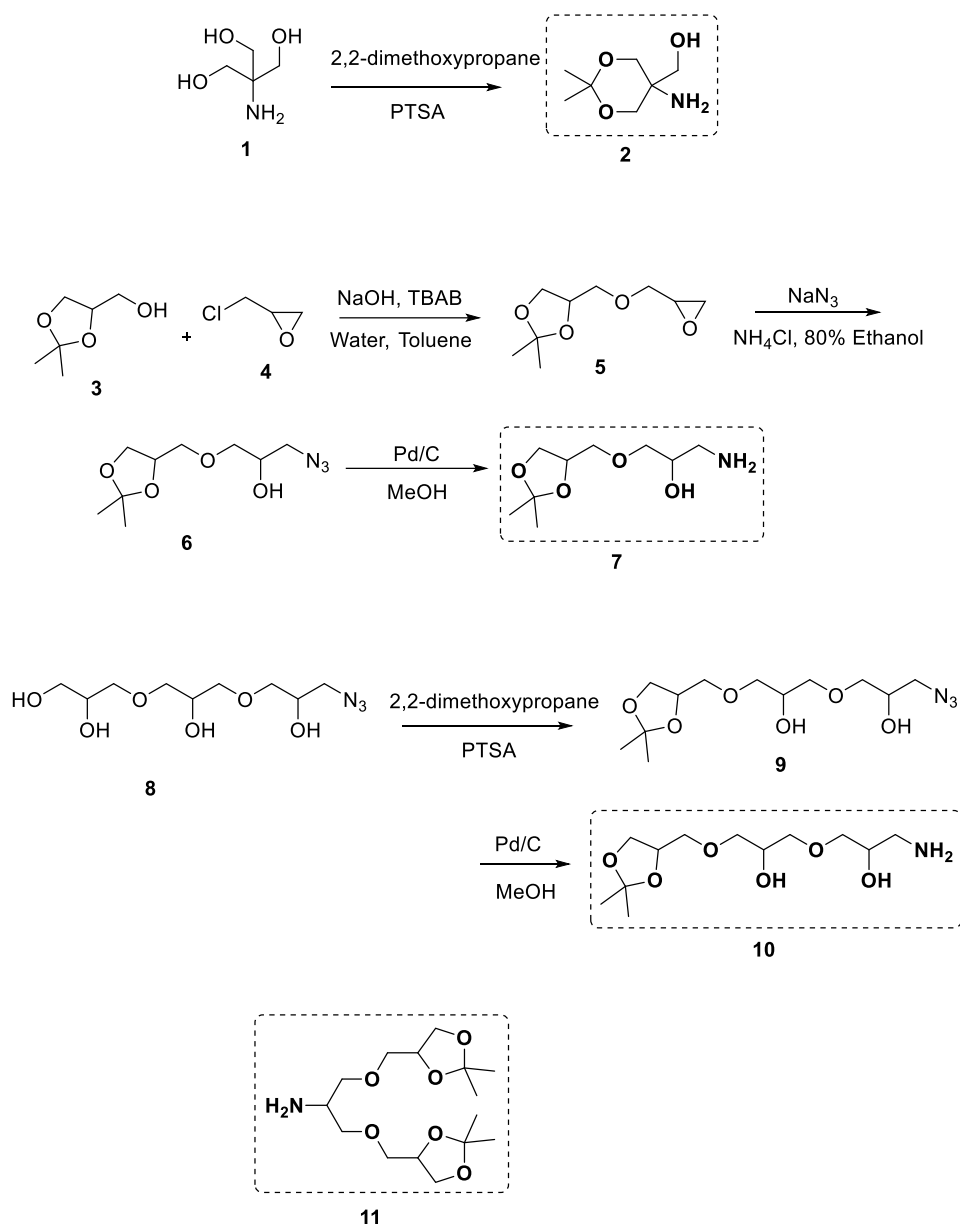
Compound 2

Commercially available tris was converted to the corresponding acetonide-protected tris amine (**2**) following the protocol by Öberg et al.[1]

Compound 5

Isopropylidenglycerol-glycidylether (**5**) was synthesized using solketal (10 g, 1 eq.) and epichlorohydrin (20.90 g, 3 eq.) in presence of NaOH (4.54 g, 1.5 eq.) and tetra-n-butylammonium bromide (TBAB) (10 wt% of starting material, 3.08 g) in water/toluene (1:1) solvent mixture at room temperature (RT). Progress of the reaction was monitored by thin layer chromatography (TLC) using hexane/ethyl acetate (1:1) with a retardation factor (Rf) of 0.3. After completion of the reaction, the mixture was suspended in water and ethyl acetate (3x30 mL). The combined organic layers were dried over anhydrous sodium sulfate and the solvent was evaporated to yield the crude product, which was purified through column chromatography to give compound **5** as a white viscous liquid in 60% isolated yield (~8.5 g).

Compound 6-7

For the synthesis of mono-azido diglycerol derivative, an isopropylidenglycerol-glycidylether (5) (5 g, 1 eq.) was refluxed overnight with NaN$_3$ (5.18 g, 3 eq.) and NH$_4$Cl (1.43 g, 1 eq.) in 80% ethanol. Progress of the reaction was monitored by TLC using methanol/dichloromethane (1:19) with a Rf of 0.45. After completion of the reaction, the mixture was suspended in water and dichloromethane (3x30 mL). The combined organic layers were dried over anhydrous sodium sulfate and the solvent was evaporated

to yield the crude product, which was purified through column chromatography using DCM and methanol to give compound **6** as a white viscous liquid in 85% isolated yield (5.22 g). Finally, to convert azide to amine functionalities, 10% (w/w) a palladium catalyst (10% Pd on charcoal) was used with respect to the weight of acetal-protected lDG-N_3 (6) for hydrogenation. The substrate was dissolved in dry methanol in a hydrogen reactor and pressurized to ~5 bar hydrogen atmosphere at RT for 3 days under vigorous stirring. Then the Pd/charcoal was filtered using a double-layer cellulose filter paper. This hydrogenation step was quantitative, which was monitored by TLC using methanol/dichloromethane (1:9) with a Rf of 0.15. Therefore, after concentrating the solution, the acetal-protected lDG-NH_2 (7) was used for surfactant synthesis without further purifications.

^{1}H NMR (500 MHz, MeOD) for compound 6: δ 4.34-4.29 (p, 1H) 4.12- 4.09 (dd, 1H), 3.95-3.91 (p, 1H), 3.79-3.76 (dd, 1H), 3.58-3.56 (m, 4H), 3.43-3.34 (m, 2H), 1.44 (s, 3H), 1.38 (s, 3H); ESI-MS m/z 231.2520 (calcd. C9H17NaN3O4 254.2560).

^{1}H NMR (500 MHz, MeOD) for compound 7: δ 4.29-4.25 (p, 1H), 4.06-4.03 (dd, 1H), 3.74-3.69 (m, 2H), 3.53-3.47 (m, 4H), 2.76-2.60 (m, 2H), 1.38 (s, 3H), 1.33 (s, 3H). ESI-MS m/z 205.1314 (calcd. C9H19NaNO4 228.1360).

Compound 8-10

Mono-azide linear triglycerol (8) was synthesized following the reported method.[2] The acetonide-protected mono-azide linear triglycerol (9) was synthesized using compound 8 (3 g, 1 eq.) and 2,2 dimethoxypropane (5.88 g, 5 eq.) under solvent-free conditions at 60 °C for 15 h. Progress of the reaction was monitored by TLC using methanol/dichloromethane (1:9) with a Rf of 0.25. After completion of the reaction, the mixture was suspended in water and dichloromethane (3x30 mL). The combined organic layers were dried over anhydrous sodium sulfate and the solvent was evaporated to yield the crude product, which had been purified through column chromatography using DCM and methanol to give compound 9 as a white viscous liquid in 75% isolated yield (2.6 g). And compound **10** was prepared according to the method mentioned above (*see compound 6-7* section for hydrogenation and work up conditions).

^{1}H NMR (500 MHz, MeOD) for compound 9: δ 4.31-4.27 (p, 1H), 4.09-4.06 (dd, 1H), 3.92-3.88 (p, 2H), 3.76-3.73 (dd, 1H), 3.59-3.49 (m, 8H), 3.40-3.31 (m, 2H), 1.41 (s, 3H), 1.35 (s, 3H); ESI-MS m/z 305.3310 (calcd. C12H23NaN3O6 328.3510).

^{1}H NMR (400 MHz, MeOD) for compound 10: δ 4.28-4.23 (p, 1H), 4.06-4.02 (m, 1H), 3.89-3.84 (m, 2H), 3.73-3.69 (m, 2H), 3.56-3.45 (m, 7H), 2.92-2.59 (m, 2H), 1.37 (s, 3H), 1.32 (s, 3H). ESI-MS m/z 279.1682 (calcd. C12H25NaNO6 302.1660).

Compound 11

Acetal-protected tri-glycerol dendron-amine (dTG-NH_2) (11) was prepared following our previously described synthetic routes.[3]

1.4 Synthesis of di-block fluorosurfactants

Synthesis of all four fluorosurfactants, which consisted of a PFPE polymer chain of low molecular weight (Krytox 157-FSL) and compounds 2, 7, 10, and 11, was conducted following our earlier reported procedures.[3]

1.5 Interfacial tension measurement

The interfacial tension of the fluorosurfactants was measured following a previously reported protocol.[4] Briefly, we measured the interfacial tensions using a drop-shape analyzer (Krüss, DSA30). We introduced an inner phase consisting of a surfactant-loaded HFE 7500 solution into a continuous phase of deionized water (18.2 M "Ohms" cm, Direct Q Merck Millipore system) via a syringe needle, and at 1 s intervals we monitored the interfacial tension between the oil drop and the water phase. For each measurement, we introduced a suitable volume of the oil phase (typically around 5 - 10 microliters) so that the oil drop broke off from the needle after 25 s or more due to gravity, which confirmed that the plateau of the interfacial tension value had been reached before the drop pinched off. We report the interfacial tension value right before the break-off of the drop. We performed five measurements using 1% (w/w) surfactant in HFE7500 to obtain the average interfacial tension value.

1.6 Post-modification of PFPE-ITG fluorosurfactant

PFPE-ITG-N_3 was prepared in two steps. In the first step, 1 equivalent of 2% PFPE-ITG (300 mg) (w/w) solution in HFE7500 oil was stirred vigorously with an equal part of dimethylformamide (DMF). Then 1 equivalent of bromoacetic acid (0.019 mg) was added to it, followed by addition of 1.5 equivalent of EDC.HCl (0.04 g) and 1.1 equivalent of HOBt (0.02 g). The mixture was then stirred overnight at 45 °C. In the second step, the DMF solvent phase was removed from the reaction mixture as it phase-separateed without stirring. Then DMF, an equal amount to the HFE7500, was used for washing (1X), removing the reactants and the by-products soluble in DMF. Then 10 equivalent of sodium azide (NaN3) (0.09 g) were added with respect to the obtained crude product. In this step, DMF was used roughly 2X the volume of HFE7500. The reaction was then heated at 75 °C for 2 d. The clear organic phase was removed. Finally, repeated washing with DMF (4X) removed the salt along with the by-product, and a pure fluorosurfactant was obtained in ~91% isolated yield (~300 mg) after rotary drying under reduced pressure.

1.7   **PDMS device fabrication**

The microfluidic PDMS devices were prepared according to our reported protocol with no further modification.[3]

1.8   **Inter-droplet molecular transport assay**

For the inter-droplet molecular transport experiment, the parallel droplet maker, flow rates for continuous oil phase, two aqueous phases, and emulsion droplet incubation conditions were used following previously reported methods with some modifications depicted below.[3] For imaging, the emulsion droplets were drawn by capillary force into a hollow rectangular capillary tube (dimension: ID 0.1 x 2.0 x 50 mm; supplier CM Scientific (UK)) and the open ends were then sealed with grease followed by fixing on microscope cover glass (thickness: 0.13-0.16 mm). The droplets were fluorescently imaged using Leica confocal microscope (TCS SP8, Germany) at days 0, 1, 2, and 3. The fluorescence intensity of the PBS-only-droplets was measured by Image J using the plot profile tool.

1.9   **From-droplet fishing**

For from-droplet-fishing assay, stock solutions of DBCO-Sulfo-Cy3, DBCO-PEG4-Biotin, and Cy®5-streptavidin were prepared following the suppliers' guidelines. MQ water was used to prepare a working solution of each compound. Prior to encapsulation, an immunocomplex consisting of 5 µM DBCO-PEG4-Biotin (8 eq.) and 0.63 µM Cy®5-streptavidin (1 eq.) was prepared in 500 µL MQ water and the freshly prepared solution was stirred in a 2 mL glass vial equipped with a magnetic stirrer bead at 200 rpm for three hours at RT. The flow-focusing nozzle used in the single droplet maker was 35 µm x 50 µm. Droplets were produced using the flow rates of 600 µL/h for the continuous phase (2% surfactant (w/w) solution in HFE 7500 oil) and 300 µL/h for the aqueous phase (dye or protein complex containing MQ water).

2.   Supporting Figures

2.1   **Thin layer chromatography (TLC)**

Figure S1. TLC analysis of PFPE-COOH, PFPE-dTG, PFPE-ITG, PFPE-IDG, and PFPE-Tris from left to right, respectively. A mixture of 20% methanol (v/v) and HFE-7100 was used as a mobile phase to run the TLC.

2.2   Inter-droplet leakage
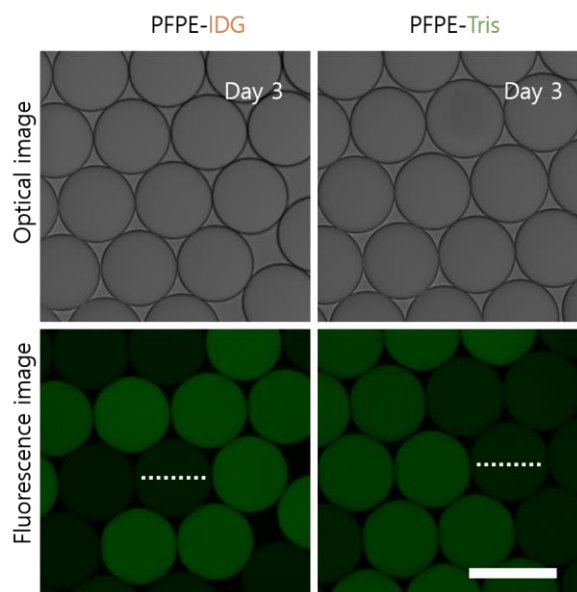
Figure S2. Micrographs showing the inter-droplet diffusion of a fluorescence dye sodium fluorescein salt after 72 h where two populations of empty and dye-containing droplets were stabilized with PFPE-IDG or PFPE-Tris. Two representative initially empty droplets are shown by the dotted lines characteristic for intensity measurements by using Image J plot profiling tool. Scale bar, 100 µm

2.3   From-droplet fishing
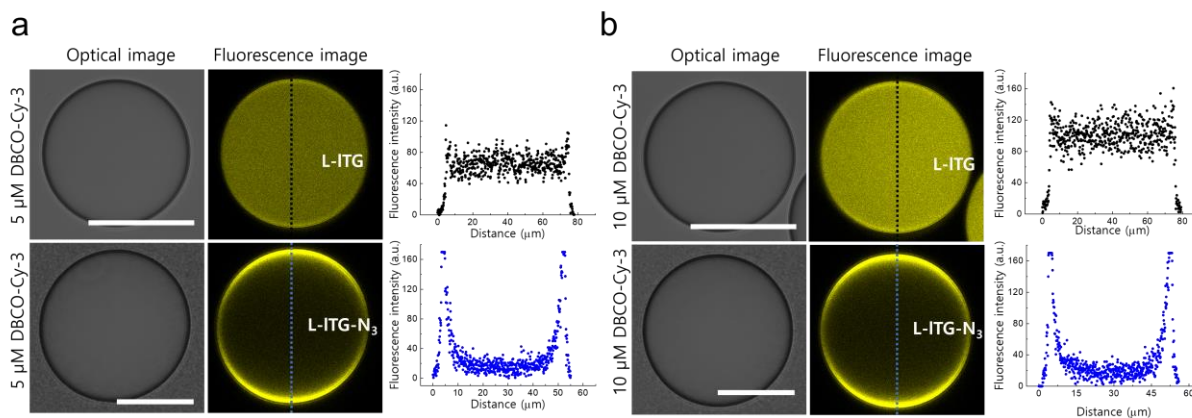
Figure S3. Confocal fluorescent images of the dye-encapsulated droplets. (a) Droplets with 5 µM DBCO-Cy-3 and (b) droplets with 5 µM DBCO-Cy-3. Droplets were stabilized with either L-ITG (top panel) or L-ITG-N_3 (bottom panel) surfactant. Unlike L-ITG, L-ITG-N_3 enabled from-droplet fishing of the dye under both conditions, as indicated by the strong fluorescence intensity at the droplet interfaces. Image J plot profiling tool was used to measure the fluorescence signal across the water-in-oil droplets stabilized with either L-ITG or L-ITG-N_3 surfactant. Scale bars: 50 µm (top panel) and 25 µm (bottom panel).

2.4 **^{1}H NMR of head groups**
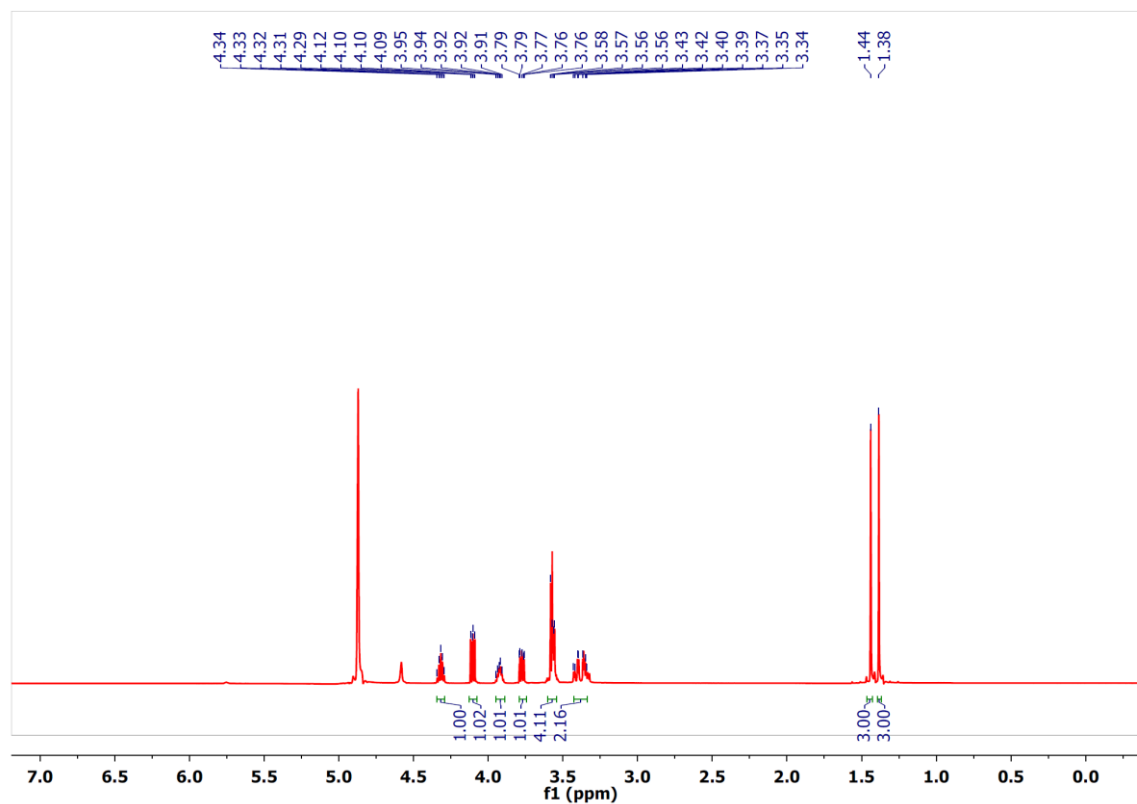
Figure S4. 1H NMR (500 MHz, MeOD) of compound **6**.
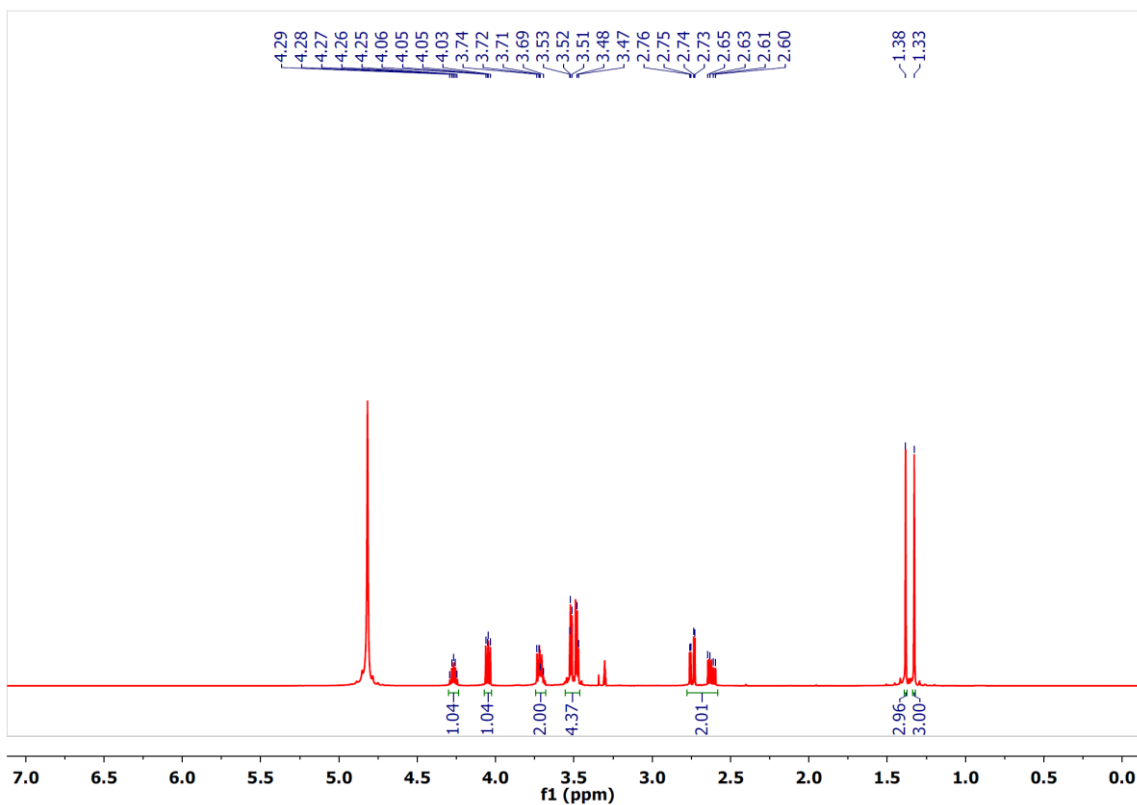
Figure S5. 1H NMR (500 MHz, MeOD) of compound **7**.
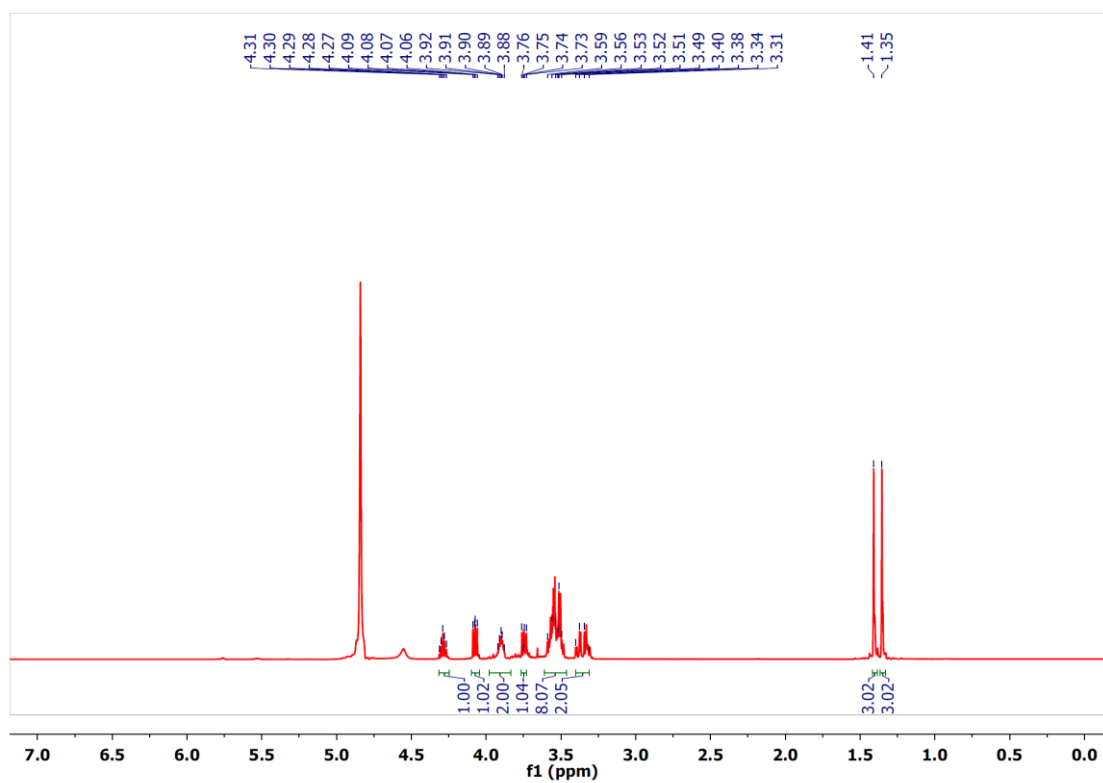
Figure S6. 1H NMR (500 MHz, MeOD) of compound **9**.
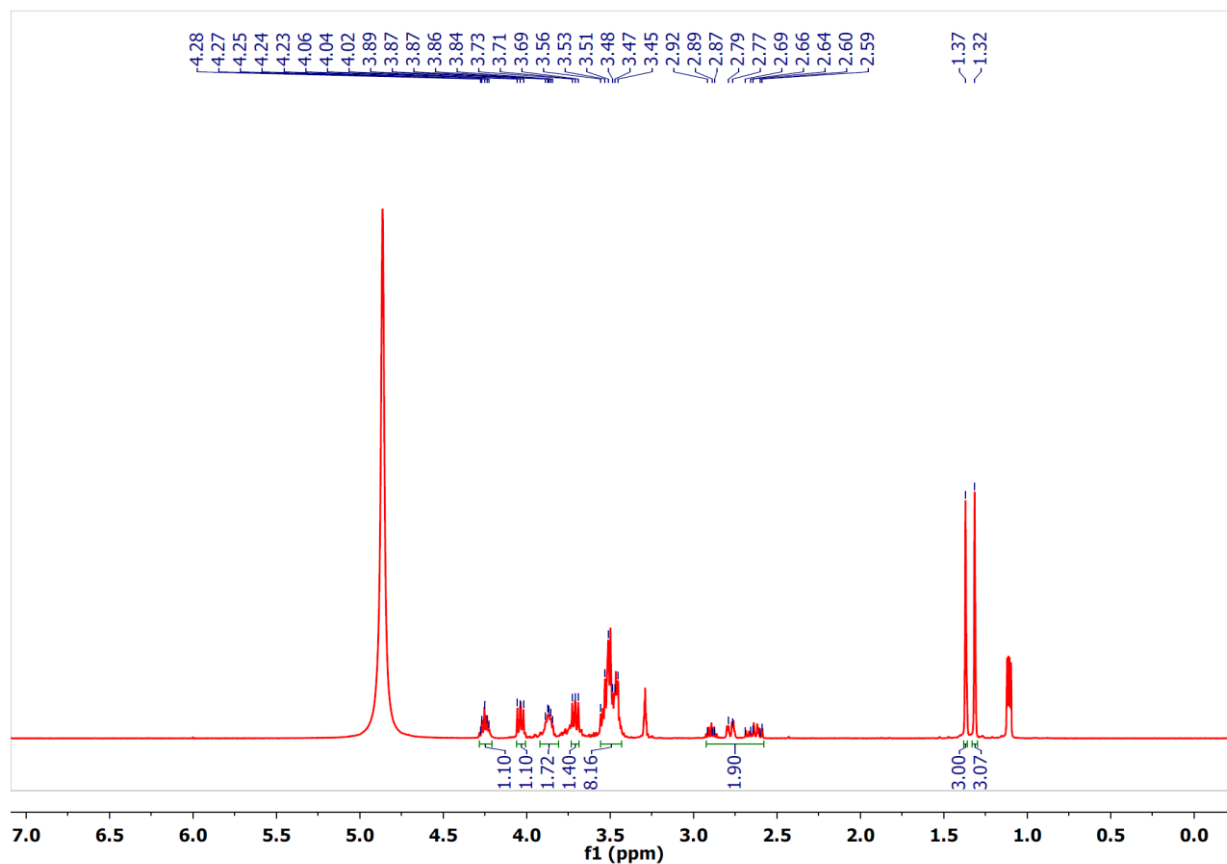
Figure S7. 1H NMR (400 MHz, MeOD) of compound **10**.

References

[1]   K. Öberg, Y. Hed, I. J. Rahmn, J. Kelly, P. Löwenhielm and M. Malkoch, *Chem. Commun.* **2013**, *49*, 6938.

[2]   M. Wyszogrodzka, R. Haag, *Langmuir* **2009**, *25*, 5703.

[3]   M.S. Chowdhury, W. Zheng, S. Kumari, J. Heyman, X. Zhang, P. Dey, D. A. Weitz, R. Haag, *Nat. Commun.* **2019**, *10*, 4546.

[4]   G. Etienne, M. Kessler, E. Amstad, *Macromol. Chem. Phys.* **2017**, *218*, 1600365.

Author Contributions

Mohammad Suman Chowdhury (M.S.C.) designed the research, synthesized the surfactants, analyzed the data and wrote the manuscript. Wenshan Zheng (W.Z.) designed the research and analyzed the data. Abhishek Kumar Singh (A.K.S.) and M.S.C. jointly synthesized the head groups. Irvine Lian Hao Ong (I.L.H.O.) performed the interfacial tension measurements. Yong Hou (Y.H.) assisted in confocal imaging. John Heyman (J.H.) analyzed the data. Abbas Faghani (A.F.) assisted in surfactant purification and analyzed the data. Esther Amstad (E.A.) and David A. Weitz (D.A.W.) supervised the study. Rainer Haag (R.H.) supervised the study, analyzed the data and wrote the manuscript.

3.3 Functional Surfactants for Molecular Fishing, Capsule Creation, and Single-Cell Gene Expression
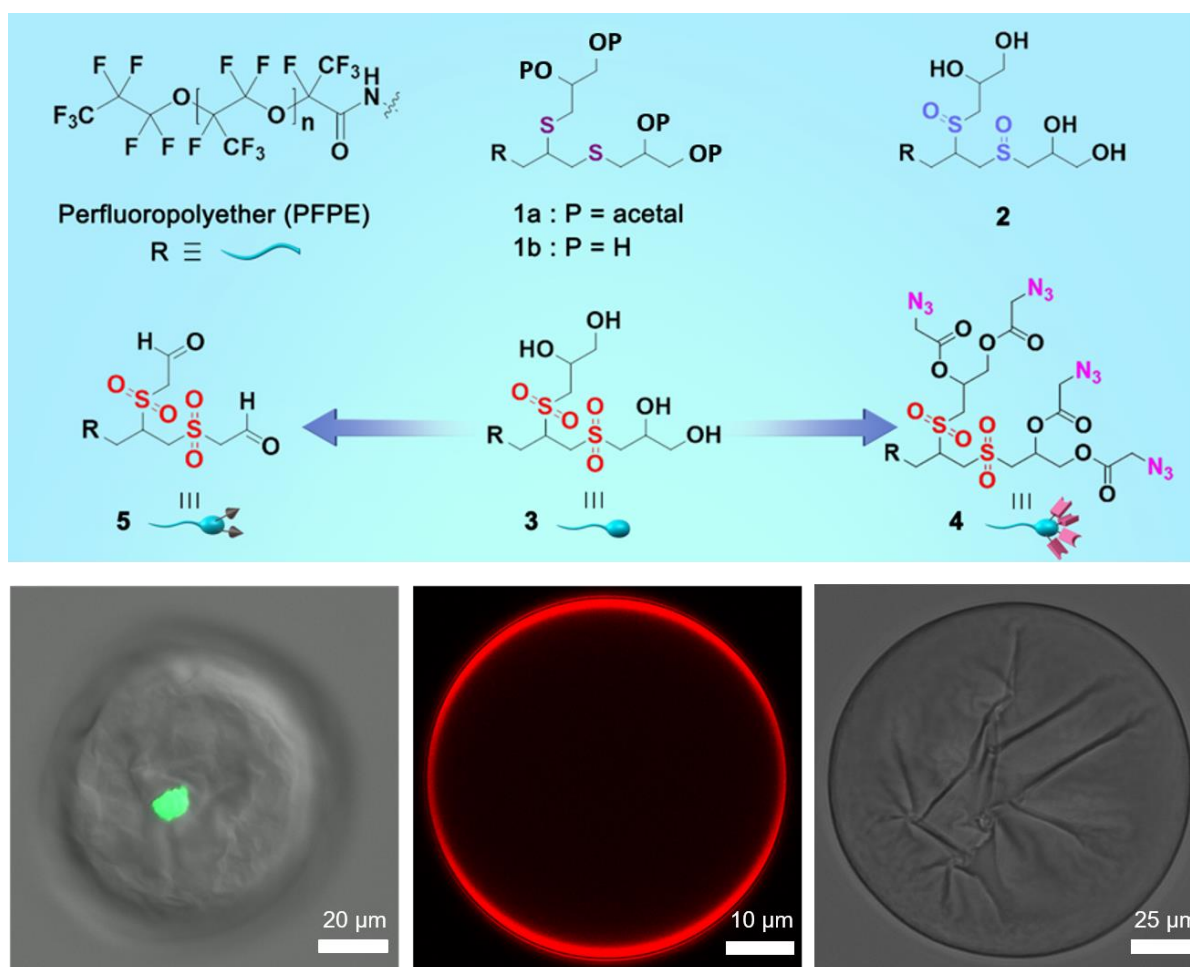
M.S. Chowdhury, X. Zhang, L. Amini, P. Dey, A. Faghani, A. K. Singh, M. Schmück-Henneresse, R. Haag

Author's contributions: In this publication the author contributed to the concept and design, and performed most of the synthesis, characterization, the data evaluation, as well as wrote the draft of the manuscript.

Functional Surfactants for Molecular Fishing, Capsule Creation, and Single-Cell Gene Expression

Mohammad Suman Chowdhury,[1#*] Xingcai Zhang,[2,3#] Leila Amini,[4] Pradip Dey,[1] Abhishek Kumar Singh,[1] Abbas Faghani,[1] Michael S. Henneresse,[4] Rainer Haag[1*]

[1]Institut für Chemie und Biochemie, Freie Universität Berlin, Takustrasse 3, 14195 Berlin, Germany

[2]John A. Paulson School of Engineering and Applied Sciences, Harvard University, Cambridge, Massachusetts 02138, USA

[3]School of Engineering, Massachusetts Institute of Technology, Cambridge, Massachusetts 02139, USA

[4]Berlin Institute of Health – Center for Regenerative Therapies, Berlin Center for Advanced Therapies, Charité Universitätsmedizin Berlin – CVK, Föhrer Str. 15, 13353 Berlin

Creating a single surfactant that is open to manipulation, while maintaining its surface activity, robustness, and compatibility, to expand the landscape of surfactant-dependent assays is extremely challenging. We report an oxidation-responsive precursor with thioethers and multiple 1,2-diols for creating a variety of functional surfactants from one parent surfactant. Using these multifunctional surfactants, we stabilized microfluidics-generated aqueous drops. The drops encapsulated different components and immersed in a bioinert oil with distinct interfaces where an azide-bearing surfactant allowed fishing of biomolecules from the drops, aldehyde-bearing surfactant allowed fabrication of microcapsules, and hydroxyl-bearing surfactants, with/without oxidized thioethers, allowed monitoring of single-cell gene expression. Creating multifunctional surfactants poses opportunities for broad applications, including adsorption, bioanalytics, catalysis, formulations, coatings, and programmable subset of emulsions.

Surfactants play an inevitable role in modern science, including proteomics (*1*), nanotransporter design (*2*), and emulsions (*3*). They typically function to solubilize, contain, shield, and deliver contents of interest ranging from hydrophobic to hydrophilic, ionic to non-ionic, solid to liquid, and protein to single-cell. For example, fluorosurfactants have been widely used in poly(dimethyl siloxane) (PDMS)-based droplet microfluidics for many low-cost (*4*) but high-performance applications, such as single-cell barcoding (*5*) therapeutic antibody discovery (*6*), microcapsule fabrication (*7*), cell-mimetic compartment construction (*8, 9*), and digital enzyme-linked immunosorbent assay (ELISA) (*10*). However, these surfactants including commercial ones cannot be used for multifunctional assays in drops as they lack functional groups and/or are vulnerable to manipulations (*11, 12, 13*). They generally suffer from low valency, unsuitability for quantitative analysis, tedious customizability, and loss of robustness, efficiency, and surface activity after modification. Encapsulation, protection, and stabilization of drops, although possible by other elegant and powerful techniques and materials, such as nanoparticle jamming (*14, 15*), wrapping with/without

prefabricated polymer films (*16*), and stimuli-responsive surfactants (*17*, *18*), still lack compatibility with varying media, biological ingredients, and/or downstream manipulation, due to material types used, charge dependency, formulations conditions, and/or solvent incompatibility, which eliminate them from high-throughput applications.

Therefore, for advanced microfluidic applications, it is necessary to have fluorosurfactants whose functionality, valency, compatibility, and polarity can be readily customized on demand. Customization of the functionality adds new chemical, biochemical, and/or biophysical properties, customization of the valency adds variable number and/or type of functional groups, and customization of the compatibility adds flexibility to work with elements, such as ionic and non-ionic molecules, biomolecules, and cells; and customization of the polarity adds freedom to choose a wide variety of polar and/or non-polar molecules as functional groups for coupling with head groups. The possibility to customize all these will certainly leverage surfactants for many functional assays and enable creating a user-friendly subset of drop-based assays, which remained unnoticed and/or unsuccessful so far.

Here, we combine a small, oxidation responsive polar head group with a non-polar perfluoropolyether (PFPE) tail to design a parent surfactant for creating a variety of multitasking surfactants that were easy to synthesize and scale-up (**Fig. 1**). By using droplet microfluidics, we further demonstrate how they can be leveraged for high-performance functional assays (**Fig. 2**). The surfactants exquisitely exploit different oxidation levels of thioethers, multivalency, tunability of -OH groups, and oxidizable 1,2-diols available in the polar part. We show the generality of the functional surfactants by using them for diverse droplet-based applications.
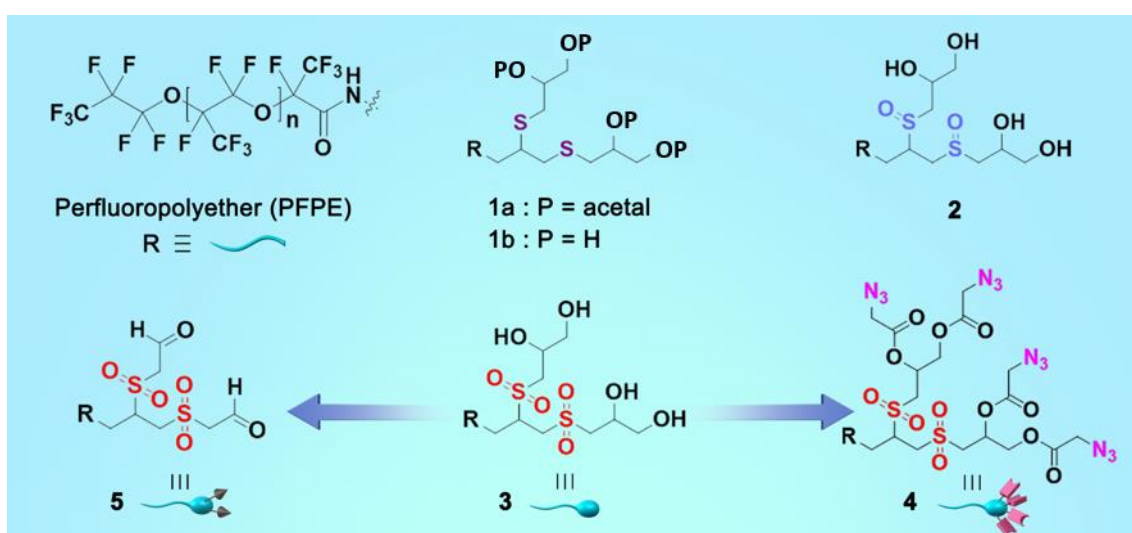
Fig. 1. Functional surfactants. The perfluoropolyether tail **R** is identical in surfactants **1a, 1b**, **2**, **3**, **4**, and **5**. Surfactant **1a** has multiple thioethers and the 1,2-diols are acetal protected (parent surfactant). Surfactants **1b**, **2**, and **3** contain multiple thioethers, sulfoxides, and sulfones, respectively with four hydroxyl groups in each of them. Surfactant **3** was functionalized to create surfactant **4** with azido moieties, while surfactant **5** with aldehyde groups was prepared by oxidizing the 1,2-diols in **3**.
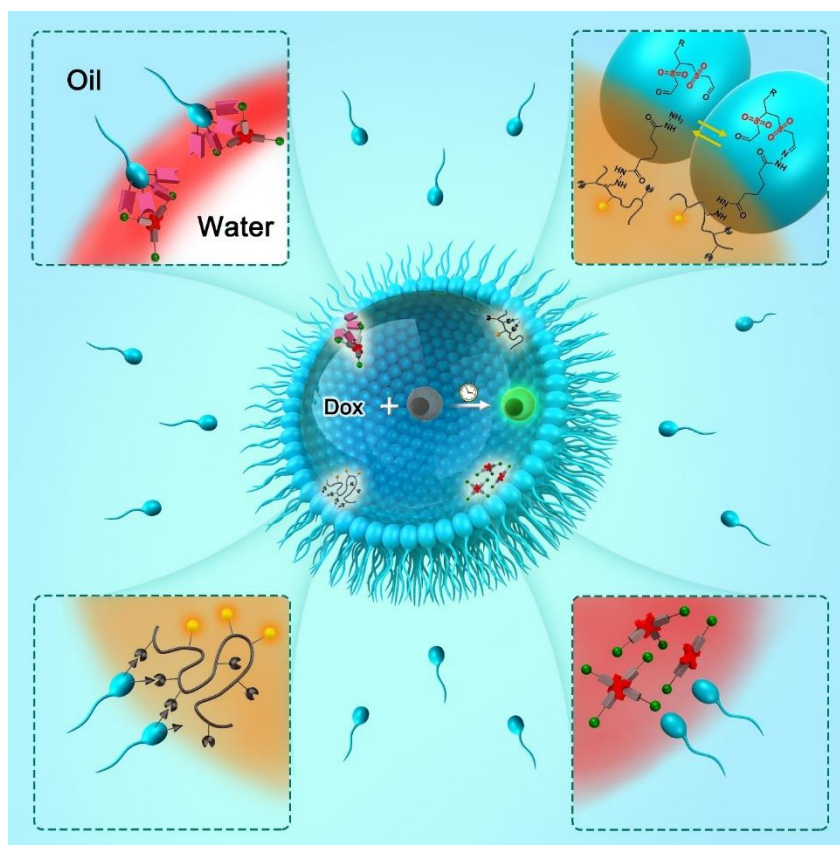
Fig. 2. Applications of functional surfactants. Scheme showing adsorption of surfactant molecules at the interface of oil (turquoise background) and water (surrounded by surfactants) to stabilize water-in-oil drop. The spherical part of the surfactant represents the polar head that meets water, while the wavy line represents the non-polar tail that stays in the oil (turquoise background). At the center of the drop, it shows co-encapsulation of Doxorubicin (Dox) and a cell that yields a fluorescent cell. The top left inset shows the interaction of azide-bearing surfactant **4** with encapsulated proteins. The bottom left inset shows the interaction of aldehyde-bearing surfactant **5** with encapsulated polymer. The bottom right inset shows no interaction of non-functional surfactant **3** with the encapsulated proteins. An exemplary reversible chemical reaction is shown between aldehyde-bearing surfactant **5** and hydrazide-bearing polymer labeled with a fluorescent dye which is encapsulated into the drop (the top right inset, which corresponds to the bottom left inset).

The synthesis of the polar surfactant part exquisitely benefits from the inexpensive, readily available propargyl amine and thioglycerol precursors, and rapid thiol-yne click chemistry. We performed the thiol-yne click reaction under UV-light that allows two thiols to be integrated into one alkyne, creating a dendritic head with two thioethers and two 1,2-diols **(fig. S1)**. After acetal protection of the diols, we synthesized a parent surfactant through amide coupling between the activated PFPE tail and the amine-bearing head **(fig. S2)**. The successful coupling reaction was confirmed by the FT-IR signal at ~1720 cm^{-1} which corresponds to the amide peak **(fig. S8)**. The protection of the diols served three purposes: it prevented the side reaction between the -OH and the activated acid; it ensured selective oxidation of thioethers; and it allowed better purification due to the good solubility of the protected head groups in common organic solvents, whereas the conjugated pro-surfactant is exclusively soluble in fluorinated solvents. When the thioethers of the parent surfactant were selectively oxidized by either

sodium periodate or meta-chloroperoxybenzoic acid they generated either sulfoxides or sulfones, respectively in their backbones, leading to a dramatic increase of the polarity. Furthermore, the oxidation sensitivity of the novel head group was confirmed by ESI-MS **(fig. S9-S11),** which would otherwise be difficult with the pro-surfactants or final surfactants due to solubility issues. Deprotection of the thioether-, sulfoxide-, and sulfone-containing surfactants under mildly acidic conditions created highly polar surfactants **1b**, **2**, and **3**, respectively, all with four hydroxyl groups **(Fig. 1)**. This posed opportunities for grafting a wide variety of polar and/or non-polar functional molecules to the available -OH groups. As both sulfoxide and sulfone groups can highly enhance the overall polarity of the surfactants, the post-functionalization of the -OH groups with small non-polar molecules should not affect the overall amphiphilic character of the surfactants.
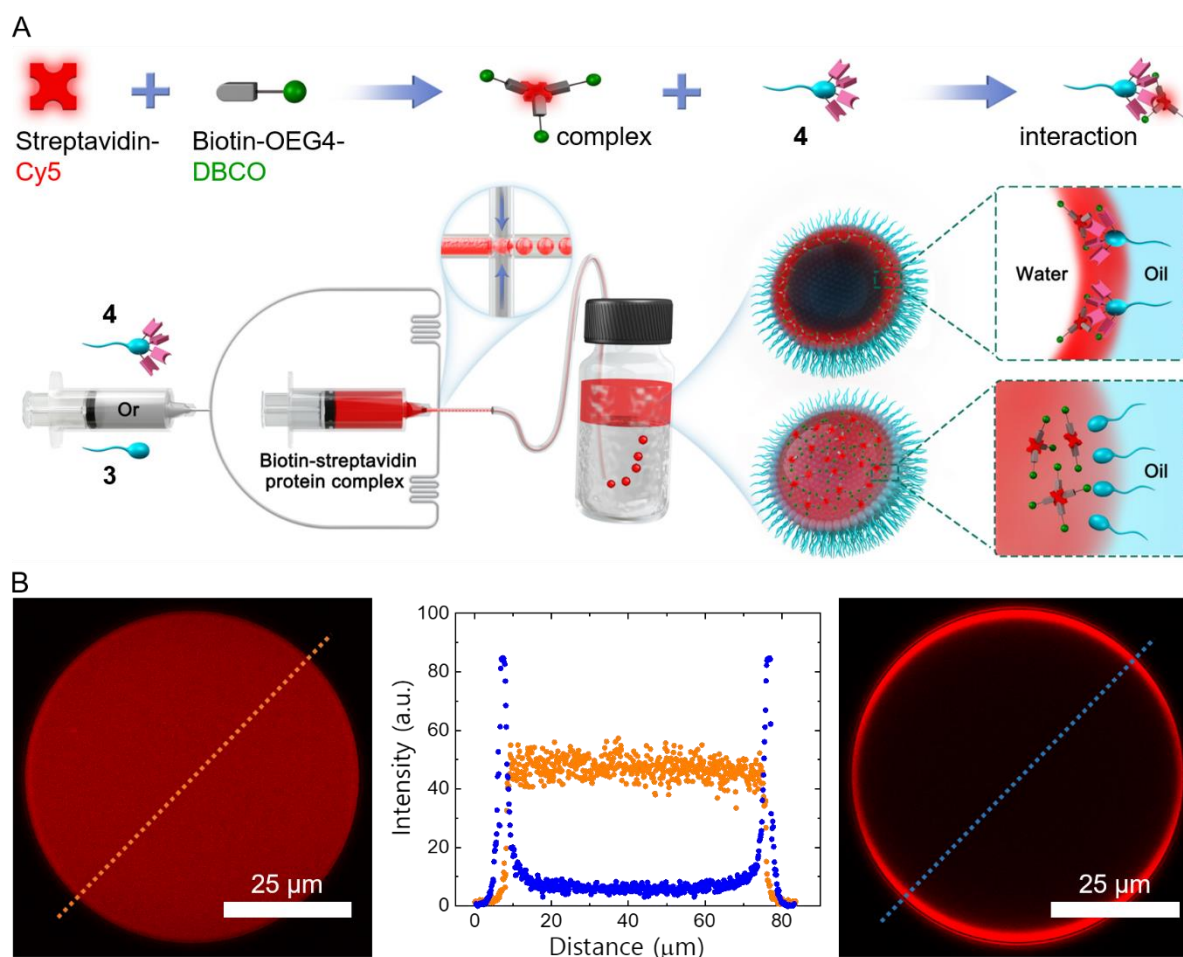
Fig. 3. Microfluidic approach to surfactant-stabilized drops for fishing biomolecules. (**A**) Mixing of Cy5 dye-labeled streptavidin (4-lock in red) with biotin (key in gray) connected via OEG4 (gray stick) to the strained cyclooctyne (green sphere) created a complex of biotin-streptavidin. This complex interacted with the surfactant **4**, which contained azide groups (pink symbols) (the top panel). The bottom panel shows microfluidics generation of the complex-encapsulated drops using either surfactant **3** or **4** where the drops are pinched-off at the channel cross-section (middle inset). The interior of the drop at the top inset shows the migration of complexes to the drop interface (successful fishing) with surfactant **4**. By contrast, the interior of the drop at the bottom inset shows a homogeneous distribution of the complexes across the drop (no fishing) with surfactant **3**. (**B**) 2D confocal fluorescent images of the complex-

encapsulated drops and their fluorescence intensity profiles. The drops were stabilized by surfactant **3** (left) and surfactant **4** (right). In the intensity profiles plotted as a function of distance (middle), the orange line represents the spatial intensity of the drop of the left image and the blue one denotes the spatial intensity of the drop of the right image.

To create a functional surfactant, we chose surfactant **3** as the starting surfactant as it had the maximum overall polarity, and it would allow grafting of azidoacetic acid to the -OH groups through facile esterification in one-step **(fig. S2)**. The azide-functionalized surfactant **4 (Fig. 1)** was characterized by FT-IR where two newly generated strong IR bands at ~1750 cm^{-1} and ~2100 cm^{-1} appeared, clearly indicating the corresponding ester and azide signals, respectively **(fig. S8)**. We then used droplet microfluidics to create water-in-oil emulsion droplets, which were stabilized either by surfactant **3** or by the azido-surfactant **4**. A 2% (w/w) solution of surfactant in HFE-7500 oil was injected into the microfluidic channel to create stable and monodisperse drops of ~80 micrometers (µm) in diameter (~250 pL) **(Fig. 3 and fig. S3)**. The flow rates of the aqueous and oil phases were 300 µL/h and 600 µL/h, respectively. The emulsion droplets were loaded with a protein complex comprised of Cy5 dye-labeled streptavidin and strained cyclooctyne-bearing DBCO-OEG4-Biotin which was pre-complexed in bulk before encapsulation into droplets. To prepare the protein complex, we employed 5 µM biotin and 0.63 µM streptavidin, providing a 2:1 ratio of biotin and biotin-binding site, respectively, and incubated them for ~3 h. Surprisingly, unlike PEG-based di-block surfactants (*13*), our azido-surfactant could generate highly monodisperse droplets with an average diameter of 68.5 ± 0.9 µm **(fig. S3)**, justifying both the well-preserved amphiphilic character and the robustness of the functional surfactant, which can be unambiguously attributed to the highly polar sulfones in the backbone of the polar head. Furthermore, when the droplets were imaged after ~10 min, we found that the functional surfactants could effectively fish the protein complex from the droplet via rapid strain-promoted azide-alkyne cycloaddition (SPAAC) reaction between the surfactant and streptavidin-biotin complex. This resulted in the higher fluorescence intensity at the rim and no fluorescence signal within the drop **(Fig. 3B and fig. S3)**, clearly suggested that the azide-bearing surfactant enabled from-droplet fishing of the complexes. On the contrary, the surfactant **3** lacks azide functionality and could not fish the complex, resulting in a homogeneous distribution of the complex across the droplet **(Fig. 3B and fig. S3)**. It is noteworthy that biotin and streptavidin are widely used in biochemistry because of their robust and high affinity that dictates the design of numerous affinity-based assays (*19*, *20*). Moreover, many high-performance assays such as sandwich ELISA, single-cell barcoding, and single-cell antibody screening require sequential capture of target analytes where functional beads are used to immobilize them (*5*, *6*, *21*). Having this in mind, we questioned whether our functional surfactant could pose any steric hindrance to the sequential fishing of biotin and streptavidin from drops and/or to fishing of the biotin-streptavidin complex that forms in drops. If not, skipping the complex formation in bulk should not be prohibitive to the from-droplet fishing of individual analytes or a complex comprised of multiple analytes. To validate this, we encapsulated biotin and streptavidin without pre-complexation into droplets that were stabilized with surfactant **4**. When the droplets were imaged at 1 h intervals for 3 h, we found that both droplet incubation and bulk incubation before encapsulation did not affect from-droplet fishing **(Fig. S4)**, suggesting that our functional surfactant does not pose any limitations to protein activity and allows sequential fishing of the biotin and streptavidin from drops. This feature indicates that our functional surfactant has a high potential to simplify the droplet-based assays requiring functional beads.

It is worth mentioning that, before using DBCO-OEG4-Biotin, we used DBCO-Sulfo-Biotin to make the protein complex with the streptavidin-Cy5. Surprisingly, we found that from-droplet fishing was not successful. The failure can be attributed to the linker type, which was also reported by others (*22*). Hence, we believe our functional surfactant can also be a powerful tool in combination with droplet microfluidics for a fast, cheap, and effective screening of the activity of a wide variety of small molecule linkers that are used in designing antibody-drug conjugate (ADC) (*23*) and digital single-biomolecule detection system (*10*).

The robustness and intact surface activity of surfactant **4** motivated us to exploit the 1,2-diols in surfactant **3**, which is also responsive to oxidation. Since the highly polar sulfones in **4** contributed to the high degree of droplet stability and monodispersity, after oxidation of the diols in surfactant **3**, it should also enable the generation of highly monodisperse drops with high stability due to sulfones. Furthermore, oxidation of the diols would create reactive aldehyde (-CHO) groups, which will bring another functionality for dynamic covalent chemistry. The dynamic covalent chemistry provides a powerful toolbox to generate reversible bonds with highly controllable reaction kinetics at different pH conditions via amine linkers with variable reactivities, such as alkoxyamine, carbazone, and hydrazide (*24*). Conscious of these scopes, we oxidized the diols in **3** by sodium periodate to create surfactant **5**, bearing -CHO groups at the dendritic terminus which were characterized by FT-IR **(fig. S8)**. This allowed us to fabricate dynamic capsules in drops in one-step using gelatin modified with adipic acid dihydrazide (ADH). It is worth mentioning that the creation of microcapsules in one-step is a powerful way to protect the inner materials (*7, 16, 25*). While the combination of droplet microfluidics and highly tunable kinetics of reversible chemistry can add advantages to generate highly monodisperse capsules with tunable degradation kinetics for pharmaceutics, perfume industries, and many other industrial applications.

We encapsulated 1% gelatin-ADH labeled with Cy-3 dye into droplets. We found that surfactant **5** was highly robust to generate monodisperse droplets and its aldehyde groups were well exposed to react with gelatin-ADH to form dynamic capsules **(Fig. 4A)**. An analogous surfactant with ethers instead of sulfones could not create stable drops **(fig. S5)**, repeatedly validated the crucial role of sulfones in surfactants in maintaining the surface activity, stabilizing the droplets, and facilitating the cross-linking chemistry. To demonstrate the pH effect on hydrazone formation and therefore on the capsule creation, we encapsulated gelatin-ADH in three different pHs. We found that capsules started to form within 3 h and displayed varying morphology rather than being purely spherical at both acidic and basic conditions **(Fig. 4B)**. While at physiological pH no change in their shape was detected, reflecting the usual slow hydrazone formation at neutral pH **(Fig. 4B)** (*23*). However, long-term incubation till 18 h caused pronounced wrinkling at the capsule surface at both acidic and basic conditions unlike at neutral conditions, which we attributed to the increasing degree of hydrazone formation at the oil-water interface between surfactant's aldehyde (-CHO) and gelatin-ADH's hydrazide **(Fig. 4B)**. Although we exploited only the reactivity of hydrazide that reacted with the aldehyde groups in our surfactants to form capsules, all other possible amine derivatives can also be exploited to fine-tune the reactivity on-demand and control the physicochemical properties of the capsules. Although we demonstrated the one-step capsule formation with the aldehyde-bearing head in the w/o system, the aldehyde-head can be used in any fluidic systems such as oil-in-water, water-in-oil-in-water, or more complex with variable hydrophobic tails.
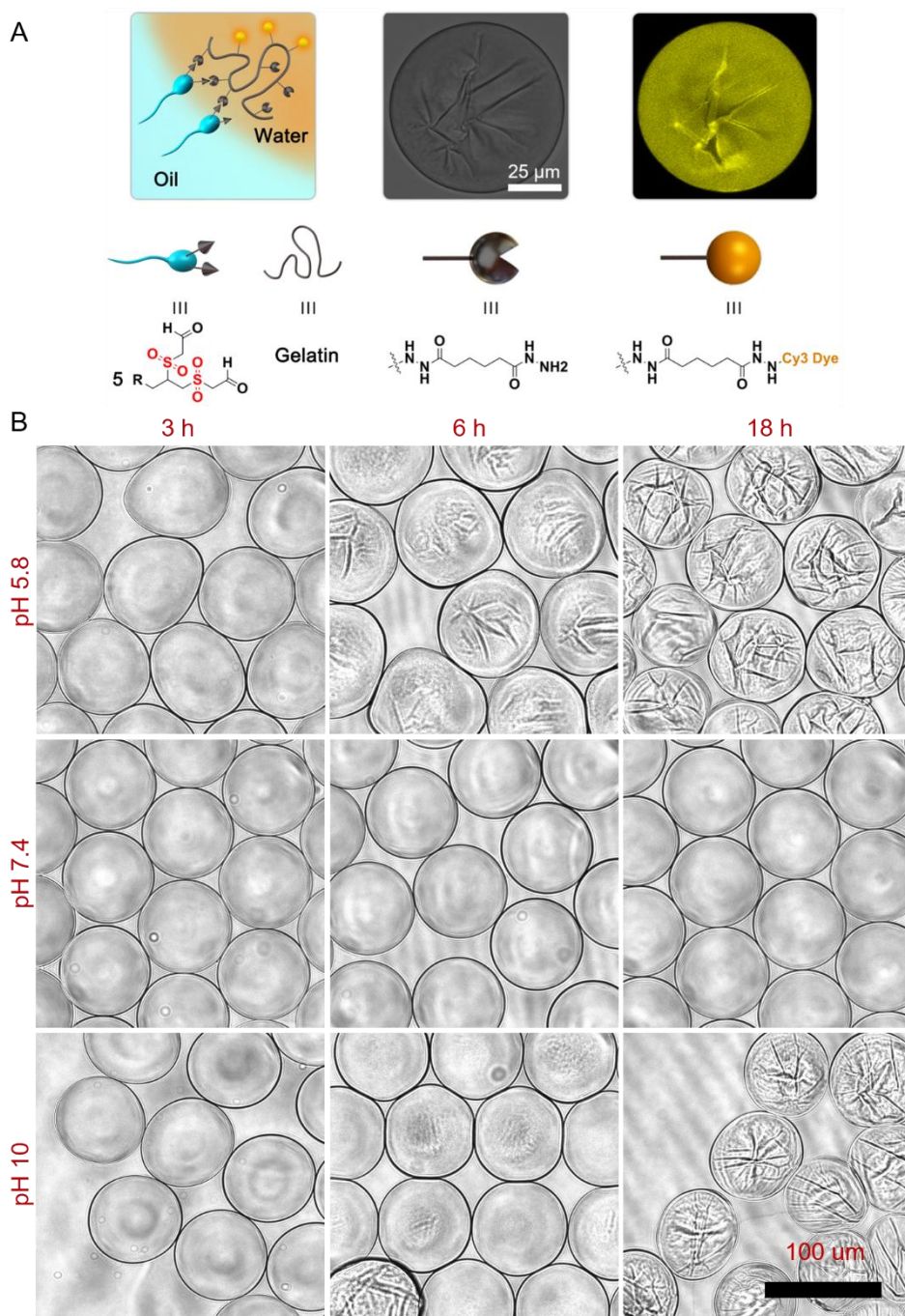
Fig. 4. One-step capsule fabrication. (**A**) The capsule formation scheme showing the reaction between the surfactant's -CHO groups and the gelatin-ADH's hydrazide groups at the water-oil interface of a drop (orange background). Drops were generated by using the single drop-maker PDMS device with two inlets for oil and aqueous solutions (used in Fig. 3A) and stabilized with surfactant **5** (left). 2D fluorescent (middle) and bright-field (right) images of a capsule were recorded with a confocal microscope after 24 h of droplet generation. The inner phase of the capsule comprised of 1% gelatin-ADH labeled with Cy-3 dye in the pH 10 borate buffer. The distribution of the fluorescent intensity across the capsule indicated that the polymer was not adsorbed at the interface due to the reversible hydrazone formation process across the capsule. (**B**) Time and pH-dependent capsule formation through reversible covalent bonds between 1% gelatin-ADH (in the aqueous phase) and the surfactant **5** (at the droplet interface).

Finally, to test the robustness and biocompatibility of the non-functional surfactants **1b**, **2**, and **3,** we co-encapsulated the drug doxycycline (Dox) and Dox-inducible green fluorescent protein (GFP)-expressing Jurkat cells into droplets that were stabilized by these surfactants **(fig. S6)**. Testing of the surfactants **1b**, **2**, and **3** under the cell culture conditions revealed three crucial things: (i) the oxidized surfactants **2** and **3** generated more robust drops than the non-oxidized surfactant **1b** even though all of them equally had four -OH groups, suggesting oxidation of the thioethers was needed to increase polarity and enhance the robustness of the head group to secure the best performance of the surfactants; (ii) none of these surfactants interfered with the GFP expression at the single-cell level **(fig. S6)**, indicating that Dox could effectively activate the transcription system in the genome of the inducible cell to facilitate the gene expression; and (iii) cells could be easily released from droplets by washing surfactants with the fluorinated oil **(fig. S6)**.

In summary, we have described five functional surfactants generated from one parent surfactant and their potential applications. The parent surfactant was synthesized using a non-polar PFPE tail and an acetal protected novel small-molecule head obtained by an efficient thiol-yne-click reaction. The fluorinated tail enabled surfactants to be used for droplet microfluidics, while the head provided multivalency, readily adjustable functionality, and oxidation responsive thioethers and 1,2-diols. These features of the small molecule were exploited to introduce multi-functionality to the surfactants and have a great potential to be exploited in designing anti-inflammatory nano-vehicles for biomedicine, and in creating a broad range of high-performance polymers for diverse applications. The thioethers were oxidized to either sulfoxides or sulfones to add extra polarity to surfactants. The sulfone-bearing surfactant was used and by grafting azido-moieties to the -OH groups, we demonstrated the efficient fishing of biotin-streptavidin complexes from microfluidics generated droplets via the efficient SPAAC reaction. This approach has the potential to replace functional-beads that are used in droplet-based biochemical assays and to avoid plate-reader-based low-throughput and expensive assays for screening small-molecule linkers for ADC and beyond. By converting the 1,2-diols to -CHO groups, we depicted a one-step capsule fabrication at high-throughput using hydrazide-functionalized gelatin and aldehyde-bearing surfactant with sulfones at the backbone at different pH conditions. We showed that the physicochemical properties of the capsule could be easily controlled by varying the pH, which can be translated to other capsule systems by tuning the non-polar tails and the reactivity of amine groups for creating capsules of various types for variable applications. Additionally, surfactants bearing -OH groups and either thioethers, sulfoxides, or sulfones exhibited excellent compatibility with the single-cell and its drug inducible gene expression in the drop and repeatedly justified the benefit of a higher degree of oxidation of thioethers by controlling microdroplet robustness. We envision that our approach to design functional surfactants will improve not only the basic research and development but also a broad range of applied sciences.

REFERENCES AND NOTES

1. L. H. Urner *et al*., *Nat. Commun.* **11**, 564 (2020).
2. Z. Tang *et al*., *Nat. Rev. Mater.* **5**, 847-860 (2020).
3. A. B. Theberge *et al*., *Angew. Chem. Int. Ed.* **49**, 5846-5868 (2010).
4. J. J. Agresti *et al*., *Proc. Natl. Acad. Sci. U.S.A.* **107**, 4004-4009 (2010).
5. A. M. Klein *et al*., *Cell* **161**, 1187-1201 (2015).

6. A. Gérard *et al*., *Nat. Biotechnol.* **38**, 715-721 (2020).
7. J. Zhang *et al*., *Science* **335**, 690-694 (2012).
8. T. E. Miller *et al*., *Science* **368**, 649-654 (2020).
9. M. Weiss *et al*., *Nat. Mater.* **17**, 89-96 (2018).
10. L. Cohen *et al*., *ACS Nano* **14**, 9491-9501 (2020).
11. C. Holtze *et al*., *Lab Chip* **8**, 1632-1639 (2008).
12. M. S. Chowdhury *et al*., *Nat. Commun.* **10**, 4546 (2019).
13. I. Platzman, J-Willi Janiesch, J. P. Spatz, *J. Am. Chem. Soc.* **135**, 3339-3342 (2013).
14. M. Cui, T. Emrick, T. P. Russell, *Science* **342**, 460-463 (2013).
15. C. Huang *et al*., *Nat. Nanotechnol.* **12**, 1060-1063 (2017).
16. D. Kumar, J. D. Paulsen, T. P. Russell, N. Menon, *Science* **359**, 775-778 (2018).
17. L. D. Zarzar *et al*., *Nature* **518**, 520-524 (2015).
18. Z. Yang, J. Wei, Y. I. Sobolev, B. A. Grzybowski, *Nature* **553**, 313-318 (2018).
19. A. S. Cheung, D. K. Y. Zhang, S. T. Koshy, D. J. Mooney, *Nat. Biotechnol.* **36**, 160-169 (2018).
20. D. M. Rissin *et al*., *Nat. Biotechnol.* **28**, 595-599 (2010).
21. C. Wu, P. M. Garden, D. R. Walt, *J. Am. Chem. Soc.* **142**, 12314-12323 (2020).
22. L. Cohen, D. R. Walt, *Bioconjugate Chem.* **29**, 3452-3458 (2018).
23. R. P. Lyon *et al*., *Nat. Biotechnol.* **33**, 733-735 (2015).
24. N. Boehnke, C. Cam, E. Bat, T. Segura, H. D. Maynard, *Biomacromolecules* **16**, 2101 (2015).
25. E. Amstad, *Science* **359**, 743 (2018).

ACKNOWLEDGMENTS

Functional Surfactants for Molecular Fishing, Capsule Creation, and Single-Cell Gene Expression

Mohammad Suman Chowdhury,[1#*] Xingcai Zhang,[2,3#] Leila Amini,[4] Pradip Dey,[1] Abhishek Kumar Singh,[1] Abbas Faghani,[1] Michael S. Henneresse,[4] Rainer Haag[1*]

[1]Institut für Chemie und Biochemie, Freie Universität Berlin, Takustrasse 3, 14195 Berlin, Germany

[2]John A. Paulson School of Engineering and Applied Sciences, Harvard University, Cambridge, Massachusetts 02138, USA

[3]School of Engineering, Massachusetts Institute of Technology, Cambridge, Massachusetts 02139, USA

[4]Berlin Institute of Health – Center for Regenerative Therapies, Berlin Center for Advanced Therapies, Charité Universitätsmedizin Berlin – CVK, Föhrer Str. 15, 13353 Berlin

Materials. Monocarboxylic acid-bearing Krytox 157-FSL (MW = ~2200 g mol^{-1}) was purchased from LUB SERVICE GmbH (Germany). Both HFE 7100- and HFE 7500-fluorinated oils were bought from 3M. Dibenzylcyclooctyne (DBCO)-OEG4-Biotin and DBCO-Sulfo-Biotin were obtained from Jena Bioscience (Germany). All other chemicals we purchased were reagent grade. These chemicals were from Acros Organics (Belgium) and/or from Merck (Germany) unless otherwise mentioned. They were used as received without further purification. For moisture-sensitive synthesis, flame-dried glasswares were used. All reactions were performed under an inert atmosphere. For droplet generation, we prepared 2% (w/w) surfactant solutions in HFE-7500 oil irrespective of surfactant types.

Instrumentation. We used an AMX 500 spectrometer (Bruker, Switzerland) to obtain the NMR spectra. δ values in ppm were used to report the chemical shift of the proton NMR. For peak calibration, we used deuterated solvent peaks. For UV-irradiation, we used a 100 W Ushio (Tokyo, Japan) USH-102d mercury short arc lamp. The FT-IR spectra were recorded from 4000 to 650 cm^{-1} wavenumbers by Nicolet AVATAR 320 FT-IR 5 SXC (Thermo Fisher Scientific, USA) with

a DTGS detector. We took fluorescence images using the Zeiss microscope (Zeiss, Germany) and the Leica confocal microscope (TCS SP8, Germany). During water-in-oil (w/o) emulsion droplet generation by microfluidic flow focusing, we used a high-resolution CCD camera with 3 MPixel (Jena, Germany) for brightfield imaging. We used OriginPro 2019b (academic version) to plot all the FT-IR spectra. We used Image J to prepare a fluorescence intensity profile from the spatial intensity of fluorescent droplets.
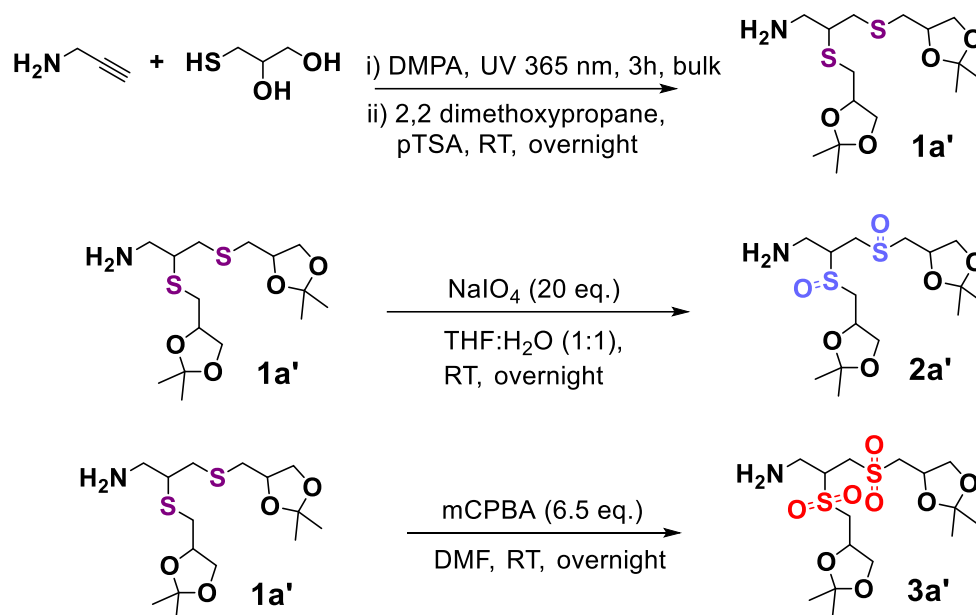
Fig. S1. Schematic synthetic approach to compounds **1a'-3a'** through thiol-yne click reaction, acetal protection, and oxidations.

Synthesis of compound 1a'

To a dry 250 mL round-bottom flask, propargyl amine (5 g, 90.8 mmol), thioglycerol (29.5 g, 272.3 mmol), and 2,2-dimethoxy-2-phenylacetophenone (DMPA) photoinitiator (0.93 g, 3.63 mmol) were added. The thiol-yne click chemistry was performed following a literature procedure with some modifications (*1*). In short, the chemicals were thoroughly mixed rotating using a rotavapor while heating at 40 °C without applying vacuum under dark conditions. Before irradiating with the 365 nm UV-light, the flask was flushed with argon and kept under inert conditions using an argon-filled balloon. The contents were then irradiated at room temperature (RT) with 365 nm UV-light at 60 W without stirring. Subsequently, the crude product was

dissolved in a minimum amount of methanol and precipitated into excess diethyl ether (2x). The crude was then dried under reduced pressure and without further purification and used for the protection of 1,2-diols by the acetal protecting group. The acetal protection was conducted following the reported method with a slight modification (**2**). 2,2-dimethoxypropane (0.73 mol, 75.63 g) and p-toluene sulfonic acid monohydrate (pTSA.H$_2$O) (9.99 mmol, 18.99 g) were added to the crude product. The mixture was then stirred overnight at RT. The reaction was quenched by adding triethylamine (13.77 g, 136 mmol). Then the solvent was evaporated in rotavapor. Next, the residue was suspended in water and dichloromethane (3x100 mL). The organic layers were combined and dried over sodium sulfate and then the solvent was evaporated to yield the crude product, which had been purified using column chromatography with DCM and methanol to give compound **1a'** as a brown viscous liquid with 30% isolated yield (~9.6 g).

^{1}H NMR (500 MHz, CDCl$_3$) for compound **1a'**: δ 4.32- 4.21 (p, 2H), 4.15-4.04 (dd, 2H), 3.82-3.56 (dd, m, 4H), 3.12-2.62 (m, 7H), 1.45-1.40 (s, 6H), 1.38-1.31 (s, 6H); ESI-MS calculated m/z for C$_{15}$H$_{30}$NO$_4$S$_2$ [M+H]$^+$: 352.1538, found: 352.1584) (**Fig. S9**).

The general procedure to prepare sulfoxide derivative (compound 2a')

Oxidation of thioether to sulfoxide was performed following the reported procedures with some modifications (**3**). To a vial equipped with a magnetic stirrer bead, compound **1a'** (100 mg, 0.28 mmol) and NaIO$_4$ (1.2 g, 5.68 mmol) were added. Then 2 mL of THF and water (1:1) mixture was added to it. The reaction mixture was vigorously stirred overnight at RT. Selective oxidation of the thioethers to the corresponding sulfoxides was monitored by ESI-MS (**Fig. S10**).

ESI-MS calculated m/z for C$_{15}$H$_{30}$NO$_6$S$_2$ [M+H]$^+$: 384.1436, found: 384.1479).

The general procedure to prepare sulfone derivative (compound 3a')

Oxidation of thioether to sulfone was performed following the reported procedures with some modifications (**4**). To a vial equipped with a magnetic stirrer bead, compound **1a'** (100 mg, 0.28 mmol) and mCPBA (320 mg, 1.82 mmol) were added. Then ~6 mL dimethylformamide (DMF) was added to it. The reaction mixture was vigorously stirred overnight at RT. Selective oxidation of the thioethers to the corresponding sulfones was monitored by ESI-MS (**Fig. S11**).

ESI-MS calculated m/z for C$_{15}$H$_{30}$NO$_8$S$_2$ [M+H]$^+$: 416.1335, found: 416.1290).
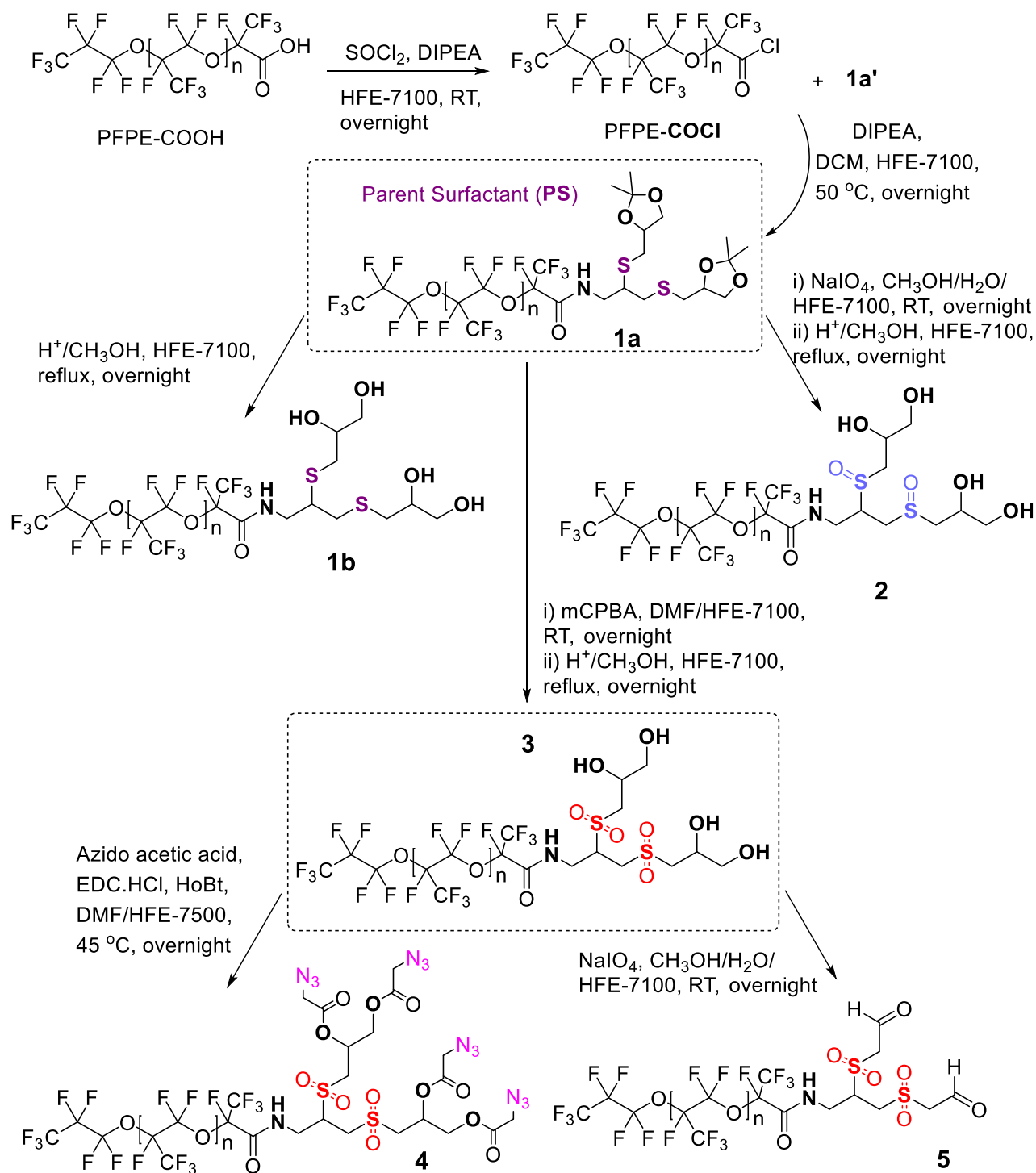
Fig. S2. Schematic synthetic approach to surfactants **1b**, **2**, **3**, **4**, and **5** through the synthesis of the parent surfactant (**PS**) **1a** and subsequent oxidations and post-functionalization.

Synthesis of parent surfactant (PS) 1a. The di-block **'PS' 1a** was synthesized in a two-step process (**Fig. S2**) following the reported protocols with some modifications (*2*, *5*). In the first step, an acid chloride derivative of PFPE-COOH was prepared by dropwise addition of thionyl chloride (1.62g, 13.63 mmol) under ice-cooled condition in a mixture of diisopropylethylamine (DIPEA) (1.37 g, 13.63 mmol) and PFPE-COOH (15 g, ~6.82 mmol) in HFE-7100 (30 mL) taken in a 100 mL round-bottomed flask equipped with magnetic stirrer bead. After thionyl chloride addition, the ice-bath was removed, and the reaction continued overnight at RT with continuous stirring under an inert atmosphere. To remove the generated salt, the crude mixture was filtered through cotton wool and dried under reduced pressure. The residue was then redissolved in 30 mL of HFE-7100. In the second step, compound **1a'** was reacted with the activated PFPE. Compound **1a'** (4.79 g, 13.63 mmol) and DIPEA (1.37 g, 13.63 mmol) were dissolved in DCM and then added dropwise into the solution of activated-PFPE. In summary, 30 mL DCM was added to provide better miscibility with HFE-7100 oil. The reaction mixture was then refluxed at 50 °C overnight. The crude reaction mixture was dried under reduced pressure and washed with methanol (5x30 mL). Thus, all the unreacted head groups (**1a'**) and possible by products were removed during washing, providing the di-block **'PS' 1a** with the protected hydroxyl groups.

Synthesis of surfactant 1b. Deprotection of the acetal groups in the **'PS' 1a** was performed overnight under reflux condition using 1.25% (w/v) HCl in methanol-HFE7100 solvent mixture, which created the water-soluble polar head group in the surfactant. The crude fluorosurfactant **1b** was then washed with methanol (3x30 mL, for a 5 g batch) to remove the acid and obtain a ~80% isolated yield after drying under reduced pressure.

Synthesis of surfactants 2 and 3. Surfactants **2** and **3** were synthesized in two steps. Firstly, the thioethers in the **'PS' 1a** were selectively oxidized to either sulfoxides or sulfones following the *general oxidation procedures* described above with slight modification in solvent composition to ensure better miscibility of the reactants. For oxidation of thioethers to sulfoxides, a solvent mixture comprised of H_2O, CH_3OH, and HFE7100 was used. For a 5 g batch, a total of ~20 mL solvent was used where these solvents were mixed at a ratio of 4:6:10, respectively. For oxidation of thioethers to sulfones, a mixture of DMF and HFE7100 (1:1) was used. For a 5 g batch, ~20 mL solvent was used. Next, the oxidized pro-surfactants were treated with mild acidic conditions for

the deprotection of the acetal groups. Refluxing them at 50 °C overnight in the 1.25% (w/v) HCl in methanol-HFE7100 solvent mixture led to the generation of either surfactant **2** or surfactant **3** containing the water-soluble polar head groups in surfactants. The crude fluorosurfactants were then washed with methanol (3x30 mL, for a 5 g batch) to remove the acid and both obtained with ~85% isolated yields after drying them under reduced pressure.

Synthesis of surfactant 4. Surfactant **4** was prepared in one step. To a 50 mL round bottom flask equipped with a magnetic stirrer bead, surfactant **3** (300 mg, 0.14 mmol), azido acetic acid (68.9 mg, 0.68 mmol), EDC.HCl (195.03 mg, 1.02 mmol), and HOBt (81.07 mg, 0.6 mmol) were added. Then 10 mL solvent consisting of a mixture of DMF and HFE7500 oil (1:1) were added to it. The mixture was vigorously stirred overnight at 45 °C. When stirring was stopped, within minutes, DMF was phase separated. After removing the DMF part, the fluorous oil phase was washed with pure DMF (3x10 mL), which removed the reactants and by-products soluble in DMF. After drying under reduced pressure, azido fluorosurfactant **4** was obtained with a ~89% isolated yield (~316 mg).

Synthesis of surfactant 5. Surfactant **5** was prepared in one step. To a 100 mL round bottom flask equipped with a magnetic stirrer bead, surfactant **3** (1.2 g, 0.91 mmol) and $NaIO_4$ (3.9 g, 18.18 mmol) were added. Then 10 mL solvent consisting of a mixture of water, methanol, and HFE7100 oil at a 2:3:5 ratio, respectively, was added to it. The reaction mixture was vigorously stirred overnight at RT. The aqueous phase was carefully removed by washing with methanol (3x10 mL). Then ~10 mL HFE7500 was added, which facilitated the precipitation of residual $NaIO_4$ and other impurities generated during the reaction. The supernatant was collected and filtered using a double-layer cellulose filter paper. After drying under reduced pressure, fluorosurfactant **5** with aldehyde functionality was obtained with a ~40% isolated yield (~0.48 g).

PDMS device fabrication. The single-drop-making PDMS device was prepared according to our reported protocol with no further modification (**2**).

Preparation of biotin and streptavidin solutions for droplet encapsulation. For the from-droplet-fishing assay, stock solutions of DBCO-OEG4-Biotin and Cy®5-streptavidin were

prepared following the suppliers' guidelines. Milli-Q (MQ) water was used to prepare a working solution of each compound. For droplet incubation, DBCO-OEG4-Biotin and Cy®5-streptavidin were mixed at a molar ratio of 8:1 to make up a final concentration of 5 µM:0.63 µM, respectively, in 500 µL MQ water. Of note, this ratio provided two biotin molecules for each biotin-binding site in the streptavidin which had four biotin-binding sites in total. The solution was then vortexed for 30 s and then immediately transferred into a 1 mL syringe for droplet encapsulation. On the contrary, for bulk incubation prior to droplet encapsulation, three samples were prepared separately containing same amounts of biotin and streptavidin in 500 µL MQ water. These freshly prepared solutions were stirred in 2 mL glass vials, equipped with magnetic stirrer beads, at 200 rpm at RT for 1 h, 2 h, and 3 h, respectively. Each sample was then transferred into a 1 mL syringe at the indicated time point for droplet encapsulation. The flow-focusing nozzle used in the single droplet maker was 35 µm x 50 µm. The flow rates of 600 µL/h for the oil phase and 300 µL/h for the aqueous phase generated ~80 µm droplets. For droplet generation, a 2% surfactant (w/w) solution in HFE 7500 oil was used.

Gelatin functionalization and capsule fabrication. The commercially available gelatin (type A) was functionalized with adipic acid dihydrazide (ADH) following a literature procedure to prepare gelatin-ADH where all the carboxylic acid groups were modified with the ADH (**6**). To prepare Cy3 dye-labeled gelatin-ADH, 3.5 mg (~4.5 µM) of NHS-activated Cy3 dye was added to a solution of 250 mg gelatin-ADH (~460 µM of ADH) dissolved in ~2.5 mL of deionized (DI) water and diisopropylamine (DIPEA). Additionally, ~2.5 mL DMSO was added to ensure better miscibility of the dye. This reaction was performed overnight at 45 °C followed by dialysis in water for 2 days at 40 °C. A regenerated cellulose (RC) dialysis membrane with a molecular weight cut-off of 3500 Da was used for dialysis. After drying the solution under reduced pressure, ~200 mg dye-labeled gelatin-ADH was obtained which was stored at 4 °C for further use.

To fabricate capsules at different pH conditions, a 1% gelatin-ADH solution was prepared in DI water at varying pHs. A 2% (w/w) solution of the -CHO bearing surfactant **5** in HFE-7500 was employed to generate droplets loaded with the gelatin solution. A single droplet maker device with two inlets (one for oil and one for aqueous media) was used as demonstrated in the main text (**Fig. 3A**). The flow rates of the aqueous and oil phases were 300 µL/h and 600 µL/h, respectively. The

generated droplets were incubated for varying time points at ~25 °C and imaged using a confocal microscope to monitor the progress of the capsule formation.

Stable DOX-inducible Jurkat cell line generation. Jurkat cells were cultured in very low endotoxin-containing Roswell Park Memorial Institute (RPMI) 1640 medium under standard cell culture conditions. The medium was supplemented with 10% (v/v) fetal bovine serum (FBS) and 1% (v/v) penicillin-streptomycin (P-S). To generate a stable Tet-On 3G doxycycline (Dox)-inducible green fluorescence protein (GFP)-expressing reporter-cell line, Jurkat cells were transfected with hyperactive *piggyBac* transposase (pCMV-hyPBase, a kind gift from the Sanger Institute, UK) (**7**) and XLone-GFP (a gift from Xiaojun Lian; Addgene plasmid # 96930) (**8**) plasmid constructs. Program CL-120 of the 4D Nucleofector (Lonza) was used to electroporate the Jurkat cells with 10 µg of the XLone-GFP and 25 µg of the pCMV-hyPBase plasmids. The plasmids and 1 million cells were dissolved in 100 µl electroporation buffer P3 before electroporation. This solution was transferred into a 48 wells plate prefilled with a 1 mL prewarmed medium. On the following day, the cells were transferred into T25 flasks and then 4 mL of fresh medium was added. On day 5, cells were treated with 4 µM Dox to turn on the green fluorescent protein (GFP) expression. On day 8, FACS was used to isolate a pure population of cells having the maximum GFP fluorescence intensity. The FACS sorted cells were then grown for three days and frozen in a freezing medium (FBS + 10% DMSO).
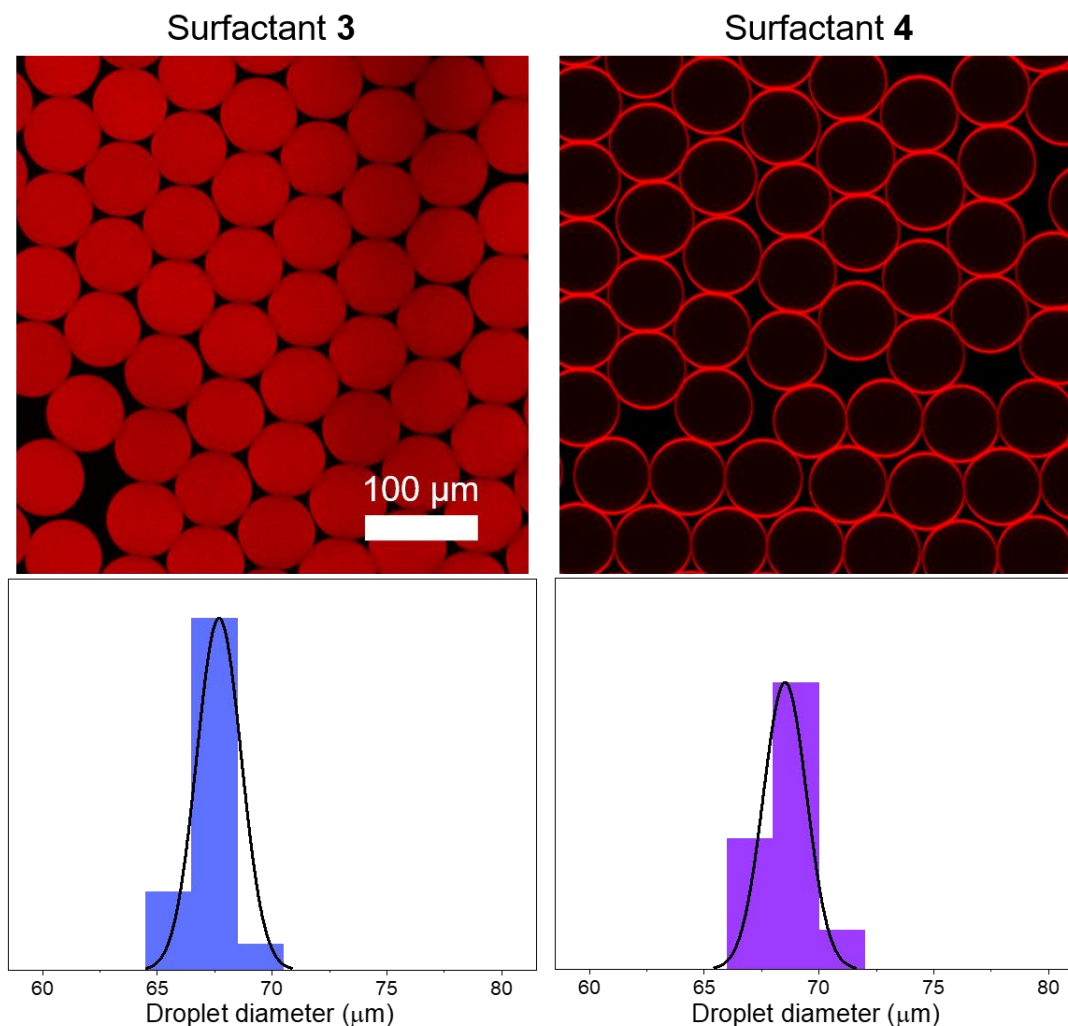
Fig. S3. From-droplet biomolecules' fishing and the droplet-size distribution. Confocal fluorescent images of the droplets loaded with biotin-streptavidin complexes (top panel). These complexes were prepared in bulk for ~3 h by mixing DBCO-OEG4-Biotin (8 eq.) with Cy®5-streptavidin (1 eq.). The final concentrations of the biotin and streptavidin molecules were 5 μM and 0.63 μM, respectively. Droplets were stabilized with surfactant **4** (top left) and surfactant **3** (top right). Unlike surfactant **3**, surfactant **4** enabled from-droplet fishing of the protein complexes, as indicated by the strong fluorescence intensity at the rim of the droplets and no fluorescence intensity within the droplets (top left). The droplets were imaged after 10 minutes of droplet generation. The size distribution of the droplets (bottom panel) showed that highly monodisperse droplets were generated by both surfactant **3** (bottom right) and surfactant **4** (bottom left), which suggested that both the modified **4** and non-modified **3** surfactants were equally good to create

highly stable and highly monodisperse droplets for the assay. In addition, it suggested that the sulfones in the backbone of the head group allowed the surfactant **4** to maintain its surface activity even though the hydroxyl groups were functionalized with the non-polar azido moieties.
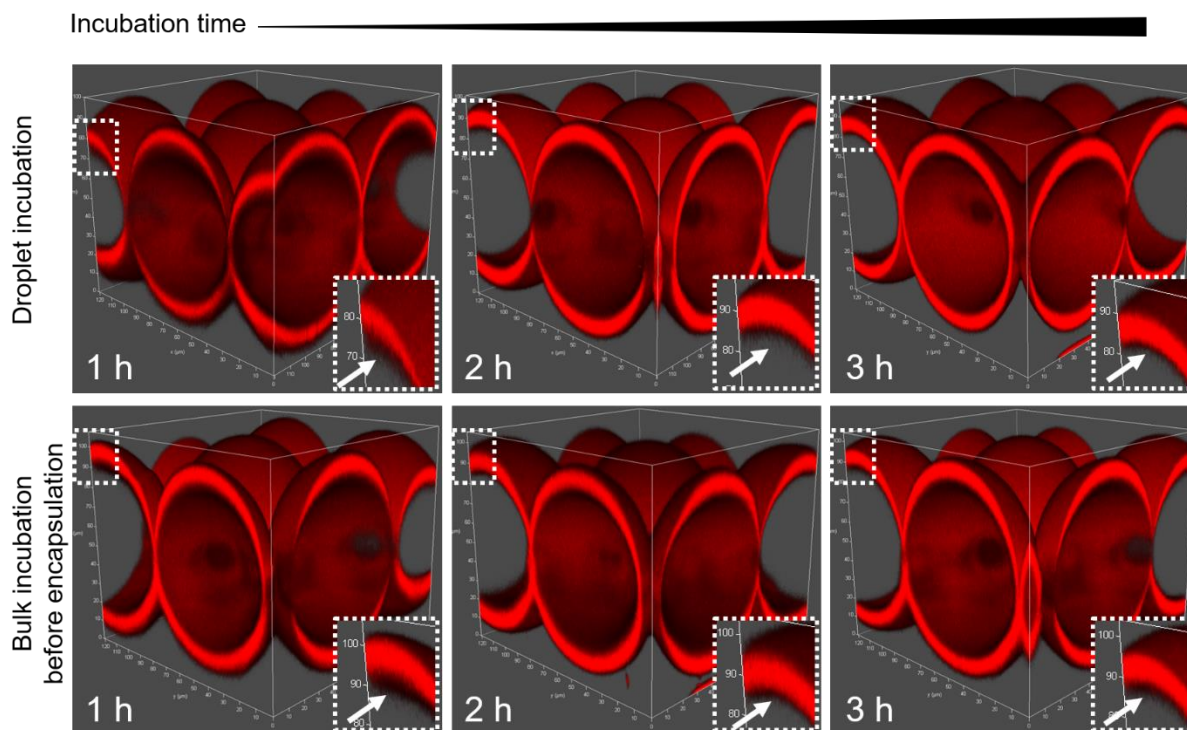
Fig. S4. Influence of droplet vs. bulk incubation of proteins on fishing efficiency. Here, bulk incubation refers to making the biotin-streptavidin complex outside the drops, while droplet incubation refers to making the complex inside drops, which poses an opportunity for both sequential fishing of individual proteins and fishing of the complex. The insets show the from-droplet fishing kinetics by means of reduced thicknesses of black areas (denoted by white arrows) under both incubation conditions at the indicated time points. Droplet incubation enabled better fishing than bulk incubation at 2 h and 3 h, revealing that sequential fishing might be more beneficial than fishing the complex only, and it is not necessary to make complex outside drops. In those images, droplets were stabilized with surfactant **4** and the aqueous phase comprised 5 µM DBCO-OEG4-Biotin and 0.63 µM streptavidin-Cy5.
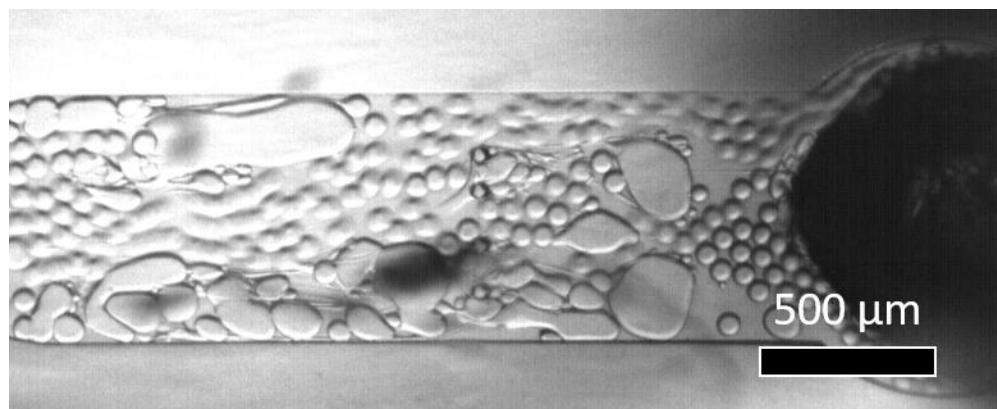
Fig. S5. Performance of 1,2-diols oxidized surfactant lacking thioethers. We used our previously reported surfactant L-dTG (*2*), which had two 1,2-diols as in surfactant **1** but lacking thioethers in the backbone. We chose this to prepare an analogous surfactant like surfactant **5** but without the possibility to have sulfones in the backbone. This allowed us to justify the role of sulfones in creating and stabilizing the droplets with surfactant-lacking hydroxyl groups and to compare its performance with surfactant **5**. Oxidation of the 1,2-diols with sodium metaperiodate was conducted following the procedures discussed above. We found that the 1,2-diols oxidized surfactant L-dTG failed to generate stable droplets even though it had a similar length and architecture as in surfactant **5**. The image of the unstable droplets was taken during droplet generation. Note, some droplets were seen to be monodisperse as shown in the figure, but they coalesced shortly after collection.
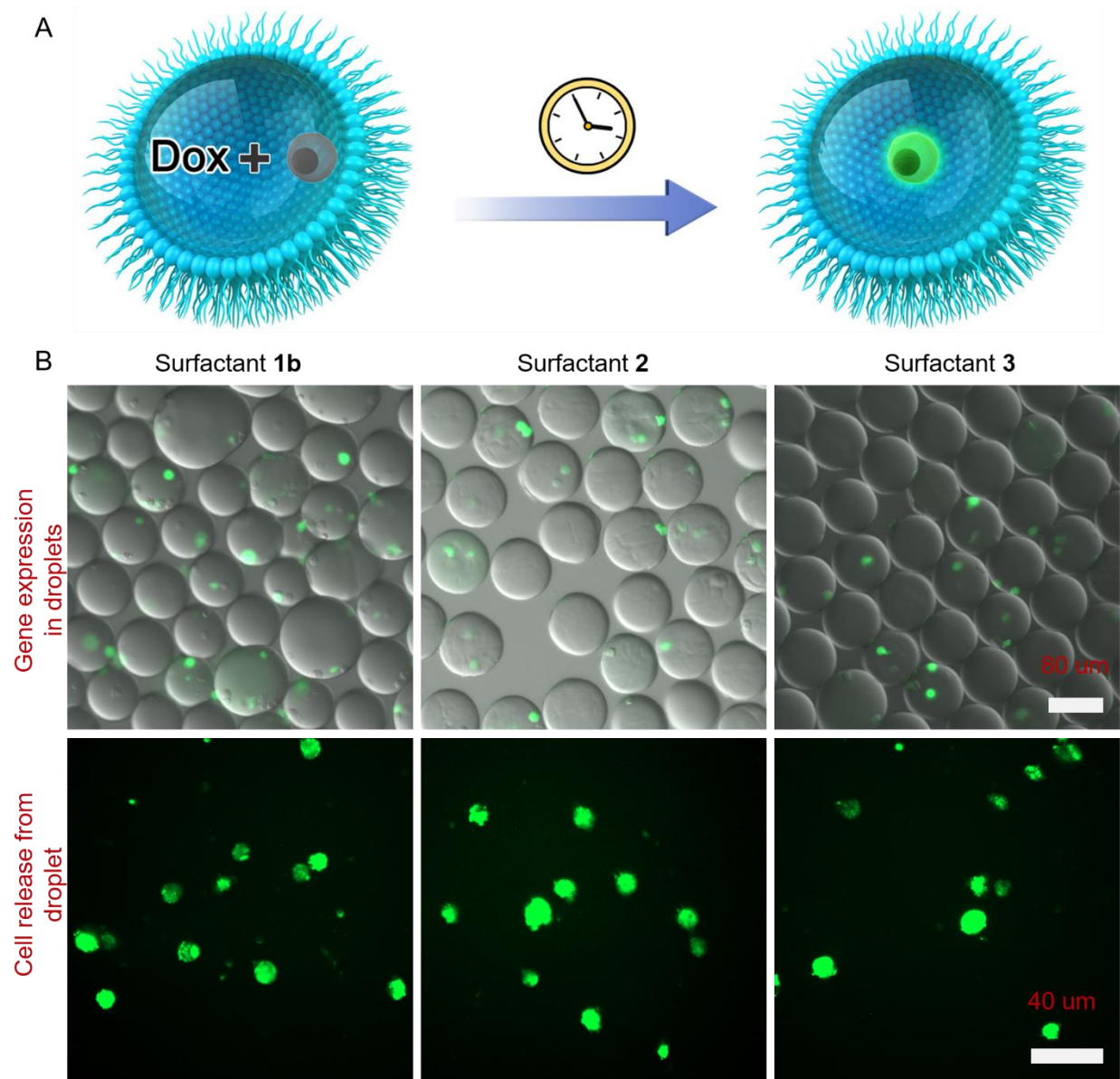
Fig. S6. Drug-inducible gene expression in single-cell cultured in droplets. (**A**) Schematic showing the co-encapsulation of the drug Dox and a non-fluorescent single-cell (grey) (within the aqueous phase) after droplet generation. The droplet was stabilized with either surfactant **1b**, surfactant **2**, or surfactant **3** as indicated in the images. The cell (green) started to express the GFP gene with time as Dox activated its transcription system to facilitate the gene expression. (**B**) Prior to cell encapsulation into droplets, Dox-inducible cells were dispersed in RPMI 1640 medium containing 4 µg/mL Dox, 5 µg/mL BSD, and 17% (v/v) Opti-prep. The cell density was 6.0×10^6 cells/mL, and the cell culture medium was supplemented with 10% FBS and 1% P-S. A single-droplet-maker device with two inlets (one for oil and one for cell culture media with cell

suspension) was used as demonstrated in the main text (**Fig. 3A**). The flow rates for droplet generation were 600 µL/h and 300 µL/h for oil and aqueous phases, respectively. The droplets were incubated for 48 h to turn on the GFP expression and, subsequently, differential interference contrast (DIC) images of the droplets were taken using a fluorescence microscope. To release the encapsulated cells from 100 µL emulsion droplets, the droplets were washed with HFE-7500 oil (10x500 µL) until the droplets coalesced into a single aqueous layer. After each wash, the excess oil underneath the emulsion and/or aqueous layer was removed by a syringe mounted with a long needle. The released cells were then imaged using a fluorescence microscope. Of note, the contaminated HFE-7500 oil can be easily recycled by distillation using a rotavapor under reduced pressure.
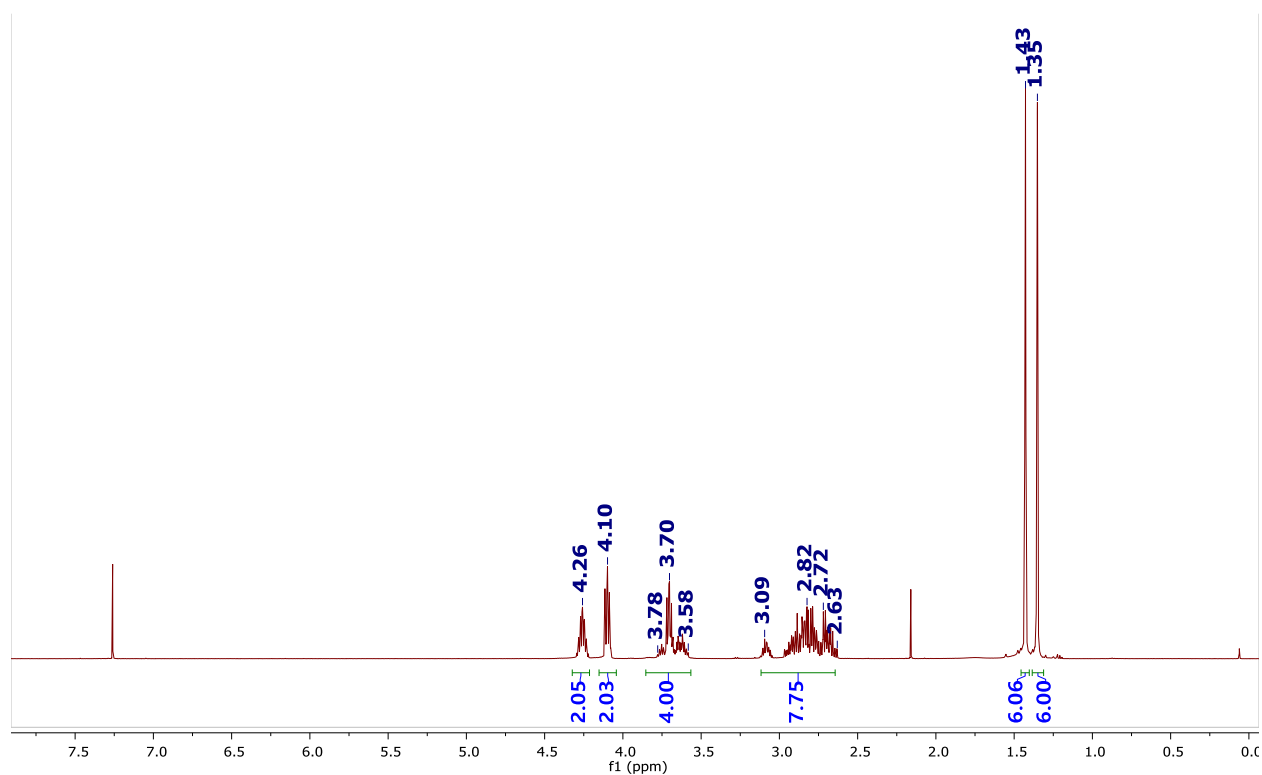
Fig. S7. ^{1}H NMR (500 MHz, CDCl$_3$) of compound **1a'**.
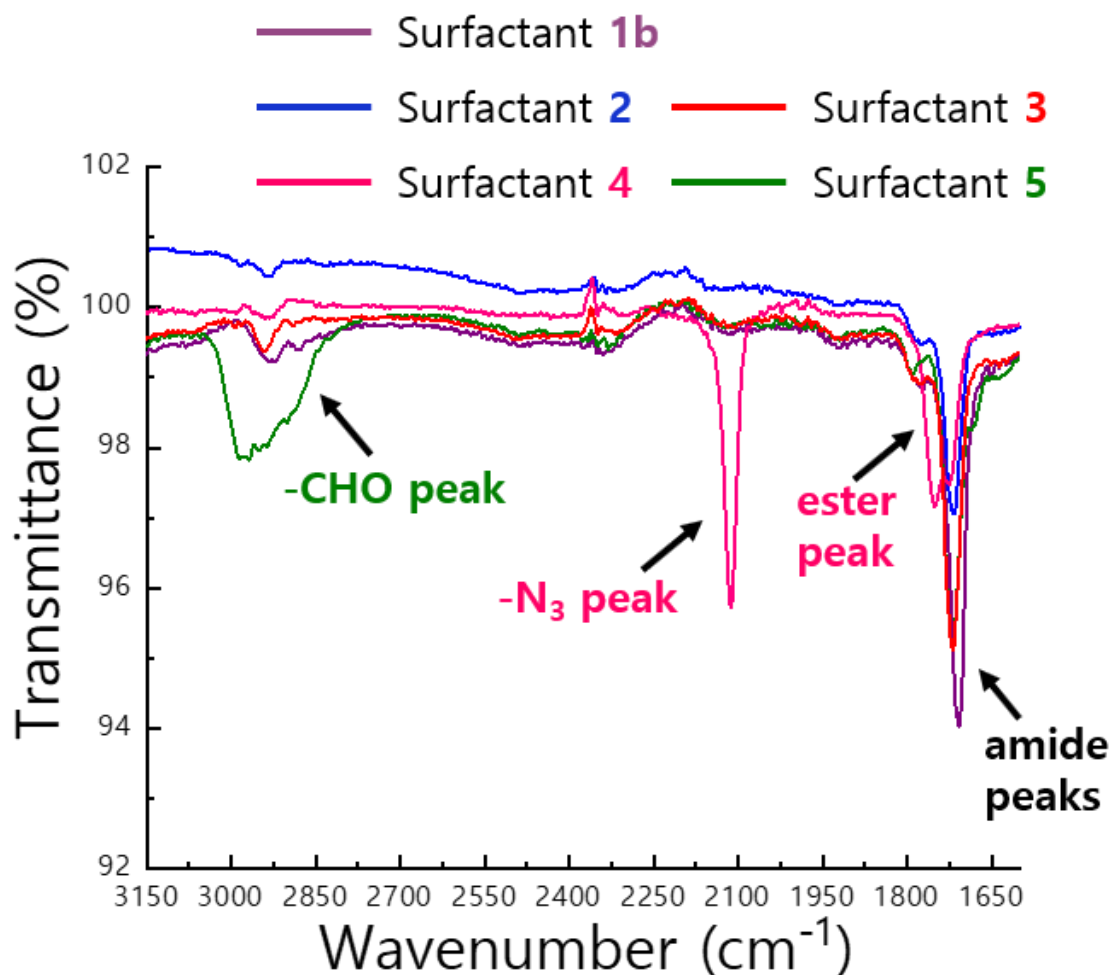
Fig. S8. Characterization of the surfactants by FT-IR. FT-IR spectra showing the presence of amide signals in the surfactants **1b**, **2**, **3**, **4** and **5** at ~1720 cm^{-1}. The successful preparation of the azido acetic acid coupled surfactant **4** was confirmed by both the ester signal at ~1750 cm^{-1} and the azide signal at ~2100 cm^{-1}. Surfactant **5**, which was created by oxidizing the 1,2-diols, showed a new signal at ~2850 cm^{-1}, which confirmed the formation of -CHO groups after the oxidation.
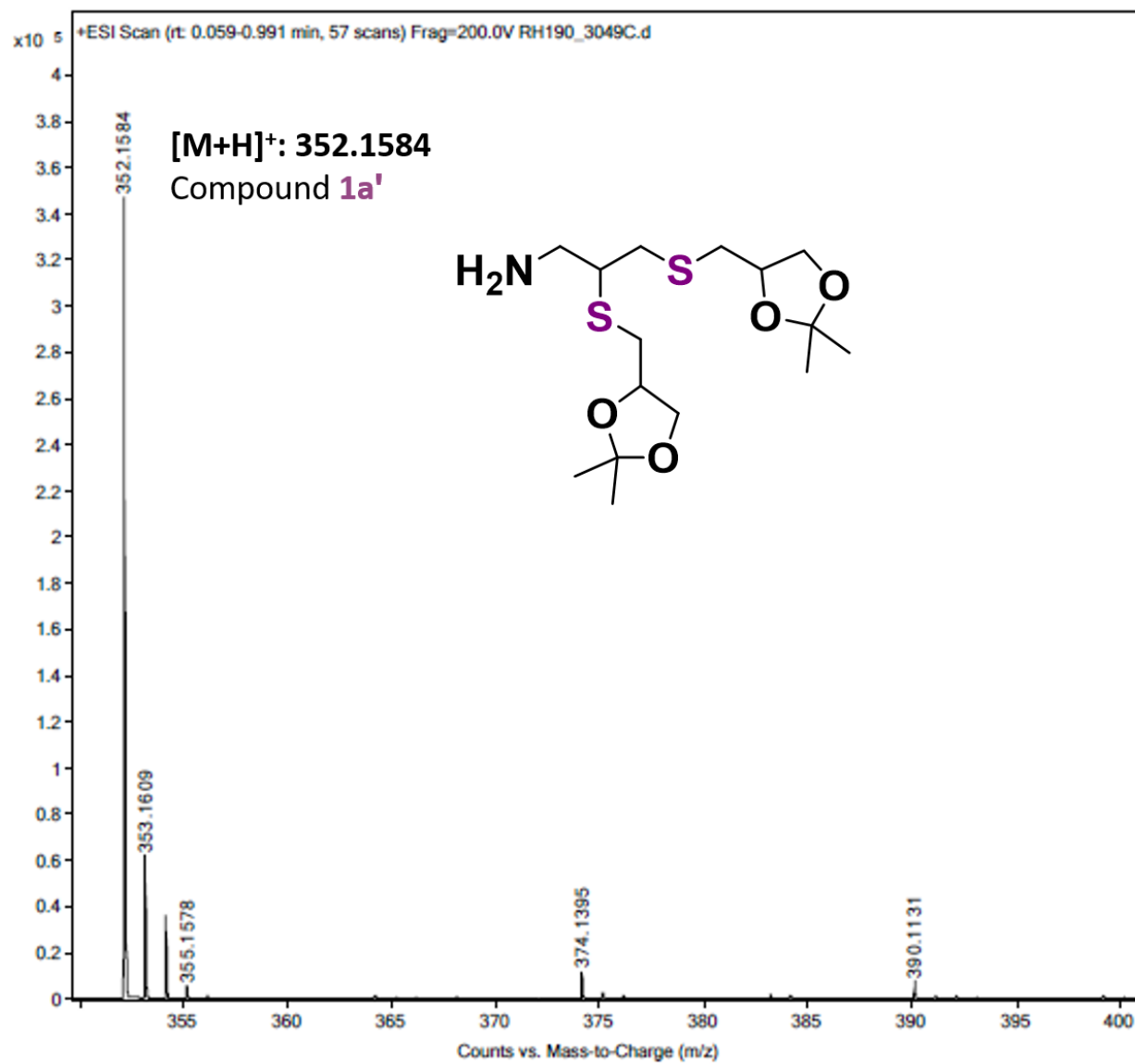
Fig. S9. ESI-MS of compound **1a'**.
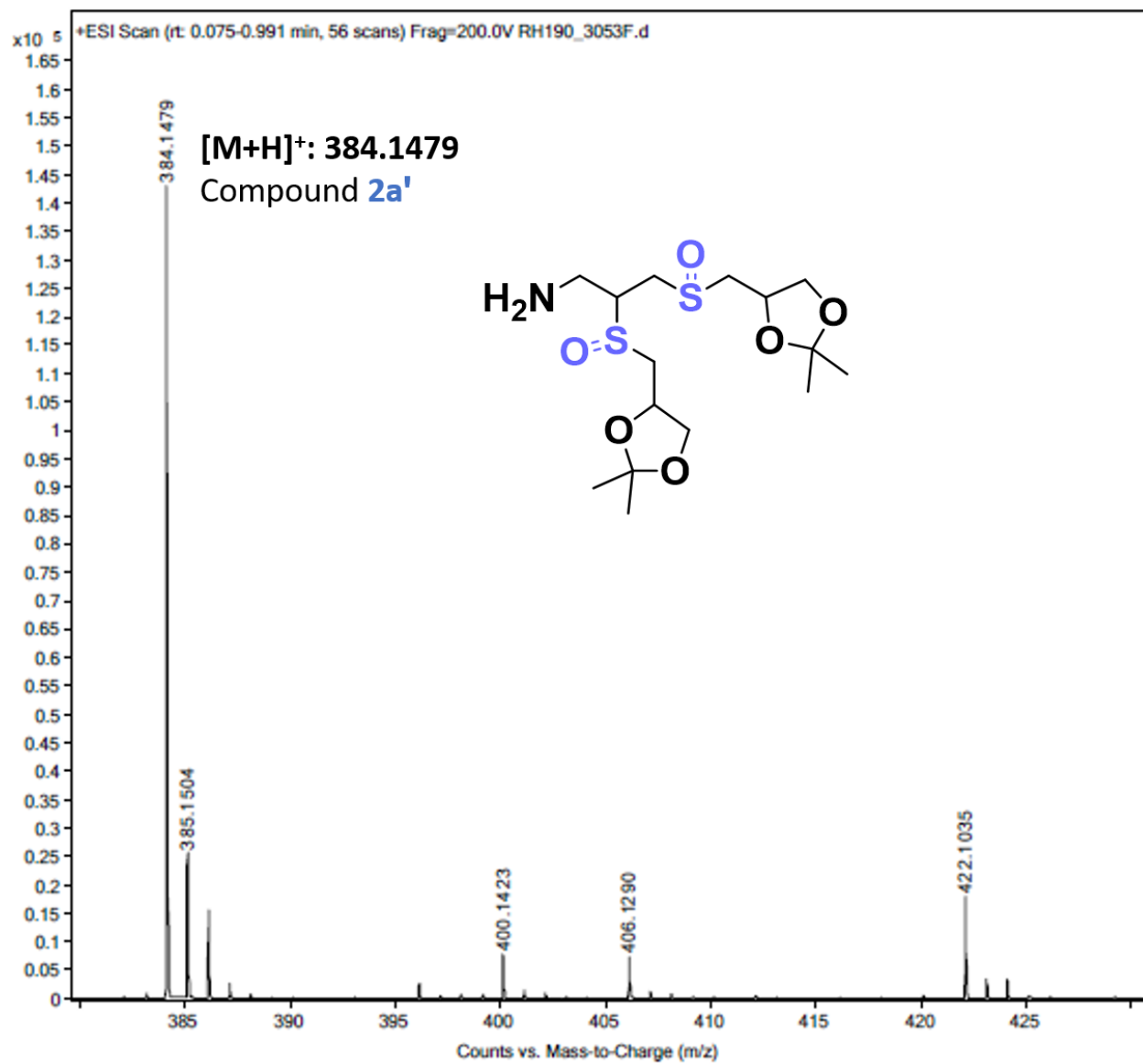
Fig. S10. ESI-MS of compound **2a'**.
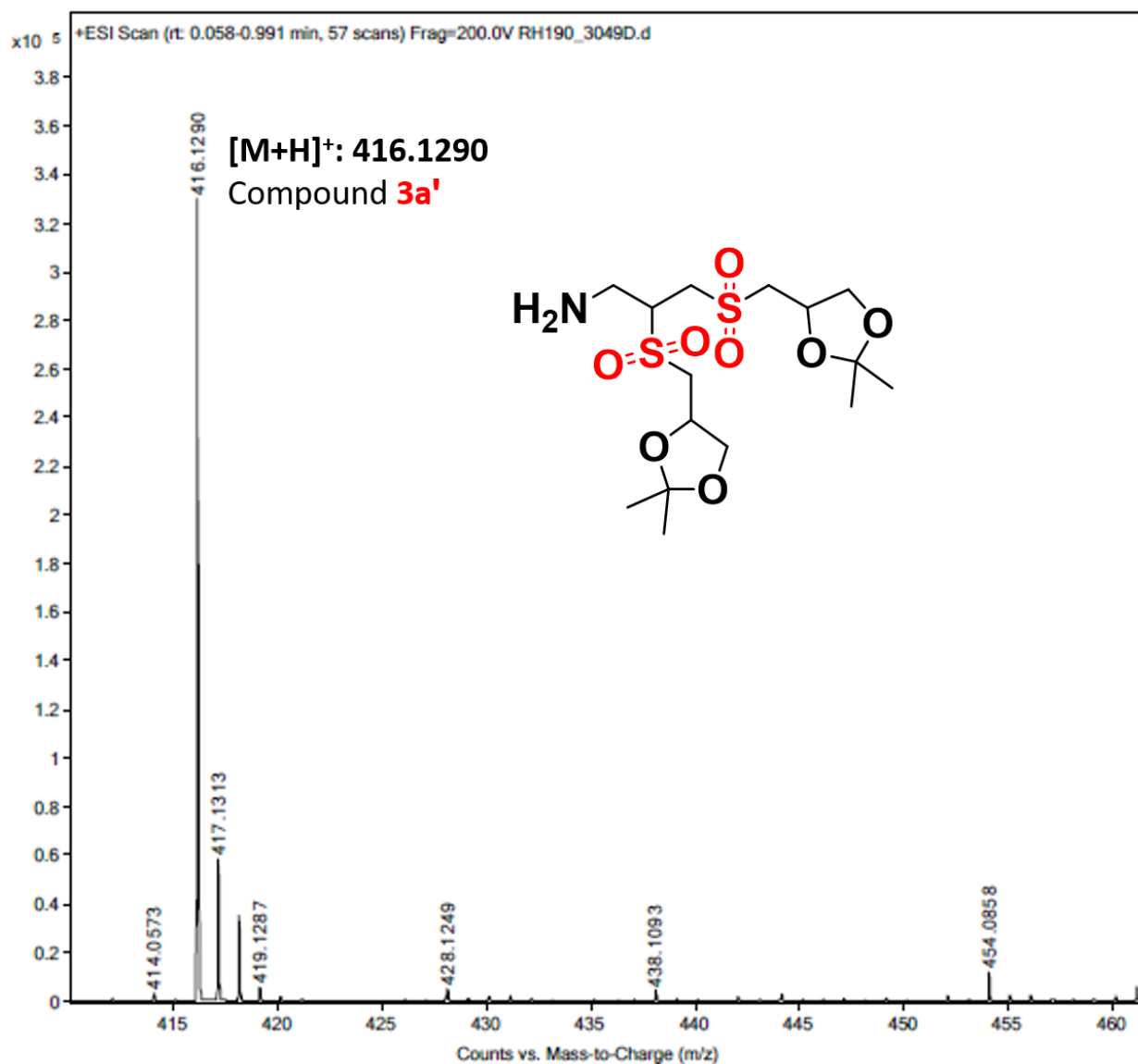
Fig. S11. ESI-MS of compound **3a'**.

REFERENCES

1. K. L. Killops, L. M. Campos, C. J. Hawker, *J. Am. Chem. Soc.* **130**, 5062-5064 (2008).
2. M.S. Chowdhury *et al.*, *Nat. Commun.* **10**, 4546 (2019).
3. S. Shahsavari *et al.*, *Beilstein J. Org. Chem.* **14**, 1750-1757 (2018).
4. J. M. Sarapas, G. N. Tew, *Angew. Chem. Int. Ed.* **55**, 15860-15863 (2016).
5. J. P. E. Human, J. A. Mills, *Nature* **158**, 877 (1946).
6. N. Boehnke, C. Cam, E. Bat, T. Segura, H. D. Maynard, *Biomacromolecules* **16**, 2101 (2015).
7. K. Yusa, L. Zhou, M. A. Li, A. Bradley, N. L. Craig, *Proc. Natl. Acad. Sci. U.S.A.* **108**, 1531-1536 (2010).
8. L. N. Randolph, X. Bao, C. Zhou, X. Lian, *Sci. Rep.* **7**, 1549 (2017).

4 Summary and Outlook

This thesis provides insight into the design of new oligoglycerol-based high-performance fluorosurfactants to stabilize pico- to nanoliter-scale droplets. Typically, these droplets are generated at kHz rates by PDMS-based droplet microfluidics for high-value biochemical assays. In addition, it demonstrated how fluorosurfactants could be rationally designed integrating variable spatial geometries of the oligoglycerol head groups. Furthermore, it illustrated how stimuli-responsive and functional surfactants can be created from readily available starting materials under mild reaction conditions. Besides, the study showed a promising direction to perform droplet-based functional assays that can benefit from the robust and reactive droplet interface which were easily created by the novel functional fluorosurfactants. Interestingly, post-customization of the head groups on functional fluorosurfactants did not alter the emulsion stability and droplet monodispersity. As the study greatly benefited from readily available starting materials, facile and scalable synthesis, and high performance fluorosurfactants, it is expected that the fluorosurfactant library should be of interest to a broader community including microfluidic users, molecular biologists, and chemists who are working with miniaturized droplet-based high-throughput platform to generate high-value products for basic research and medical diagnostics.

In the first project, novel fluorosurfactants using dendritic glycerol oligomers and linear perfluoropolyethers (PFPEs) were synthesized. Since polymeric surfactants are more effective than small molecule surfactants for stabilizing emulsion droplets, for surfactant synthesis, we employed mono- and triglycerol dendrons as the polar heads and commercially available low, medium, and high molecular weight PFPEs as the fluorinated tails. We employed mild reaction conditions and produced fluorosurfactants on a gram scale with high purity. Thus, five novel fluorosurfactants were created for droplet-microfluidics based water-in-oil (w/o) emulsion generation. The small library of fluorosurfactants allowed us to systematically investigate their ability to generate stable emulsions with exquisitely monodisperse droplets with or without viscous liquid. When the stable droplets were used for high-value biochemical assays, it revealed that the triglycerol dendron-based surfactants are robust, efficient, and significantly better than the gold standard PEG-surfactant to address two long-standing problems: droplet coalescence at temperature >80 ºC and inter-droplet leakage of small molecules. Besides, the surfactants showed a high degree of biocompatibility with bio-organisms, and they enabled monodisperse microgel synthesis at kilohertz rate.

In the second project, the effect of different polar head group architectures on the performance of fluorosurfactants was investigated regarding their polarity, surface activity, and ability to control inter-droplet leakage kinetics of small molecules. Both linear and dendritic triglycerol with same molecular weight and a common low chain length PFPE tail were applied to synthesize two linear and dendritic fluorosurfactants. Besides, three hydroxyl groups-bearing linear and dendritic fluorosurfactants were synthesized. By doing so, the interfacial tension values of the fluorosurfactants with three to four hydroxyl groups did not significantly differ from each other despite having variable hydroxyl groups and architectures in the hydrophilic head groups. When all surfactants were subjected to thin layer chromatography analysis on silica plates, it revealed that the more hydroxyl groups there are in a fluorosurfactant the higher the polarity of the surfactant is. However, surfactants with equal number of hydroxyl groups but with different architectures showed a marginal deviation in polarity from each other. Surprisingly, fluorosurfactants with linear triglycerol showed superior performance in controlling the inter-droplet small molecule transfer, while maintaining the robustness of the droplets. This necessitates designing of linear triglycerol-bearing fluorosurfactants with a high molecular weight PFPE in future studies, as high molecular weight PFPE can further control the inter-droplet transfer kinetics of small molecules. Above all, the linear triglycerol-based fluorosurfactant was post-modified with a small azido moiety to create a functional surfactant which allowed selective reactions to occur exclusively at the droplet interface. The post-modified surfactant was robust to generate monodisperse droplets at kHz rate, and highly efficient to fish 5-10 µM DBCO-bearing biotin-streptavidin complex from the aqueous droplets via SPAAC reaction.

In the third project, a novel thioether-based oxidation responsive fluorosurfactant was developed for droplet microfluidics. The polarity of the surfactant was varied by selectively oxidizing the thioethers present in the head groups. Therefore, by employing facile thiol-yne click chemistry, a dendritic triglycerol-amine polar head group with two thioethers in the backbone was synthesized from readily available propargyl amine and thioglycerol. Following an acetal protection of the cis-1,2-diols, the head group was then covalently coupled to a low molecular weight PFPE via amide coupling under mild reaction conditions. The surfactant with two thioethers in the backbone was selectively oxidized to create either sulfoxide- or sulfone-bearing surfactants. Following an acetal deprotection step, purely polar surfactant with either thioether, sulfoxides, or sulfones in the backbone and two cis-1,2-diols in the branch was created. Since sulfone among all can dramatically increase the solubility of the surfactant, post-functionalization or further oxidation of the cis-1,2-diols should not alter the polarity of the

surfactant. By post-modifying the hydroxyl groups with azido acetic acid, a novel multivalent surfactant with multiple azides was synthesized. In addition, by oxidizing the cis-1,2-diols, another new surfactant with multiple aldehyde groups per head group was synthesized. Both the functional surfactants demonstrated their ability to create robust and stable emulsions, and to generate highly monodisperse droplets. The multivalent azide-bearing surfactant could efficiently react with the DBCO-bearing biotin via a SPAAC reaction. It then enabled in-situ fishing of streptavidin from the aqueous droplet within an hour of incubation via selective interaction between biotin and streptavidin. The aldehyde-bearing surfactants could exquisitely react with hydrazide modified gelatin at the droplet interface via dynamic hydrazone reaction to form reversible capsules under both slightly acidic and slightly basic conditions. Besides, the novel surfactants showed excellent biocompatibility with single-cell gene expression. Thus, the oxidation responsive fluorosurfactants hold a great promise to explore many appealing droplet-based high-performance assays for a wide variety of applications, including capture of target biomolecules and fabrication of capsules in one-step at kHz rates.

Since decades, it has long been a dream of the droplet microfluidics users that water-in-oil (w/o) emulsion droplet should be highly robust but easy to break to release the encapsulated materials, be like a sealed container but allow exquisitely the exchange of respiratory gases for living cells, and be able to create reactive interfaces to conduct functional assays but without compromising with the droplet stability. Moreover, for industrial-scale production, breaking tens to thousands of liters of emulsion droplets by washing with the de-emulsification chemicals will certainly be extremely challenging despite it works for small-scale research work. Although droplets mimic a sealed container and allow long-term storage of the more polar contents without cross-contamination, short-term to long-term strorage of the less polar contents is undoubtely a challenge for droplet-based screening. Although functional droplet interfaces can be created by using functional surfactants for high-performance assays, such as from-droplet fishing of biomolecules by exploiting highly specific, affinity-based biochemistry that allows capturing and bringing the target analytes at the interfaces, isolation of the analytes from the surfactant is an obvious bottleneck of the analytics.

To address these, smart, readily-tunable, user-friedly, and high-performance surfactants with cleavable and cross-linkable features should be designed and tested under appropriate experimental conditions. To design a cleavable surfactatnt, a wide variety of stimuli responsive moieties can be integrated into it that will be sensitive to a diverse stimuli, including chemical and physical stimuli, such as pH, temperature, light, redox, electromagnetic radiation, and

soundwave. To design a rapid crosslinkable surfactant, various functional groups can be added that will allow the surfactant to undergo a broad range of in situ click-chemistries. The ability to integrate both the stimuli-responsiveness and crosslinking functionality into one surfactant will enhance the storage time of not only the more polar contents but also the less-polar contents. Moreover, it will allow breaking the crosslinked networks on-demand. Above all, it can be concluded that the design of stimuli-responsive surfactant with rapidly crosslinkable moieties will push the limit of droplet microfluidics-based much exciting research and development that is trying to tackle the ever growing analytical challenges for chemistry, biology, and medical diagnostics.

5 Kurzzusammenfassung

Diese Arbeit bietet einen Einblick in das Design neuer Hochleistungs-Fluortenside auf Oligoglycerinbasis zur Stabilisierung von Tröpfchen im Piko- bis Nanoliter-Maßstab. Typischerweise werden diese Tröpfchen bei kHz-Raten durch PDMS-basierte Tröpfchenmikrofluidik für hochwertige biochemische Assays erzeugt. Außerdem konnte gezeigt werden, wie Fluortenside rational designet werden können, indem variable räumliche Geometrien der Oligoglycerin-Kopfgruppen integriert werden. Darüber hinaus wurde untersucht, wie stimulierende und funktionelle Tenside aus leicht verfügbaren Ausgangsmaterialien unter milden Reaktionsbedingungen hergestellt werden können. Des Weiteren zeigte die Studie eine vielversprechende Richtung für die Durchführung tröpfchenbasierter funktioneller Assays auf, die von der robusten und reaktiven Tröpfchengrenzfläche profitieren können, die durch die neuartigen funktionellen Fluortenside leicht erzeugt werden können. Interessanterweise veränderte die Nachanpassung der Kopfgruppen an funktionelle Fluortenside die Emulsionsstabilität und die Tröpfchenmonodispersität nicht. Da die Studie in hohem Maße von den leicht verfügbaren Ausgangsmaterialien, der einfachen und skalierbaren Synthese und den leistungsstarken Fluortensiden profitierte, wird erwartet, dass die Fluortensid-Bibliothek für eine breitere Gemeinschaft von Interesse sein dürfte, einschließlich Anwendern der Mikrofluidik, Molekularbiologen und Chemiker, die mit einer auf miniaturisierten Tröpfchen basierenden Hochdurchsatz-Plattform arbeiten, um hochwertige Produkte für die Grundlagenforschung und medizinische Diagnostik zu erzeugen.

Im ersten Projekt wurden neuartige Fluortenside unter Verwendung von dendritischen Glycerin-Oligomeren und linearen Perfluorpolyethern (PFPEs) synthetisiert. Da polymere Tenside für die Stabilisierung von Emulsionströpfchen wirksamer sind als niedermolekulare Tenside, verwendeten wir für die Tensidsynthese Mono- und Triglycerindendrone als polare Köpfe und kommerziell erhältliche PFPEs mit niedrigem, mittlerem und hohem Molekulargewicht als fluorierte Schwänze. Wir verwendeten milde Reaktionsbedingungen und stellten Fluortenside im Gramm-Maßstab mit hoher Reinheit her. Auf diese Weise wurden fünf neuartige Fluortenside für die Erzeugung von Wasser-in-Öl-Emulsionen (w/o) auf der Basis von Tröpfchen-Mikrofluidik geschaffen. Die kleine Bibliothek von Fluortensiden ermöglichte es uns, systematisch ihre Fähigkeit zu untersuchen, stabile Emulsionen mit exquisit monodispersen Tröpfchen mit oder ohne viskose Flüssigkeit zu erzeugen. Als die stabilen Tröpfchen für hochwertige biochemische Assays verwendet wurden, zeigte sich, dass die auf

Triglycerin-Dendron basierenden Tenside robust, effizient und deutlich besser als sind, um zwei seit langem bestehende Probleme zu lösen: die Tröpfchenkoaleszenz bei Temperaturen >80 °C und das Austreten kleiner Moleküle zwischen den Tröpfchen. Außerdem zeigten die Tenside einen hohen Grad an Biokompatibilität mit Bioorganismen, und sie ermöglichten eine monodisperse Mikrogelsynthese bei einer Kilohertzrate.

Im zweiten Projekt wurde der Einfluss verschiedener polarer Kopfgruppen-architekturen auf die Leistung von Fluortensiden hinsichtlich ihrer Polarität, Oberflächen-aktivität und der Fähigkeit zur kinetischen Kontrolle über den Austritt kleiner Moleküle zwischen den Tröpfchen. Sowohl lineares als auch dendritisches Triglycerin mit demselben Molekulargewicht und einem gleichen PFPE-Schwanz mit niedriger Kettenlänge wurden zur Synthese von zwei linearen und dendritischen Fluortensiden verwendet. Außerdem wurden drei Hydroxylgruppen tragende lineare und dendritische Fluortenside synthetisiert. Dabei unterschieden sich die Grenzflächenspannungswerte der Fluortenside mit drei bis vier Hydroxylgruppen nicht signifikant voneinander, obwohl sie variable Hydroxylgruppen und Architekturen in den hydrophilen Kopfgruppen aufwiesen. Bei dünnschichtchromatografischer Untersuchung aller Tenside, zeigte sich, dass die Polarität des Tensids umso höher ist, je mehr Hydroxylgruppen in einem Fluortensid vorhanden sind. Tenside mit gleicher Anzahl von Hydroxylgruppen, aber mit unterschiedlicher Architektur zeigten eine marginale Abweichung in der Polarität voneinander. Überraschenderweise zeigten Fluortenside mit linearem Triglycerin eine überlegene Performance bei der Kontrolle des Transfers kleiner Moleküle zwischen den Tröpfchen, wobei die Robustheit der Tröpfchen erhalten blieb. Dies erfordert in zukünftigen Studien die Entwicklung von linearen triglycerinhaltigen Fluortensiden mit einem PFPE mit hohem Molekulargewicht, da PFPE mit hohem Molekulargewicht die Kinetik des Transfers kleiner Moleküle zwischen den Tröpfchen weiter kontrollieren kann. Vor allem wurde das lineare triglycerinhaltige Fluortensid mit einer kleinen Azidogruppe nachmodifiziert, um ein funktionelles Tensid zu schaffen, das selektive Reaktionen ausschließlich an der Tröpfchengrenzfläche ermöglicht. Das postmodifizierte Tensid war ausreichend robust, um monodisperse Tröpfchen bei kHz-Rate zu erzeugen, und hocheffizient, sodass 5-10 µM DBCO-haltige Biotin-Streptavidin-Komplexe mittels SPAAC-Reaktion aus den wässrigen Tröpfchen gefischt wurden.

Im dritten Projekt wurde ein neuartiges oxidationsreaktives Fluortensid auf Thioetherbasis für die Tröpfchenmikrofluidik entwickelt. Die Polarität des Tensids wurde durch selektive Oxidation der in den Kopfgruppen vorhandenen Thioether variiert. Daher

wurde unter Verwendung einer einfachen Thiol-Yne-Click-Chemie eine polare dendritische Triglycerin-Amin-Kopfgruppe mit zwei Thioethern in der Hauptkette aus leicht verfügbarem Propargylamin und Thioglycerin synthetisiert. Nach einem Acetalschutz der cis-1,2-Diole wurde die Kopfgruppe dann unter milden Reaktionsbedingungen über eine Amidkopplung kovalent an ein PFPE mit niedrigem Molekulargewicht gekoppelt. Das Tensid mit zwei Thioethern in der Hauptkette wurde selektiv oxidiert, um entweder sulfoxid- oder sulfonhaltige Tenside zu erzeugen. Nach Entschützung der Acetalgruppen wurde ein rein polares Tensid mit entweder Thioethern, Sulfoxiden oder Sulfonen in der Hauptkette und zwei cis-1,2-Diolen in der Verzweigung erzeugt. Da das Sulfon die Löslichkeit des Tensids dramatisch erhöhen kann, sollte eine Nachfunktionalisierung oder weitere Oxidation der cis-1,2-Diole die Polarität des Tensids nicht verändern. Durch Nachmodifizierung der Hydroxylgruppen mit Azidoessigsäure wurde ein neuartiges mehrwertiges Tensid mit mehreren Aziden synthetisiert. Darüber hinaus wurde durch Oxidation der cis-1,2-Diole ein weiteres neues Tensid mit mehreren Aldehydgruppen pro Kopfgruppe synthetisiert. Beide funktionellen Tenside zeigten ihre Fähigkeit, robuste und stabile Emulsionen zu erzeugen und hochgradig monodisperse Tröpfchen zu erzeugen. Das multivalente, azidhaltige. Tensid konnte über eine SPAAC-Reaktion effizient mit dem DBCO-haltigen Biotin reagieren. Dies ermöglichte dann das in-situ-Fischen von Streptavidin aus dem wässrigen Tröpfchen innerhalb einer Stunde nach der Inkubation durch selektive Interaktion zwischen Biotin und Streptavidin. Die aldehydhaltigen Tenside konnten mit Hydrazid-modifizierter Gelatine an der Tröpfchengrenzfläche über eine dynamische Hydrazonreaktion unter leicht sauren und leicht basischen Bedingungen hervorragend reagieren und reversible Kapseln bilden. Außerdem zeigten die neuartigen Tenside eine ausgezeichnete Biokompatibilität mit der Einzelzell-Genexpression. Daher versprechen die oxidationsreaktiven Fluortenside die Erforschung vieler attraktiver, tröpfchenbasierter Hochleistungsassays für eine Vielzahl von Anwendungen, einschließlich des Einfangens von Ziel-Biomolekülen und der Herstellung von Kapseln in einem Schritt bei kHz-Raten.

Seit Jahrzehnten ist es ein Traum der Anwender von Tröpfchenmikrofluidik, dass Wasser-in-Öl-Emulsionströpfchen (w/o) einerseits sehr robust und trotzdem leicht zu brechen sind, um eingekapselte Materialien kontrolliert freizusetzen, und außerdem wie ein versiegelter Behälter wirken, die den Austausch den Gasaustausch für lebende Zellen in hervorragender Weise ermöglichen. Des Weiteren sollten sie in der Lage sein reaktive Grenzflächen zur Durchführung funktioneller Assays zu schaffen, ohne die Tröpfchenstabilität zu beeinflussen.

Nichtsdestotrotz wird das Brechen von tausenden bis zehntausenden. Litern Emulsionströpfchen durch Waschen mit Deemulgierungschemikalien für die Produktion im industriellen Maßstab sicherlich eine große Herausforderung darstellen, obwohl es für Forschungsarbeiten im kleinen Maßstab funktioniert. Da die Tröpfchen einen versiegelten Behälter imitieren und eine langfristige Lagerung des eher polaren Inhalts ohne Kreuzkontamination ermöglichen, ist die kurz- bis langfristige Lagerung des weniger polaren Inhalts zweifellos eine Herausforderung für das tröpfchenbasierte Screening. Obwohl funktionelle Tröpfchengrenzflächen durch die Verwendung von funktionellen Tensiden für Hochleistungsassays geschaffen werden können, wie z.B. das Fischen von Biomolekülen aus Tröpfchen durch Ausnutzung der hochspezifischen, affinitätsbasierten Biochemie, die es ermöglicht, die Zielanalyten an den Grenzflächen zu fangen und an diese zu bringen, ist die Isolierung der Analyten vom Tensid ein offensichtlicher Engpass der Analytik.

Um diese Probleme anzugehen, sollten in Zukunft intelligente, leicht abstimmbare, anwenderfreundliche und leistungsstarke Tenside mit spaltbaren und vernetzbaren Eigenschaften entwickelt und unter geeigneten experimentellen Bedingungen getestet werden. Um ein spaltbares Tensid zu entwerfen, können eine Vielzahl von auf externe Reize reagierende. Einheiten in das Tensid integriert werden, einschließlich chemischer und physikalischer Reize wie pH-Wert, Temperatur, Licht, Redox, elektromagnetische Strahlung und Ultraschall. Um ein schnell vernetzbares Tensid zu entwerfen, können verschiedene funktionelle Gruppen hinzugefügt werden, die es ermöglichen, das Tensid durch ein breites Spektrum an Click-Chemie zu modifizieren. Die Fähigkeit, sowohl die Reizempfindlichkeit als auch die Vernetzungsfunktionalität in ein einziges Tensid zu integrieren, wird die Lagerzeit nicht nur der eher polaren, sondern auch der weniger polaren Inhaltsstoffe verbessern. Darüber hinaus wird es möglich sein, die Netzwerke bei Bedarf aufzubrechen. Vor allem aber lässt sich schlussfolgern, dass das Design von auf Stimuli-sensitiven Tensiden mit schnell vernetzbaren Komponenten die Grenzen der auf Tröpfchenmikrofluidik basierenden, sehr spannenden Forschung und Entwicklung beeinflussen wird, um die ständig wachsenden analytischen Herausforderungen für Chemie, Biologie und medizinische Diagnostik zu bewältigen.

6 References

[1]   P. Gruner, B. Riechers, B. Semin, J. Lim, A. Johnston, K. Short, J. C. Baret, *Nat. Commun.* **2016**, *7*, 10392.

[2]   T. Kong, J. Wu, M. To, K. Wai Kwok Yeung, H. Cheung Shum, L. Wang, *Biomicrofluidics* **2012**, *6*, 34104.

[3]   I. Lim, A. Vian, H. L. van de Wouw, R. A. Day, C. Gomez, Y. Liu, A. L. Rheingold, O. Campas, E. M. Sletten, *J. Am. Chem. Soc.* **2020**, *142*, 16072-16081.

[4]   A. B. Theberge, F. Courtois, Y. Schaerli, M. Fischlechner, C. Abell, F. Hollfelder, W. T. Huck, *Angew. Chem. Int. Ed. Engl.* **2010**, *49*, 5846-5868.

[5]   F. Goodarzi, S. Zendehboudi, *Can. J. Chem. Eng.* **2018**, *97*, 281-309.

[6]   M. Tupinamba Lima, S. N. Kurt-Zerdeli, D. Brüggemann, V. J. Spiering, M. Gradzielski, R. Schomäcker, *Colloids Surf., A* **2020**, *588*.

[7]   R. R. Raju, F. Liebig, A. Hess, H. Schlaad, J. Koetz, *RSC Adv.* **2019**, *9*, 19271-19277.

[8]   N. Pal, M. Vajpayee, A. Mandal, *Energy Fuels* **2019**, *33*, 6048-6059.

[9]   C. F. Santa Chalarca, R. A. Letteri, A. Perazzo, H. A. Stone, T. Emrick, *Adv. Funct. Mater.* **2018**, *28*.

[10]   E. Baba, T. Yatsunami, T. Yamamoto, Y. Tezuka, *Polym. J.* **2015**, *47*, 408-412.

[11]   A. D. Dinsmore, M. F. Hsu, M. G. Nikolaides, M. Marquez, A. R. Bausch, D. A. Weitz, Science **2002**, *298*, 1006-1009.

[12]   S. M. Hashemnejad, A. Z. M. Badruddoza, B. Zarket, C. Ricardo Castaneda, P. S. Doyle, *Nat. Commun.* **2019**, *10*, 2749.

[13]   R. E. Wachtel, V. L. L. Mer, *J. Colloid Sci.* **1962**, *17*, 531-564.

[14]   G. M. Whitesides, *Nature* **2006**, *442*, 368-373.

[15]   S. K. Sia, G. M. Whitesides, *Electrophoresis* **2003**, *24*, 3563-3576.

[16]   A. Rotem, O. Ram, N. Shoresh, R. A. Sperling, A. Goren, D. A. Weitz, B. E. Bernstein, *Nat. Biotechnol.* **2015**, *33*, 1165-1172.

[17]   S. Nawar, J. K. Stolaroff, C. Ye, H. Wu, D. T. Nguyen, F. Xin, D. A. Weitz, *Lab Chip* **2020**, *20*, 147-154.

[18]   L.-Y. Chu, A. S. Utada, R. K. Shah, J.-W. Kim, D. A. Weitz, *Angew. Chem. Int. Ed. Engl.* **2007**, *46*, 8970-8974.

[19]   A. S. Utada, E. Lorenceau, D. R. Link, P. D. Kaplan, H. A. Stone, D. A. Weitz, *Science* **2005**, *308*, 537-541.

[20]   Y. Lu, D. Chowdhury, G. T. Vladisavljevic, K. Koutroumanis, S. Georgiadou, *Membranes (Basel)* **2016**, *6*.

[21]   S. A. Nabavi, G. T. Vladisavljevic, M. V. Bandulasena, O. Arjmandi-Tash, V. Manovic, *J. Colloid Interface Sci.* **2017**, *505*, 315-324.

[22]   L. L. A. Adams, T. E. Kodger, S.-H. Kim, H. C. Shum, T. Franke, D. A. Weitz, *Soft Matter* **2012**, *8*.

[23]   J. G. Werner, B. T. Deveney, S. Nawar, D. A. Weitz, *Adv. Funct. Mater.* **2018**, *28*.

[24]   M. V. Bandulasena, G. T. Vladisavljevic, B. Benyahia, *J. Colloid Interface Sci.* **2019**, *542*, 23-32.

[25]   L. Mazutis, J. Gilbert, W. L. Ung, D. A. Weitz, A. D. Griffiths, J. A. Heyman, *Nat. Protoc.* **2013**, *8*, 870-891.

[26]   J. N. Lee, C. Park, G. M. Whitesides, *Anal. Chem.* **2003**, *75*, 6544-6554.

[27]   S. H. Kim, J. W. Kim, J. C. Cho, D. A. Weitz, *Lab Chip* **2011**, *11*, 3162-3166.

[28]   P. K. Kilpatrick, *Energy Fuels* **2012**, *26*, 4017-4026.

[29]   D. J. McClements, *Soft Matter* **2012**, *8*, 1719-1729.

[30] C. Holtze, A. C. Rowat, J. J. Agresti, J. B. Hutchison, F. E. Angile, C. H. Schmitz, S. Koster, H. Duan, K. J. Humphry, R. A. Scanga, J. S. Johnson, D. Pisignano, D. A. Weitz, *Lab Chip* **2008**, *8*, 1632-1639.

[31] S. A. Raya, I. Mohd Saaid, A. Abbas Ahmed, A. Abubakar Umar, *J. Pet. Explor. Prod. Technol.* **2020**, *10*, 1711-1728.

[32] L. He, J. Hu, W. Deng, *Polym. Chem.* **2018**, *9*, 4926-4946.

[33] H. Lee, C. H. Choi, A. Abbaspourrad, C. Wesner, M. Caggioni, T. Zhu, S. Nawar, D. A. Weitz, *Adv. Mater.* **2016**, *28*, 8425-8430.

[34] B. Zhang, Z. Jiang, X. Zhou, S. Lu, J. Li, Y. Liu, C. Li, *Angew. Chem. Int. Ed. Engl.* **2012**, *51*, 13159-13162.

[35] T. Shimizu, M. Masuda, H. Minamikawa, *Chem. Rev.* **2005**, *105*, 1401-1443.

[36] D. A. Balazs, W. Godbey, *J. Drug Deliv.* **2011**, *2011*, 326497.

[37] B.-J. Lin, W.-H. Chen, W. M. Budzianowski, C.-T. Hsieh, P.-H. Lin, *Appl. Energy* **2016**, *178*, 746-757.

[38] A. Hidalgo, A. Cruz, J. Perez-Gil, *Eur. J. Pharm. Biopharm.* **2015**, *95*, 117-127.

[39] C. Love, J. Steinkuhler, D. T. Gonzales, N. Yandrapalli, T. Robinson, R. Dimova, T. D. Tang, *Angew. Chem. Int. Ed. Engl.* **2020**, *59*, 5950-5957.

[40] A. J. Kirby, P. Camilleri, J. B. Engberts, M. C. Feiters, R. J. Nolte, O. Soderman, M. Bergsma, P. C. Bell, M. L. Fielden, C. L. Garcia Rodriguez, P. Guedat, A. Kremer, C. McGregor, C. Perrin, G. Ronsin, M. C. van Eijk, *Angew. Chem. Int. Ed. Engl.* **2003**, *42*, 1448-1457.

[41] P. Raffa, A. A. Broekhuis, F. Picchioni, *J. Pet. Sci. Eng.* **2016**, *145*, 723-733.

[42] P. Raffa, D. A. Wever, F. Picchioni, A. A. Broekhuis, *Chem. Rev.* **2015**, *115*, 8504-8563.

[43] A. Wołowicz, K. Staszak, *J. Mol. Liq.* **2020**, *299*.

[44] X. Han, Y. Lu, J. Xie, E. Zhang, H. Zhu, H. Du, K. Wang, B. Song, C. Yang, Y. Shi, Z. Cao, *Nat. Nanotechnol.* **2020**, *15*, 605-614.

[45] J. M. Sarapas, G. N. Tew, *Angew. Chem. Int. Ed. Engl.* **2016**, *55*, 15860-15863.

[46] R. Bej, K. Achazi, R. Haag, S. Ghosh, *Biomacromolecules* **2020**, *21*, 3353-3363.

[47] M. Meier, J. Kennedy-Darling, S. H. Choi, E. M. Norstrom, S. S. Sisodia, R. F. Ismagilov, *Angew. Chem. Int. Ed. Engl.* **2009**, *48*, 1487-1489.

[48] M. Wyszogrodzka, R. Haag, *Langmuir* **2009**, *25*, 5703-5712.

[49] L. H. Urner, K. Goltsche, M. Selent, I. Liko, M.-P. Schweder, C. V. Robinson, K. Pagel, R. Haag, *Chem. - Eur. J.* **2020**.

[50] Y.-L. Chiu, H. F. Chan, K. K. L. Phua, Y. Zhang, S. Juul, B. R. Knudsen, Y.-P. Ho, K. W. Leong, *ACS Nano* **2014**, *8*, 3913-3920.

[51] J. C. Baret, F. Kleinschmidt, A. El Harrak, A. D. Griffiths, *Langmuir* **2009**, *25*, 6088-6093.

[52] J. C. Baret, *Lab Chip* **2012**, *12*, 422-433.

[53] L. S. Roach, H. Song, R. F. Ismagilov, *Anal. Chem.* **2005**, *77*, 785-796.

[54] A. Lee, S. K. Tang, C. R. Mace, G. M. Whitesides, *Langmuir* **2011**, *27*, 11560-11574.

[55] A. M. Klein, L. Mazutis, I. Akartuna, N. Tallapragada, A. Veres, V. Li, L. Peshkin, D. A. Weitz, M. W. Kirschner, *Cell* **2015**, *161*, 1187-1201.

[56] G. Etienne, M. Kessler, E. Amstad, *Macromol. Chem. Phys.* **2017**, *218*.

[57] Z. Cao, S. Jiang, *Nano Today* **2012**, *7*, 404-413.

[58] D. J. Holt, R. J. Payne, W. Y. Chow, C. Abell, *J. Colloid Interface Sci.* **2010**, *350*, 205-211.

[59] O. Wagner, J. Thiele, M. Weinhart, L. Mazutis, D. A. Weitz, W. T. Huck, R. Haag, *Lab Chip* **2016**, *16*, 65-69.

[60] D. Grun, L. Kester, A. V. Oudenaarden, *Nat. Methods*, **2014**, *11*, 637-640.

[61] R. Zilionis, J. Nainys, A. Veres, V. Savova, D. Zemmour, A. M. Klein, L. Mazutis, *Nat. Protoc.* **2017**, *12*, 44-73.
[62] K. Matula, F. Rivello, W. T. S. Huck, *Adv. Biosyst.* **2020**, *4*, e1900188.
[63] A. C. Daly, L. Riley, T. Segura, J. A. Burdick, *Nat. Rev. Mater.* **2019**, *5*, 20-43.
[64] A. S. Mao, J. W. Shin, S. Utech, H. Wang, O. Uzun, W. Li, M. Cooper, Y. Hu, L. Zhang, D. A. Weitz, D. J. Mooney, *Nat. Mater.* **2017**, *16*, 236-243.
[65] C. Holtze, *J. Phys. D: Appl. Phys.* **2013**, *46*.
[66] D. A. Weitz, *Lab Chip* **2017**, *17*, 2539.
[67] D. Pekin, Y. Skhiri, J. C. Baret, D. Le Corre, L. Mazutis, C. B. Salem, F. Millot, A. El Harrak, J. B. Hutchison, J. W. Larson, D. R. Link, P. Laurent-Puig, A. D. Griffiths, V. Taly, *Lab Chip* **2011**, *11*, 2156-2166.
[68] F. Lan, J. R. Haliburton, A. Yuan, A. R. Abate, *Nat. Commun.* **2016**, *7*, 11784.
[69] R. Ding, W. L. Ung, J. A. Heyman, D. A. Weitz, *Biomicrofluidics* **2017**, *11*, 014114.
[70] T. J. Abram, H. Cherukury, C. Y. Ou, T. Vu, M. Toledano, Y. Li, J. T. Grunwald, M. N. Toosky, D. F. Tifrea, A. Slepenkin, J. Chong, L. Kong, D. V. Del Pozo, K. T. La, L. Labanieh, J. Zimak, B. Shen, S. S. Huang, E. Gratton, E. M. Peterson, W. Zhao, *Lab Chip* **2020**, *20*, 477-489.
[71] N. Shembekar, C. Chaipan, R. Utharala, C. A. Merten, *Lab Chip* **2016**, *16*, 1314-1331.
[72] R. Schekman, *Proc. Natl. Acad. Sc.i U. S. A.* **2010**, *107*, 6551.
[73] S. Sarkar, N. Cohen, P. Sabhachandani, T. Konry, *Lab Chip* **2015**, *15*, 4441-4450.
[74] A. Kulesa, J. Kehe, J. E. Hurtado, P. Tawde, P. C. Blainey, *Proc. Natl. Acad. Sc.i U. S. A.* **2018**, *115*, 6685-6690.
[75] G. R. Zimmermann, J. Lehar, C. T. Keith, *Drug Discovery Today* **2007**, *12*, 34-42.
[76] I. Levin, A. Aharoni, *Chem. Biol.* **2012**, *19*, 929-931.
[77] J. Clausell-Tormos, D. Lieber, J. C. Baret, A. El-Harrak, O. J. Miller, L. Frenz, J. Blouwolff, K. J. Humphry, S. Koster, H. Duan, C. Holtze, D. A. Weitz, A. D. Griffiths, C. A. Merten, *Chem. Biol.* **2008**, *15*, 427-437.
[78] I. Platzman, J. W. Janiesch, J. P. Spatz, *J. Am. Chem. Soc.* **2013**, *135*, 3339-3342.
[79] M. Wyszogrodzka, R. Haag, *Langmuir*, **2009**, *25*, 5703-5712.
[80] M. Hamada, T. Kishimoto, N. Nakajima, *Heterocycles* **2012**, *86*.
[81] O. Nachtigall, C. Kordel, L. H. Urner, R. Haag, *Angew. Chem. Int. Ed. Engl.* **2014**, *53*, 9669-9673.
[82] A. K. Singh, R. Nguyen, N. Galy, R. Haag, S. K. Sharma, C. Len, *Molecules* **2016**, *21*.
[83] L. H. Urner, I. Liko, H. Y. Yen, K. K. Hoi, J. R. Bolla, J. Gault, F. G. Almeida, M. P. Schweder, D. Shutin, S. Ehrmann, R. Haag, C. V. Robinson, K. Pagel, *Nat. Commun.* **2020**, *11*, 564.
[84] M. Wyszogrodzka, R. Haag, *Langmuir*, **2009**, *25*, 5703-5712.
[85] M. Wyszogrodzka, R. Haag, *Chemistry* **2008**, *14*, 9202-9214.
[86] S. Gupta, J. Pfeil, S. Kumar, C. Poulsen, U. Lauer, A. Hamann, U. Hoffmann, R. Haag, *Bioconjug. Chem.* **2015**, *26*, 669-679.
[87] L. H. Urner, Y. B. Maier, R. Haag, K. Pagel, *J. Am. Soc. Mass. Spectrom.* **2019**, *30*, 174-180.
[88] S. Alpugan, G. Garcia, F. Poyer, M. Durmuş, P. Maillard, V. Ahsen, F. Dumoulin, *J. Porphyrins Phthalocyanines* **2013**, *17*, 596-603.
[89] S. Kumar, K. Ludwig, B. Schade, H. von Berlepsch, I. Papp, R. Tyagi, M. Gulia, R. Haag, C. Bottcher, *Chemistry* **2016**, *22*, 5629-5636.
[90] A. Tschiche, B. N. Thota, F. Neumann, A. Schafer, N. Ma, R. Haag, *Macromol. Biosci.* **2016**, *16*, 811-823.
[91] S. Kumari, K. Achazi, P. Dey, R. Haag, J. Dernedde, *Biomacromolecules* **2019**, *20*, 1157-1166.

[92] B. Schade, A. K. Singh, V. Wycisk, J. L. Cuellar-Camacho, H. von Berlepsch, R. Haag, C. Bottcher, *Chemistry* **2020**, *26*, 6919-6934.

[93] J. M. William, M. Kuriyama, O. Onomura, *Adv. Synth. Catal.* **2014**, *356*, 934-940.

[94] F. Mecozzi, J. J. Dong, P. Saisaha, W. R. Browne, *Eur. J. Org. Chem.* **2017**, *2017*, 6919-6925.

[95] D. D. McKinnon, D. W. Domaille, J. N. Cha, K. S. Anseth, *Adv. Mater.* **2014**, *26*, 865-872.

[96] A. Hebel, R. Haag, *J. Org. Chem.* **2002**, *67*, 9452-9455.

[97] X. Zhang, K. Achazi, R. Haag, *Adv. Healthc. Mater.* **2015**, *4*, 585-592.

[98] B. Marco-Dufort, R. Iten, M. W. Tibbitt, *J. Am. Chem. Soc.* **2020**, *142*, 15371-15385.

[99] A. Mittal, A. K. Singh, A. Kumar, Parmanand, K. Achazi, R. Haag, S. K. Sharma, *Polym. Adv. Technol.* **2020**, *31*, 1208-1217.

[100] J. M. Sarapas, G. N. Tew, *Angew. Chem. Int. Ed. Engl.* **2016**, *55,* 15860-15863.

[101] A. B. Lowe, C. E. Hoyle, C. N. Bowman, *J. Mater. Chem.* **2010**, *20*.

[102] R. Hoogenboom, *Angew. Chem. Int. Ed. Engl.* **2010**, *49*, 3415-3417.

[103] B. M. Rosen, G. Lligadas, C. Hahn, V. Percec, *J. Polym. Sci., Part A: Polym. Chem.* **2009**, *47*, 3940-3948.

[104] G. Chen, J. Kumar, A. Gregory, M. H. Stenzel, *Chem. Commun.* **2009**, 6291-6293.

[105] M. K. Jeon, J. B. Lim, G. M. Lee, *BMC Biotechnol.* **2010**, *10*, 70.

7 Appendix

7.1 Publications, patent and contributions

1. **M.S. Chowdhury**, X. Zhang, L. Amini, P. Dey, A. K. Singh, A. Faghani, M. S. Henneresse, R. Haag. *Functional Surfactants for Molecular Fishing, Capsule Creation, and Single-Cell Gene Expression,* **2020**, in preparation.

2. **M.S. Chowdhury**, W. Zheng, A. K. Singh, I. L. H. Ong, Y. Hou, J. Heyman, A. Faghani, E. Amstad, D. A. Weitz, R. Haag. *Linear triglycerol-based fluorosurfactants show high potential for droplet-microfluidics-based biochemical assays,* **2020**, submitted.

3. **M. S. Chowdhury**, W. Zheng, S. Kumari, J. Heyman, X. Zhang, P. Dey, D. A. Weitz, R. Haag, *Nat. Commun.* **2019**, *10***,** 4546. *Dendronized fluorosurfactant for highly stable water-in-fluorinated oil emulsions with minimal inter-droplet transfer of small molecules.*

4. R. Randriantsilefisoa, J. L. Cuellar-Camacho, **M. S. Chowdhury**, P. Dey, U. Schedler, R. Haag, *J. Mater. Chem. B* **2019**, *7*, 3220. *Highly sensitive detection of antibodies in a soft bioactive three-dimensional bioorthogonal hydrogel.*

5. P. Dey, T. Bergmann, J. L. Cuellar-Camacho, S. Ehrmann, **M. S. Chowdhury**, M. Zhang, I. Dahmani, R. Haag, W. Azab, *ACS Nano* **2018**, *12*, 6429. *Multivalent flexible nanogels exhibit broad-spectrum antiviral activity by blocking virus entry.*

6. **M. S. Chowdhury**, D. A. Weitz, R. Haag, **2018**, *International Patent #* PCT/EP2018/070036. *Di-block Copolymer: A Manufacturing Method and Suited Applications.*

7.2 Curriculum Vitae

The CV is not included for personal reasons.